2012

The Role of NADPH Oxidase in Ischemia/Reperfusion-Induced Alterations to AMPA Receptor Trafficking and NMDA Receptor Function

Phillip Howard Beske
The University of Montana

THE ROLE OF NADPH OXIDASE IN ISCHEMIA/REPERFUSION-INDUCED ALTERATIONS TO AMPA RECEPTOR TRAFFICKING AND NMDA RECEPTOR FUNCTION

By

Phillip Howard Beske

B.A, Luther College, Decorah, IA, USA, 2006

Dissertation Paper

Presented in partial fulfillment of the requirements for the degree of

Doctor of Philosophy
in Neuroscience

The University of Montana
Missoula, MT

January 2012

Approved by:

Stephen Sprang,
Associate Provost for Graduate Education and Dean of The Graduate School
Graduate School

Darrell Jackson, Chair
Department of Biomedical and Pharmaceutical Sciences

Howard Beall
Department of Biomedical and Pharmaceutical Sciences

Jesse Hay
Division of Biological Sciences

David Poulsen
Department of Biomedical and Pharmaceutical Sciences

J.B Alexander (Sandy) Ross, Associate Dean of the Graduate School
Department of Chemistry and Biochemistry

Beske, Phillip, Ph.D, January 2012 Neuroscience

The Role of NADPH Oxidase in Ischemia/Reperfusion-Induced Alterations to AMPA Receptor Trafficking and NMDA Receptor Function.

Chairperson: Dr. Darrell Jackson

ABSTRACT

Following a stroke, the pathological increase in intracellular calcium arising from the over-activation of post-synaptic glutamatergic receptors has long been established as a key contributor to neuronal death. Also contributing to ischemic/reperfusion-induced neuronal death is oxidative stress, chemically defined as a pathologic state within the cell arising from the increased generation of reactive oxygen and nitrogen species and/or a decrease in the ability of the cell to scavenge and detoxify the reactive intermediates. Strong evidence supports the notion that oxidative stress serves as an important mediator in leading to alterations in intracellular signaling events, ultimately affecting cellular function. However, few studies to date have investigated the role of a key reactive oxygen species generator, NADPH oxidase, in mediating the signaling events leading to alterations in NMDA and AMPA receptor function following ischemia/reperfusion. Therefore, the current series of studies examines the role of reactive oxygen species production from NADPH oxidase following oxygen-glucose deprivation/reperfusion (OGD/R) and the downstream redox-dependent signaling pathways leading to changes in NMDA and AMPA receptor function. *In-vitro* studies using differentiated SH-SY5Y human neuroblastoma cells were performed to test the hypothesis that NADPH oxidase-dependent ROS production mediates the increased tyrosine phosphorylation status of the NMDA receptor NR2A subunit following OGD/R, ultimately resulting in an enhancement of NMDA receptor mediated cell death. *In-situ* studies using acute organotypical hippocampal slices prepared from adult male rats were performed to examine the role of the OGD/R-induced increase in NADPH oxidase activity in accelerating the endocytic machineries involved in the surface removal and selective degradation of the AMPA receptor GluR2 subunit following OGD/R. These studies demonstrated that the increased NADPH oxidase-dependent reactive oxygen species production during reperfusion of OGD treated slices was involved in mediating the internalization of the GluR2 subunit, not only through increasing the serine 880 phosphorylation of the GluR2 subunit, thereby leading to a decreased anchoring of GluR2 with membrane scaffolding proteins, but also by enhancing the activity of the endocytic machinery responsible for the internalization of AMPA receptors. Collectively, these studies begin to elucidate a role for NADPH oxidase-dependent signaling pathways in the ischemic/reperfusion-induced pathologic alterations in NMDA and AMPA receptors known to occur following stroke.

ACKNOWLEDGMENTS

First, I owe a great deal of gratitude to the faculty and staff of the Department of Biomedical and Pharmaceutical Sciences for allowing me the opportunity to further my education, not only as a scientist and a professional-in-training, but also as a person.

Second, I would like to give an enormous thank you to my dissertation advisor Dr. Darrell Jackson, not only for your unwavering support, guidance, mentorship, and faith in me as your graduate student, but also as for your friendship.

Third, I would like to thank and acknowledge my dissertation committee, Dr. Howard Beall, Dr. Jesse Hay, Dr. David Poulsen, and Dr. Sandy Ross. Your patience, guidance, and encouragement have been of crucial influence in the pages that follow.

Fourth, I would like to thank all of those in my life that have endured these past 5+ years with me. To my fellow graduate students, a million thank you's for all of the laughs and smiles we've shared, both in the lab and outside of it. To Josh Ballman, thanks for being one of the best homies a guy could ask for. To all my friends, word yo! To Taco Bell and the creator of Ramen noodles, thank you for providing me delicious and affordable nourishment off my graduate student stipend. To my dog Maddie, while you weren't always the easiest to deal with at times, you always greeted me with nothing but happiness and joy upon returning home from the lab. Thank you for all of the stress-reliving cuddle sessions. and I'm sorry for all of the times I was too busy with work to take you out for a walk. To my entire extended family, words can't express how grateful I

am for the solid foundation you've laid for all of us children to blossom into adults within. To my Grandma Alice Beske, who taught me among many things, "Attitude is everything." To my parents, this would have never gotten completed without the un-conditional love, support, and inspiration you've given to me. Thank you for all of the times I had to retreat back to Minnesota to relax and re-group in the comfort of our home. Finally and most importantly, the largest possible thank to you guys for giving me the motivation to have the confidence in myself to reach for large goals. We did it! Mom and Dad, this is dedicated to you…

TABLE OF CONTENTS

LIST OF DIAGRAMS

LIST OF FIGURES

LIST OF ABBREVIATIONS

ABP – AMPA receptor binding protein

aCSF – Artificial cerebral spinal fluid

ADAR2 – Adenosine deaminase enzyme, 2

AIF - Apoptosis-inducing factor

AMPA – α-amino-3-hydroxyl-5-methyl-4-isoxazole-propionate

AMPAR – AMPA receptor

ANOVA – Analysis of variance

AP2 – Adaptor protein 2

APAF-1 – Apoptosis peptidase activation factor 1

Apo - Apocynin

ATP/ADP – Adenosine Triphosphate/adenosine Diphosphate

ASICs – Acid Sensing Ion Channels

BAR domain – Bin-Amphisphysin-Rvs domain

BSA – Bovine serum albumin

CA1/3 – *Cornus ammonis* area 1/3

CaMKII – Ca^{2+}/calmodulin-dependent protein kinase II

Caspase – Cysteine-dependent aspartate-directed proteases

CdK5 – Cyclin-dependent kinase, 5

CKII – Casein Kinase, 2

CNS – Central Nervous System

CREB – Cyclic-AMP response element binding protein

DPI – Diphenylene Iodonium

DISC - Death-inducing signaling complex

D-MEM/F-12 – Dulbecco's modified eagle medium/F-12

Duox 1/2 – Dual oxidase, 1/2

ER – Endoplasmic reticulum

ERK 1/2 – Extracellular signal-regulated kinase, 1/2

FAD – Flavin adenine dinucleotide

GAIP – G α-interacting protein

GDI – Guanosine nucleotide dissociation inhibitor

GluR2 – Glutamate receptor subunit, 2

GRIP1 – Glutamate receptor interacting protein

GPIC – G α-interacting protein C-terminus (GPIC)

GTP/GDP – Guanosine triphosphate/guanosine diphosphate

HNE – 4-hydroxynonenal

IP3R - Inositol triphosphate receptor

LTP/LTD – Long term potentiation/depression

MAC - Mitochondrial apoptosis-induced channel

mGluR – Metabotropic glutamate receptor

NADPH – Nicotinamide adenine dinucleotide phosphate

NADPH Oxidase – Nicotinamide adenine dinucleotide phosphate-oxidase

NBT – Nitro blue tetrazolium chloride

NCX – Sodium calcium exchanger

NMDA – N-methyl-D-aspartic acid

NMDAR – NMDA receptor

NR2A – NMDA receptor subunit 2A

nNOS – Neuronal nitric oxide synthase

Nox2 – NADPH Oxidase subunit, 2

NSF – N-Ethylmaleimide-Sensitive Fusion Protein

OGD/R – Oxygen-glucose deprivation/reperfusion

p38 MAPK – p38 mitogen activated protein kinase

PARP - Poly(ADP-ribose) polymerase

PBS – Phosphate buffered saline

PDZ domain – Post-synaptic density protein (PSD-95), Drosophila disc large tumor suppressor (DlgA), zonula occludens-1 protein (Zo-1) domain

PI – Propidium Iodide

PICK1 – Protein interacting with C kinase 1

PKA – Protein kinase A

PKCα – Protein kinase C, alpha

PKCδ – Protein kinase C, delta

PMCA – Plasma membrane Ca^{2+} ATPase

PP1– Protein phosphatase, 1

PP2A – Protein phosphatase, 2A

PSD-93 – Post-synaptic density protein, 93 kDa

PSD-95 – Post-synaptic density protein, 95 kDa

PTP – Protein tyrosine phosphatase

PUMA - p53-upregulated modulator of apoptosis

Q/R editing – Glutamine/arginine editing

RNS – Reactive Nitrogen Species

ROS – Reactive Oxygen Species

SDS-PAGE - Sodium dodecyl sulfate polyacrylamide gel electrophoresis

SFKs – Src family kinases

SH3 domain – SRC homology 3 domain

SNARE – Soluble N-ethylmaleimide-sensitive fusion attachment protein receptor

SOD – Superoxide dismutase

SAP 97 – Synapse associated protein, 97 kDa

SAP 102 – Synapse associated protein, 102 kDa

STEP – Striatal-enriched tyrosine phosphatase

TRPM2/7 – Transient receptor potential cation channel, subfamily M, member 2/7

GENERAL INTRODUCTION

Stroke Classifications and Pathophysiology

Every year in the United States, approximately 795,000 people suffer from a stroke, making it the leading cause of disability and the third leading cause of death in the United States after heart disease and cancer (Falluji *et al.,* 2011). In its most basic form, a stroke is defined as a medical emergency arising from the loss of brain function due to a disruption in blood delivery to affected areas of the brain. Normal brain function operates at a high metabolic rate, and since the brain does not store glucose, a nutrient necessary for energy production, it remains very susceptible to any decreases in the delivery of glucose through the bloodstream.

However, while most strokes can be generally classified as the deprivation of oxygen and glucose through inadequate blood delivery to the brain, a stroke can occur in various forms. About 10 to 15% of stroke patients suffer from hemorrhagic stroke (Broderick *et al.,* 2007), or a rupture of a blood vessel within the brain, resulting in the deprivation of both oxygen and glucose to the regions of brain tissue surrounding the blood vessel rupture.

The most common form of stroke, which constitutes about 80-85% of all strokes, is termed "ischemic stroke," occurring when blood flow to an area of the brain is decreased or completely absent as a result of a vessel occlusion, typically from a thrombus or embolus (Falluji *et al.,* 2011). A thrombotic stroke results from a blood clot blocking an blood vessel, which most frequently forms around an atherosclerotic plaque. Because the blockage of the blood vessel is gradual in nature, the onset of thrombotic stroke symptoms is frequently at a slower rate (Broderick *et al.,* 2007). The other frequent type of ischemic stroke results from an embolus, or a travelling particle of debris in the bloodstream originating from elsewhere in the body. Most often, the travelling particle is a blood clot, but can also be other substances including plaque, cancer cells, air, or clumps of bacteria from an infection of the endocardium. Other types of ischemic stroke include systemic hypoperfusion, or a general decrease in blood supply often as a result of circulatory shock or heart attack. Cerebral venous sinus thrombosis, a blood clot of the dural venous sinuses responsible for draining blood from the brain, can also result in an ischemic stroke.

Despite the fact that stroke type is fairly easily categorized in various forms, stroke outcome cannot be classified or diagnosed so simply. The severity of each case of ischemic stroke varies greatly depending on a variety of factors, including the time of ischemia, the area of the brain in which blood supply is significantly reduced, the presence and effectiveness of collateral circulation, and numerous other factors.

While a disturbance in blood flow leading to a complete lack of oxygen (anoxia) or low levels of oxygen (hypoxia) coupled with no/low glucose delivery levels is in itself a damaging event (ischemia), the reintroduction of blood supply (reperfusion) after a period of ischemia further damages the brain tissue. This phenomena is often termed the "oxygen paradox," where the reintroduction of blood supply is necessary for survival, but also results in further damage via inflammation, oxidative stress, and delayed cellular death. However, while injury from reperfusion does cause further damage, the general objective of stroke patient care is to restore blood flow as soon as possible without causing intracerebral hemorrhage (Falluji *et al.,* 2011).

The brain damage resulting from ischemia/reperfusion is often sub-divided into two areas, frequently termed the "necrotic core" and the "penumbra." The necrotic core is defined as the irreversibly damaged area of the brain immediately surrounding the area of blood flow blockage (Schaller and Graf, 2004). Cells undergoing necrotic death die among living neighboring cells without eliciting an inflammatory response via the activation of microglial cells and do so because of physical, chemical, or osmotic damage to the plasma membrane. This un-organized cellular death results in a build-up of dead tissue and cell debris at or near the site of blood vessel occlusion, which after microglial invasion and subsequent debris removal leads to tissue scarring. In terms of stroke pathology, these areas of the brain do not have the potential to recover.

In contrast to the necrotic core, the ischemic penumbra is characterized as tissue that is damaged but still viable in the areas surrounding the necrotic core (Schaller and Graf, 2004). However, the life expectancy of cells within the penumbra is short, as cells in the area have enough energy to survive for a short period of time but not enough to properly maintain function (Hakim, 1998). Also in contrast to the necrotic core, tissue in the penumbra does not typically die by necrosis, but rather through signals arising within the cell resulting in programmed cell death (often called "apoptosis"). Therefore, since tissue within the penumbra is not necessarily fated to die and may have the potential to recover, the goal of many current stroke therapeutic development involves the design of compounds with the ability to save as much of the penumbric tissue as possible. As to date, while there have been and currently are many promising drugs in clinical testing designed for stroke patient care, an effective and reliable therapeutic used for minimizing stroke-induced neuronal damage has yet to reach the public.

Stroke and Excitotoxicity

Calcium cytotoxicity, or more simply put, a pathologically elevated rise in cytoplasmic calcium concentration, is a central mechanism involved in neuronal death in many chronic as well as acute neurodegenerative diseases (Alzheimer's disease, Parkinson's disease, Traumatic brain injury, and others). Initial reports of the cytotoxic nature of high intracellular calcium concentrations date back over 30 years ago and have long been established as a key event involved in the neurodegeneration observed with ischemic/reperfusion injury (Szydlowska and Tymianski, 2010). While physiologic increases in cytoplasmic calcium levels are responsible for many cellular processes such as cell growth, differentiation, synaptic activity for example, abberent regulation of neuronal activity leading to the accumulation of high intracellular calcium levels is also responsible for much of the neuronal death associated with stroke (Arudine *et al.,* 2003).

During ischemia/reperfusion, the abrupt lack of available energy in brain tissue disrupts the ATP-dependent processes necessary to maintain ionic gradients critical to normal cellular function and ionic homeostasis. As a consequence of the ion gradient collapse, excessive levels of neurotransmitter are released into the synapse. Of particular importance is the excessive release of the neurotransmitter glutamate, the primary excitatory neurotransmitter in the brain. Additionally, the function of excitatory amino acid transporters (EAATs) on both neurons and astrocytes is compromised by the lack of ionic homeostatsis that occurs during ischemia/reperfusion, ultimately impairing the ability of the transporters to clear glutamate from the synapse, leading to prolonged elevated glutamate concentrations in the synapse (Camacho and Massieu, 2006). In turn, excessive levels of glutamate in the synapse over-activate post-synaptic glutamatergic targets such as NMDA, AMPA, and kainate receptors, thereby causing the ion channels to open and allow for the excessive influx of calcium.

In addition to increased calcium influx through post-synaptic receptors, intracellular stores of calcium are also released from the mitochondria and endoplasmic reticulum (via the inositol triphosphate receptor (IP3R)) due to the activation of post-synaptic metabotropic glutamate receptors (mGluRs), as well as the activation of other metabotropic receptors as a consequence of acetylcholine, dopamine, and serotonin neurotransmitter release (Arudine *et al.,* 2003). Furthermore, enhanced calcium entry into the neuron following ischemia has also been linked to include other ion channels and transporters such as the transient receptor potential cation channel, subfamily M, member 2 and 7 (TRPM2/7), Na^{+}/Ca^{2+} exchangers (NCX), acid-sensing ion channels (ASICs) or plasma membrane Ca^{2+} ATPase (PMCA), and L-type voltage-dependent calcium channels (Szydlowska and Tymianski, 2010).

Stroke and Apoptosis

One of the damaging consequences of the pathologic increase in cytosolic calcium during ischemia/reperfusion arising from the over-activation of NMDA and calcium-permeable AMPA receptors is the opening of the mitochondrial permeability transition pore. When mitochondria absorb too much calcium, the organelle opens a pore to release excess calcium. In addition to calcium exit from the mitochondria, proteins are also released, particularly cytochrome *c*, which can initiate programmed cell death (Stavrovskaya and Kristal, 2006). In conditions of normal physiologic mitochondrial function, cytochrome *c* is an essential component of the electron transport chain in the mitochondria, responsible for transferring electrons between Complexes III (Coenzyme Q – Cytochrome C reductase) and IV (Cytochrome C oxidase), which is necessary for the production of ATP. Typically, cytochrome *c* is associated with the inner membrane of the mitochondria, but during stress-like cellular conditions, or in response to pro-apoptotic stimuli, cytochrome *c* is released into the cytoplasm (Tafani *et al*., 2002). The release of cytochrome *c* is responsible for the activation of cysteine-dependent aspartate-directed proteases (caspases), which play an essential role in programmed cell death. Termed the "intrinsic apoptotic pathway", once cytochrome *c* is released, it binds with Apoptotic protease activating factor-1 (Apaf-1), which also binds pro-caspase-9 to form a protein complex known as the apoptosome (Dejean *et al*., 2006). Consequently, the apoptosome cleaves pro-caspase-9 to its active cleaved form of caspase-9, which then cleaves pro-capase-3 to active caspase-3. Through caspase-3-dependent proteolysis of other caspases, proteins, and poly(ADP-ribose) polymerase (PARP), caspase-3 activation serves as a central step responsible for killing the cell from within (Stravrovskaya and Kristal, 2006).

However, while the release of cytochrome *c* from the mitochondria is a crucial event leading to ischemia/reperfusion-induced apoptosis, numerous pathways upstream of cytochrome *c* release also affect apoptotic signaling. Oxidative stress, or the overproduction of reactive oxygen species (ROS) following ischemia/reperfusion, activates a number of pathways that have been demonstrated to modulate the intrinsic pathway of apoptosis (Niizuma *et al.*, 2010). Bcl-2 proteins are a family of evolutionarily related proteins which are important in governing mitochondrial membrane permeabilization and are typically classified in three sub-groups: anti-apoptotic (Bcl-2, Bcl-X_L, Bcl-w), pro-apoptotic (Bax, Bak, Bad, Bim, Noxa), and p53-upregulated modulator of apoptosis (PUMA; Niizuma *et al.*, 2010). The pro-apoptotic protein Bax, which competes with the anti-apoptotic protein Bcl-2 proper, has been shown to be up-regulated following ischemia/reperfusion, which further contributes to cytochrome *c* release from the mitochondria via promoting the formation of the mitochondrial apoptosis-induced channel (MAC; Xi *et al.*, 2011) through which cytochrome *c* can exit. Another key regulator of apoptosis is p53, which has been shown to transcriptionally up-regulate a number of pro-apoptotic proteins after ischemia (Bax, Bid, Noxa, and PUMA), as well as directly regulate apoptosis in a transcription-independent manner by translocating to the mitochondria and interacting with the anti-apoptotic Bcl-X_L protein, thereby aiding directly in cytochrome *c* release (Endo *et al.,* 2006).

Opposing the activity of pro-apoptotic signaling during ischemia is the kinase Akt, a downstream target of PI3-kinase. Akt is responsible for the phosphorylation and inactivation of the pro-apoptotic protein Bad following ischemia/reperfusion, ultimately diminishing the ability of Bad to inhibit the activity of pro-survival Bcl-2 family proteins

(Kamala *et al.,* 2007). Additionally, Akt is responsible for the phosphorylation of MDM2, which in turn increases the degradation of p53, thereby diminishing the contribution of p53 in ischemic-induced apoptotic signaling (Niizuma *et al.*, 2010).

While the "intrinsic" apoptotic pathway is perhaps the best studied in ischemia/reperfusion, the "extrinsic" or receptor-mediated pathway has also been shown to contribute to stroke-induced apoptosis. Fas, a death receptor, is also involved in ischemic apoptosis through the up-regulation of Fas receptor and Fas ligand expression (Rosenbaum *et al.*, 2000). The Fas receptor forms the death-inducing signaling complex (DISC) upon ligand binding, which in turn activates procaspase-8, thereby cleaving and activating the pro-apoptotic protein Bid as well as directly activating caspase-3.

In addition to the intrinsic and extrinsic caspase-dependent apoptotic pathways, caspase-independent pathways are involved in ischemic/reperfusion mediated programmed cell death as well (Niizuma *et al.,* 2010). Apoptosis-inducing factor (AIF) is released from the mitochondria following stroke and translocates to the nucleus, ultimately leading to large-scale DNA fragmentation and apoptosis via an unidentified caspase-independent mechanism (Culmsee *et al.,* 2005). In a similar manner, endonuclease G contributes to caspase-independent apoptosis following ischemia/reperfusion by translocating from the mitochondria to the nucleus where it is responsible for DNA fragmentation (Lee *et al.*, 2005). Taken together, the cell undergoes a complex and multifaceted apoptotic signal involved in the delayed neuronal death seen within cells of the penumbra following stroke.

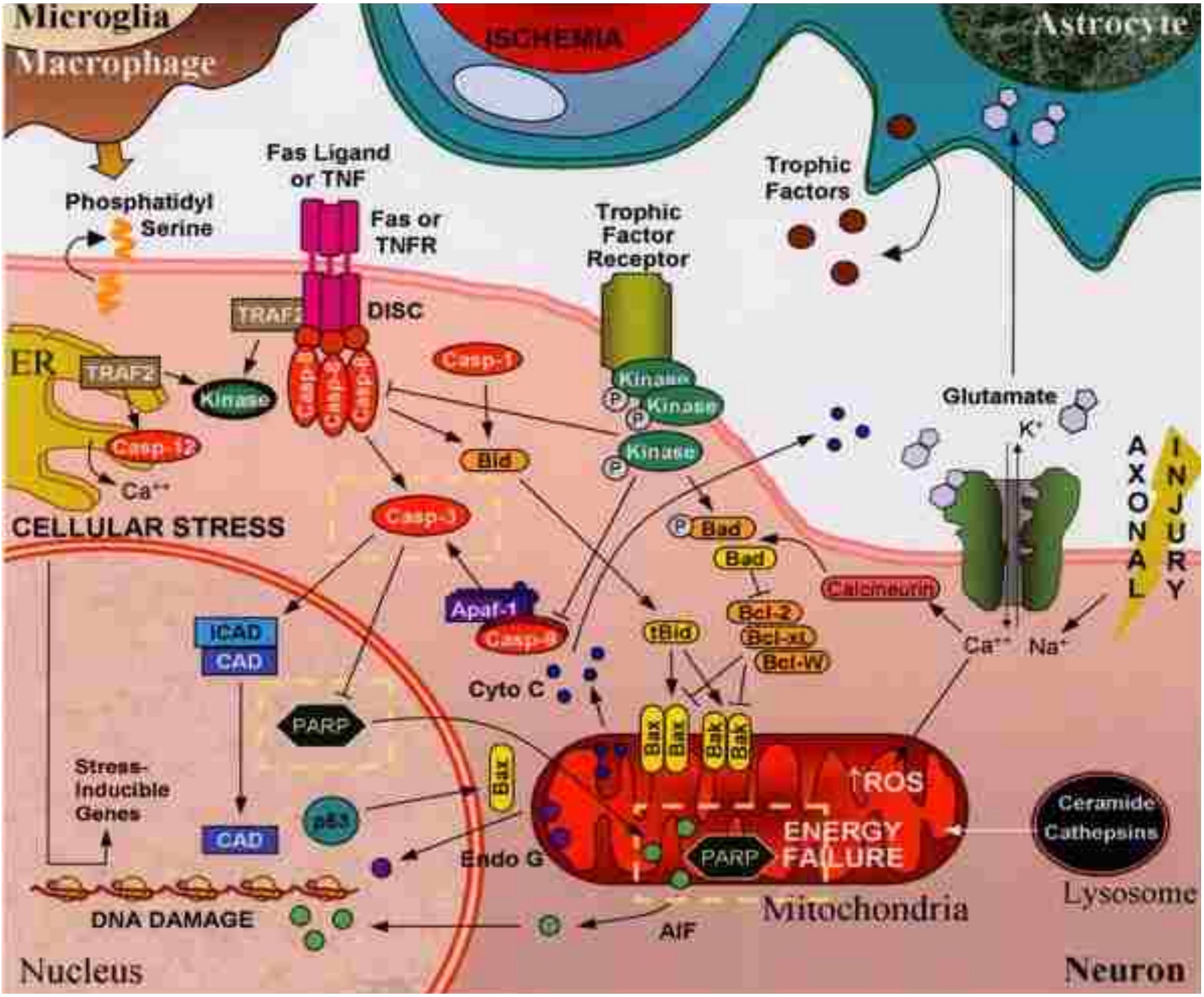
Microglia
Macrophage
ISCHEMIA
Astrocyte
Fas Ligand or TNF
Phosphatidyl Serine
Fas or TNFR
Trophic Factors
Trophic Factor Receptor
TRAF2
DISC
ER
TRAF2
Kinase
Casp-8
Casp-8
Casp-8
Casp-1
Kinase
Kinase
Kinase
Glutamate
K+
Casp-12
Ca++
Bid
CELLULAR STRESS
Casp-3
Bad
Bad
AXONAL INJURY
Apaf-1
Casp-9
Calcineurin
ICAD
CAD
tBid
Bcl-2
Bcl-xL
Bcl-W
Ca++
Na+
Cyto C
PARP
Bax
Bax
Bak
Bak
Stress-Inducible Genes
Bax
↑ROS
Ceramide
Cathepsins
p53
ENERGY FAILURE
CAD
Endo G
PARP
Lysosome
DNA DAMAGE
Mitochondria
AIF
Nucleus
Neuron

Diagram 1. Schematic representation of the initiation and regulation of neuronal apoptosis after ischemia. Pathologic mechanisms triggering apoptosis after ischemia include oxidative stress, energy failure, excitotoxicity (primarily excess glutamate), axonal injury, trophic factor withdrawal, ER stress, and/or death receptor-ligand binding (for example TNF, Fas). Regulation of apoptosis occurs through multiple pathways including kinase-dependent intracellular signaling pathways and Bcl-2 family proteins. Execution of apoptosis involves the caspase cascade and/or release of apoptogenic factors from organelles such as mitochondria and lysosomes. Ultimately DNA fragmentation, cytoskeletal disintegration, and externalization of membrane phosphatidylserine occurs, signaling macrophages and microglia to engulf cellular debris. Potential therapeutic targets discussed in this review are highlighted within the dashed yellow lines. AIF, apoptosis-inducing factor; Apaf-1, apoptotic protease activating factor-1; Bcl, B-cell lymphoma; CAD, caspase-activated deoxyribonuclease; casp, caspase; cyto c, cytochrome *c*; DISC, death-inducing signaling complex; Endo G, endonuclease G; ER, endoplasmic reticulum; iCAD, inhibitor of CAD; ROS, reactive oxygen species; tBid, truncated Bid; TNF, tumor necrosis factor; TNFR, TNF receptor; TRAF2, TNF receptor associated factor. (From Zhang X *et al.,* 2005).

NADPH Oxidase Structure and Function

Nicotinamide adenine dinucleotide phosphate-oxidase (NADPH oxidase) is a multi-subunit enzyme responsible for the single electron transfer from NADPH to oxygen (O_2) to form superoxide ($O_2^{\cdot-}$) and $NADP^+$, with flavin adenine dinucleotide (FAD) serving as a necessary co-factor. NADPH oxidase was first characterized over 40 years ago as the enzyme responsible for the oxidative burst observed in neutrophils to provide host defense against bacteria (Infanger *et al.,* 2006). While the role NADPH oxidase was once thought to be limited only in the modulation of immunological responses, numerous studies within the past 15 years that have clearly demonstrated that the function of NADPH oxidase ROS production is much more diverse, involving a large variety of cellular functions in a wide array of cells and tissues. The NADPH oxidase (Nox) family has been shown to arise from numerous Nox proteins (Nox1-5 and Duox1/2) in a tissue specific manner to produce superoxide in not only the immune system, but also the brain, the vasculature, the kidneys and the digestive tract, ultimately mediating a number of physiologic processes including the regulation of gene expression, proliferation, differentiation, migration, apoptosis, and learning and memory (Brown and Griendling, 2009).

Although seven distinct NOX genes have been identified, all share the commonality of producing superoxide. However, due to subcellular compartmentalization and expression patterns, specificity is achieved in proper downstream physiologic targeting from Nox-derived superoxide (Brown and Griendling, 2009). Nox1, the first novel NADPH oxidase subunit to be cloned, is most highly expressed in the colon (Rokutan *et al.,* 2008), but has also been discovered in endothelial cells, the uterus, the placenta (Cui *et al*., 2006), the prostate, osteoclasts (Lee *et al.,* 2005), retinal pericytes, neurons, astrocytes, and microglia (Sacre and Krausse, 2009). Nox1 is activated through association with the membrane subunit $p22^{phox}$, subsequently forming a complex with the cytosolic activators $p47^{phox}$, $p67^{phox}$, and the small GTPase Rac. Additionally, Nox1 can associate with the $p47^{phox}$ and $p67^{phox}$ homologues, NoxO1 and NoxA1 (Brown and Griendling, 2009) to produce superoxide.

Nox2, also often called neutrophil NADPH oxidase, was the first discovered Nox family member. Nox2 is most highly expressed in phagocytes, but has also been discovered in the central nervous system (CNS; Sacre and Krause, 2009), fibroblasts, cardiomyocytes, skeletal muscle, hepatocyctes in the liver, and hematopoietic stem cells (Bedard and Kruase, 2007). Nox2 is formed through the constitutive association with the membrane subunit $p22^{phox}$. The cytosolic activator, $p47^{phox}$, when phosphorylated on 8-9 serine residues by protein kinase C (PKC), results in the exposure of an SH3 binding site on $p47^{phox}$. The exposed SH3 binding site consequently interacts with a proline-rich region of p22phox, thereby allowing for the translocation of $p47^{phox}$ to the membrane (El Benna *et al.,* 1996). In turn, $p67^{phox}$ binds to the translocated $p47^{phox}$, which provides a binding site for activated Rac, thereby forming a functional holoenzyme along with $p40^{phox}$ (Brown and Griendling, 2009).

Nox3 is most highly expressed in the inner ear, but has also been detected in the fetal spleen, kidney, lung, and skull (Banfi *et al*., 2004). Nox3 is activated through association with $p22^{phox}$, as well as NoxO1 and $p67^{phox}$, but many studies done on Nox3 activity have been contradictory, as the exact mechanisms of Nox3 regulation remain muddled (Cheng *et al*., 2004; Uneo *et al*., 2005).

Nox4 is most highly expressed in the kidney, but is also expressed in smooth muscle cells, endothelial cells, fibroblasts, keratinocytes, osteoclasts, neurons, and hepatocytes (Brown and Griendling, 2009). However, unlike the other Nox family members, Nox4 is unique in that the only requirement for ROS production is the presence of the membrane subunit $p22^{phox}$. As a consequence of this constitutive activity, Nox4 is not dependent on any cellular signals from cytosolic activators, as its activity is governed solely by the proportional expression of the Nox4 protein (Chen *et al*., 2008). Nox4 also differs from other Nox family enzymes because the superoxide produced via Nox4 activity is so rapidly converted to hydrogen peroxide (H_2O_2) that the superoxide produced is almost undetectable, thereby making hydrogen peroxide responsible for carrying out the downstream effects of Nox4 (Serrander *et al*., 2007).

Nox5 has been demonstrated to be present in lymphatic tissue, the testis, endothelial cells, the spleen, the uterus, and prostate cancer cells (Brown and Griendling, 2009). Nox5 is also unique in that its activation is regulated by calcium instead of by the cytosolic activators necessary for Nox1-3 activation (Banfi *et al*., 2001). Various Nox5 isoforms exist, but most contain an EF-hand motif at the N-terminus, which regulates and increases Nox5 activity with increasing calcium concentrations (Banfi *et al.*, 2001). Additionally, PKC mediated phosphorylation of Nox5 increases the sensitivity of Nox5 to calcium, allowing for greater Nox5 activation at lower calcium concentrations (Jagnandan *et al.,* 2007).

Duox1/Duox2 proteins were originally isolated from the thyroid but are also expressed in respiratory epithelium (Brown and Griendling, 2009). Duox proteins have a dual nature because of the presence of an extracellular peroxidase domain along with the

EF-hand calcium-binding domain seen in Nox5 proteins (De Deken *et al*., 2000). PKC phosphorylation of the Duox enzyme also positively modulates Duox1/2 activity, but uniquely, Duox proteins directly produce hydrogen peroxide via a two electron reduction of oxygen, rather than via a two step single electron reduction with superoxide as an intermediate (Dupuy *et al*., 1989).

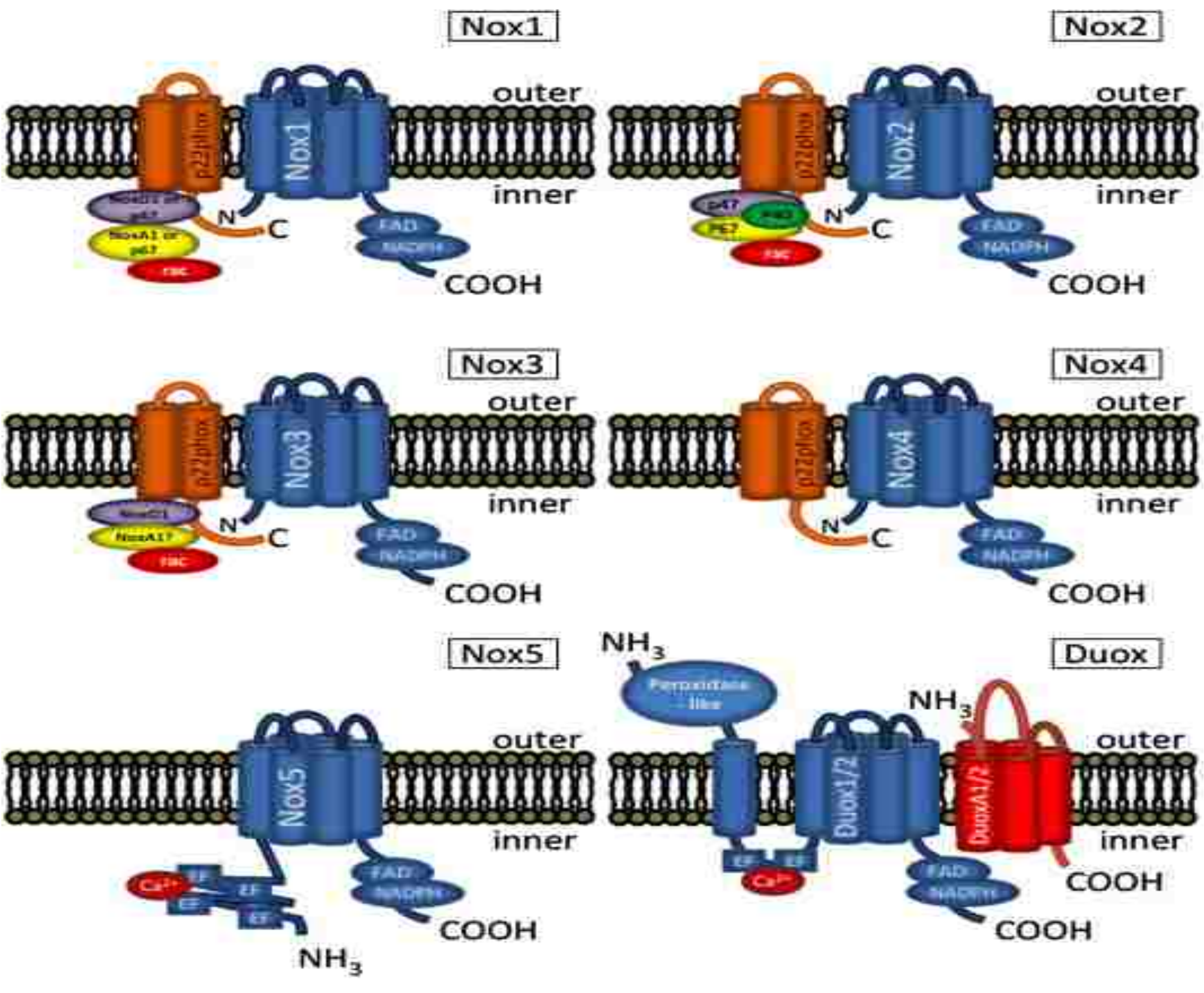
Nox1
outer
inner
Nox1
p22phox
N
C
FAD
NADPH
COOH
Nox2
outer
inner
Nox2
p22phox
N
C
FAD
NADPH
COOH
Nox3
outer
inner
Nox3
p22phox
N
C
FAD
NADPH
COOH
Nox4
outer
inner
Nox4
p22phox
N
C
FAD
NADPH
COOH
Nox5
outer
inner
Nox5
EF
FAD
NADPH
COOH
NH3
Duox
NH3
outer
inner
Duox1/2
DuoxA1/2
NH3
EF
COOH
FAD
NADPH
COOH

Diagram 2. Nox family members and their regulatory subunits. Although no three-dimensional crystallization of Nox proteins has been performed, they are believed to contain six transmembrane domains based on hydrophobicity analysis (seven for Duox1/2). Oxidase activity occurs when NADPH binds to Nox on the cytosolic side, where it transfers electrons to FAD and the heme centers (not shown) and finally to oxygen on the outer membrane surface, resulting in $O_2\bullet^-$ formation. In Nox1-4, the transmembrane subunit $p22^{phox}$ associates with active and inactive Nox. It is believed to have between two and four transmembrane segments. Nox1 is believed to primarily interact with the cytosolic subunits NoxO1, NoxA1, and GTP-Rac on activation; however, $p47^{phox}$ and $p67^{phox}$ can replace NoxO1 and NoxA1, respectively. Nox2 activation involves association with GTP-Rac, $p47^{phox}$, $p67^{phox}$, and $p40^{phox}$. Nox3 activation is less well defined, but is believed to primarily involve GTP-Rac, $p47^{phox}$, and NoxA1 in the inner ear. Nox4 is constitutively active when associating with the cytosolic $p22^{phox}$ subunit. Nox5 and Duox1/2 activation involves Ca^{2+} binding to EF-hand domains in the cytosol. Duox1/2 require the association of DuoxA1/2, respectively, for localization to the plasma membrane. (From Brown and Griendling, 2009).

NADPH Oxidase in CNS Physiology

While multiple Nox proteins are often expressed in the same cell or tissue, each of these enzymes are responsible for regulating a host of different functions in different cell types. Since all Nox proteins produce the same reactive oxygen species ($O_2^{\cdot-}$ or H_2O_2), it is clear that the various subcellular localizations and the coupling to external stimuli are of crucial importance in ultimately determining the response to Nox activation for downstream signaling (Infanger *et al*. 2006).

In the CNS, Nox1, Nox2, Nox3, and Nox4 transcripts have been detected (Sorce and Krause, 2009). In terms of cell specific expression of Nox proteins, Nox1, Nox2, and Nox4 isoforms are present in neurons, astrocytes, and microglial, while the exact localization of Nox3 has not yet been fully elucidated (Sorce and Krause, 2009). Spatial localization studies have indicated that Nox proteins not only have a synaptic localization, as shown by axonal and dendritic expression on neurons, but are also localized to the soma (Tejada-Simon *et al.,* 2005).

While data exists for the Nox1 and Nox3-dependent neurologic function (locomotor activity, movement coordination, blood pressure regulation, and inflammation), the most documented Nox-dependent CNS physiologic studies revolve around the Nox2 isoform (Sorce and Kruase, 2009). Nox2 is important in the processes of long-term potentiation (LTP) and hippocampal dependent memory (Infanger *et al.,* 2006), which is consistent with histological studies that have demonstrated Nox2 is most highly expressed in the hippocampus (Serrano *et al*. 2003; Tejada-Simon *et al.,* 2005). A controlled intracellular redox environment in hippocampal neurons has as been strongly implicated in the processes of learning and memory. First, overexpression of superoxide dismutase (SOD), the enzyme responsible for converting superoxide to hydrogen peroxide, has been shown to impair memory function in mice, which can be reversed with pharmacological inhibition of SOD (Thiels *et al.,* 2000). Also, general ROS production during neuron-glia signaling in the hippocampus is important in the translational modifications of neighboring cells that enhance LTP (Atkins and Sweatt, 1999). More direct approaches linking hippocampal function with NADPH oxidase activity have shown that genetic ablation of proteins in the Nox2 enzyme complex ($gp91^{phox}$, $p47^{phox}$, $p67^{phox}$, $gp22^{phox}$) which render Nox2 unable to produce superoxide lead to impaired cognitive function in mice (Kishida *et al.,* 2006).

At a receptor level, NADPH oxidase activity also has effects on NMDAR signaling, one of the best-studied post-synaptic receptors involved in hippocampal learning and memory. NMDAR activity is controlled, in part, by redox potential. Oxidation of cysteine residues on NR1 and NR2A subunits modify channel conformation and modulate ligand-binding in an allosteric manner (Lipton *et al*., 2002). Pharmacologic Nox inhibition blocks NMDAR dependent LTP, either through oxidant regulation of the receptor itself (Sorce and Krause, 2009), or the activation of ERK 1/2, which has both been identified as necessary for LTP (English and Sweatt, 1997) and a downstream target for NADPH oxidase-derived ROS during LTP (Kishida *et al*., 2005).

While NADPH oxidase activity is important in the modulation of NMDA receptor function, NMDA receptors themselves are in turn responsible for regulating Nox enzyme activity. Stimulation of NMDA receptors produces an intraceullar burst of superoxide from Nox2, identified mechanistically through calcium entry from NMDAR stimulation leading to the activation of PKC delta (PKCδ) and subsequent phosphorylation/translocation of the cytosolic activators required for Nox2 activity (Brennan *et al*., 2009).

NADPH oxidase activity must therefore be carefully regulated, as the under-production of ROS can impair the processes of learning and memory, and the over-production of ROS can lead to cellular damage and death. Uncontrolled ROS production from NADPH oxidase has been linked to a number of neurodegenerative disorders, from acute injuries such as stroke (Wang *et al*., 2006) and traumatic brain injury (Dohi *et al*., 2010) to chronic disorders such as Alzheimer's (Bianca *et al.,* 1999) and Parkinson's disease (Norris and Giasson, 2005).

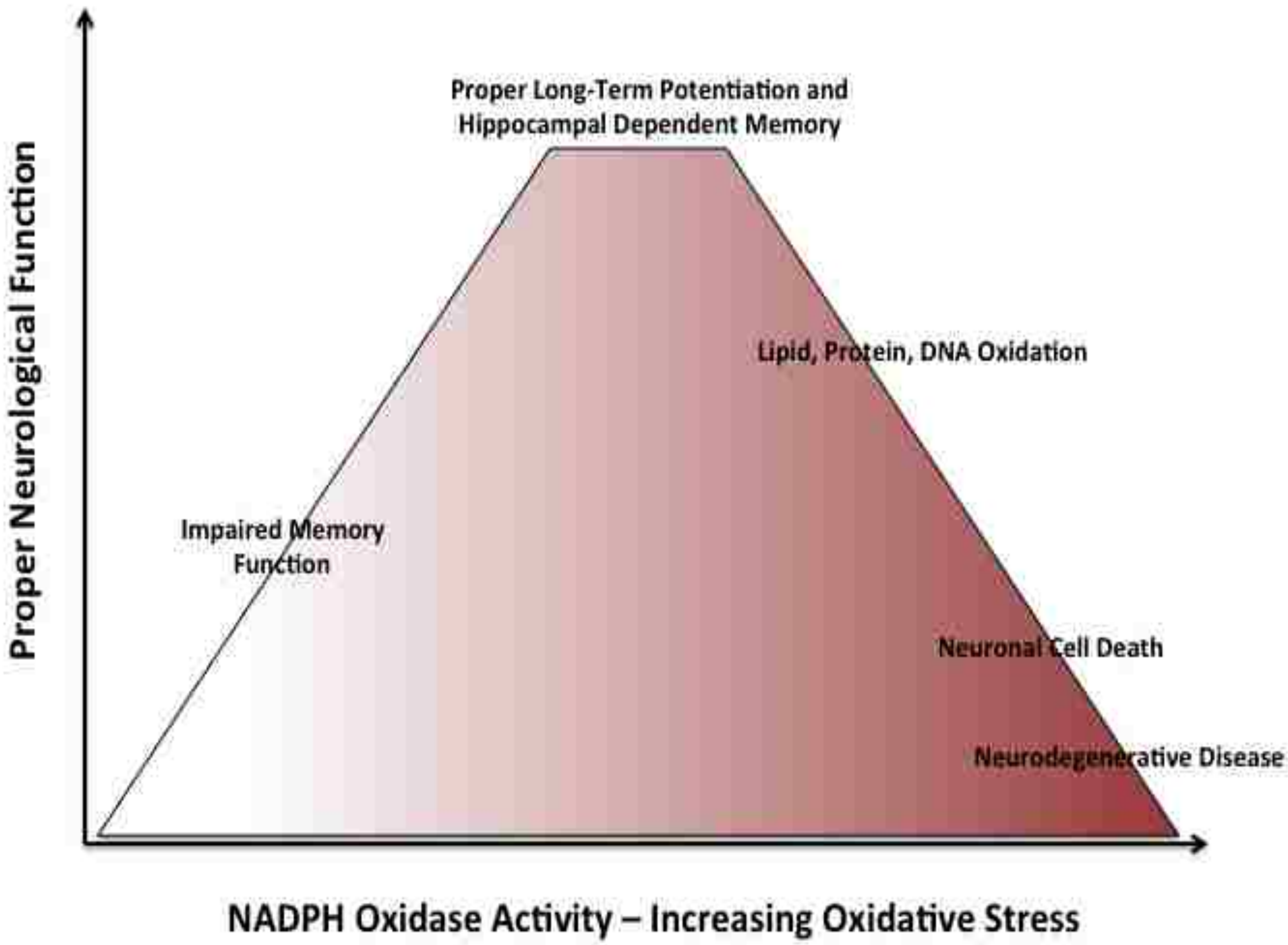
Proper Long-Term Potentiation and
Hippocampal Dependent Memory
Lipid, Protein, DNA Oxidation
Impaired Memory
Function
Neuronal Cell Death
Neurodegenerative Disease
Proper Neurological Function
NADPH Oxidase Activity – Increasing Oxidative Stress

Diagram 3. Normal CNS function depends on a balanced oxidant environment. Hippocampal processes, such as long-term potentiation and memory, are inhibited in mice in which basal ROS levels are reduced by scavengers. On the other hand, excessive production of oxidant radicals is linked to improper neuronal signaling in this and other brain regions, and in some instances can lead to neuronal cell death. Neurodegenerative diseases such as Alzheimer's and Parkinson's are characterized by increased oxidative stress, lipid, protein, and DNA oxidation, and neuronal cell death in brain regions associated with these diseases. More recently NADPH oxidase upregulation and activation in both neurons and microglia has emerged as an important mechanism of oxidative stress in CNS. (Adapted from Infanger *et al.*, 2006).

NADPH Oxidase and Oxidative Stress in Ischemia/Reperfusion

It is well established that ROS, resulting from Nox activity, is a key contributor to the oxidative stress and subsequent neuronal death associated with stroke. Nox2 knockout mice, the same which display decreased cognitive abilities, show decreased injury after global ischemia (Walder *et al.,* 1997). Furthermore, the administration of the NADPH oxidase inhibitor diphenylene iodonium (DPI) significantly decreased superoxide production following ischemia (Miller *et al.,* 2006). Additionally, pretreatment and pharmacologic inhibition of NADPH oxidase prior to the induction of ischemia/reperfusion with apocynin, a compound demonstrated to inhibit the assembly of the functional Nox2 holoenyme (Stolk *et al*., 1994), is neuroprotective in the hippocampus (Wang *et al.,* 2006).

However, NADPH oxidase activity is not the only source of ROS contributing to oxidative stress following stroke. During the ischemic phase, when oxygen and glucose are deprived, little superoxide is produced from NADPH oxidase since the molecular oxygen necessary for the conversion of oxygen to superoxide through NADPH oxidase activity is not available. Two other sources of ROS do produce superoxide during the ischemic phase however in a di-phasic manner, first from the mitochondria (due to alterations in mitochondrial electron transport function) and second from the cytosolic enzyme xanthine oxidase (Abramov *et al*., 2007). It is not until the reperfusion phase in which oxygen and glucose delivery is restored that NADPH oxidase produces a large burst of superoxide (Abramov *et al.,* 2007). Additional sources of ROS production following stroke can result from the action of other oxidase enzymes, such as monoamine oxidase, lipooxygenase, and cyclooxygenase, oxidation of unsaturated fatty acids, metabolism of catecholamines, and quinone formation (Allen and Bayraktutan, 2009).

However, superoxide is not the only reactive species produced during ischemic injury. Nitric oxide (NO) is also produced at neurotoxic levels in neurons through the calcium dependent activation of neuronal Nitric oxide synthases (nNOS) following stroke (Castillo *et al*., 2000). NOS enzymes catalyze the production of NO from L-arginine and are thought to function as a retrograde neurotransmitter in normal physiologic function, but similar to NADPH oxidase, when excessively activated in numerous pathologies, are known to contribute to cellular death (Allen and Bayraktutan, 2009).

During the extreme state of oxidative stress that occurs during ischemia/reperfusion, superoxide and NO are not the only known ROS and reactive nitrogen species (RNS) to be formed within the cellular environment. In normal cellular physiology, superoxide (O_2^-) typically undergoes dismutation into hydrogen peroxide (H_2O_2) via the activity of the antioxidant family of superoxide dismutases (SODs). The enzymatic activities of glutathione peroxidase or catalase are then responsible for the decomposition of hydrogen peroxide to water (H_2O) and oxygen (O_2). However, in the presence of transition metals such as iron (Fe^{2+}), hydrogen peroxide (H_2O_2) can undergo a Fenton reaction, leading to the formation of the highly reactive hydroxyl radical ($^{\cdot}OH$) (Crack and Taylor, 2005). Superoxide can also react with NO to form peroxynitrite ($ONOO^-$), also a very potent oxidizing agent (Allen and Bayraktutan, 2009).

The effects of increased ROS and RNS levels within the cell have numerous detrimental results. Lipid peroxidation, a process in which free radicals oxidize lipids in the cell membrane resulting in cell damage, is one of the major consequences of ROS-mediated injury. Most frequently, polyunsaturated fatty acids are the targets of lipid peroxidation because of the reactive hydrogens they posses. A ROS species, such as the ˙OH radical, combines with a hydrogen atom to produce water and a fatty acid radical. Due to the unstable nature of the fatty acid radical, it reacts quickly with molecular oxygen, thereby creating a peroxyl-fatty acid radical, which reacts with a different fatty acid, thereby producing a new fatty acid radical and a lipid peroxide. The reaction then propagates in a chain reaction until it either reacts with another radical to produce a non-radical species (which only occurs when the concentration of radical species is high enough for there to be a high probability of collision with two radicals) or is caught by an antioxidant within the cell. One of the harmful products of lipid peroxidation is 4-hydroxynonenal (HNE), which is used as a marker for lipid peroxidation and is known to be toxic in neurons and induce apoptosis (McCracken *et al.,* 2000). Other detrimental outcomes from increased ROS and RNS levels include protein oxidation/denaturation, DNA modification leading to fragmentation, phosphatase inactivation and abnormal kinase signaling, as well as activation of apoptotic pathways through the induction of mitochondrial cytochrome *c* release (Allen and Bayraktutan, 2009).

While oxidative stress can be damaging in any cell/tissue/organ, the brain is particularly susceptible to ROS and RNS-induced damage. Reasons for this include a high concentration of peroxidisable lipids, low levels of antioxidant protection (especially catalase), high oxygen and energy consumption, high levels of iron (which can act as a pro-oxidant under pathologic conditions), and the oxidation reactions of both glutamate and dopamine which occur at a high rate in neurons (Crack and Taylor, 2005; Saeed *et al*., 2007). Furthermore, during ischemia/reperfusion, lactic acid accumulates in neurons due to energy depletion, consequently leading to acidosis (Chan, 1996). This acidic environment within the neuron further promotes a pro-oxidant effect by increasing the H^+ concentration, consequently enhancing the conversion of superoxide and hydrogen peroxide to more reactive species (Allen and Bayraktutan, 2009).

Glutamatergic Receptors and NMDAR Structure, Function, and Localization

Glutamate, the primary excitatory neurotransmitter within the mammalian CNS, is responsible for the activation of various receptors that are central to neurotransmission, synaptic plasticity, and a diverse set of cognitive processes. Synaptic receptor targets for glutamate can be sub-divided into two groups, ionotropic and metabotropic receptors. The category of glutamatergic ionotropic receptors, which are all ligand-gated, nonselective, cation channels, includes the *N*-methyl *D*-asparte receptor (NMDAR), the 2-amino-3-(3-hydroxy-5-methylisoazol-4-yl)propionic acid receptor (AMPAR), and the Kainate receptor (Traynelis *et al.,* 2010). Metabotropic glutamate receptors (mGluRs), members of the family of G-protein-coupled receptors, also bind glutamate, but fall into three distinct groups: Type I ($mGluR_1$ and $mGluR_5$) which are G_q coupled and predominantly located on the post-synapse, Type II ($mGluR_2$ and $mGluR_3$), which are G_i/G_o coupled and are mainly presynaptic, and Type III ($mGluR_4$, $mGluR_6$, $mGluR_7$, and $mGluR_8$) which are also G_i/G_o coupled and located primarily on the presynapse (Shigemoto *et al*., 1997). Taken together, the coordinated action of glutamatergic receptors, along with the input of other receptors, allows for a wide array of functions based on assorted receptor spatial expression arrangements, temporal activation patterns, receptor trafficking, protein-protein interactions, phosphorylation events, translation and transcriptional regulation, and downstream coupled signals necessary for normal synaptic physiology.

Of all glutamatergic receptors, perhaps the most extensively studied in both physiology and pathology is the NMDAR. The ionotropic NMDAR arises from seven different NMDAR subunits: NR1, NR2A-D, and NR3A-B to form a tetrameric complex, most typically consisting of two NR1 and two NR2 subunits (Stephenson *et al.,* 2008). The NMDAR subunits are large in structure, consisting of over 900 amino acid residues, and assemble as integral membrane proteins that form a central ion pore, with an extracellular N-terminus and an intracellular C-terminus, which is responsible for facilitating cytoplasmic protein-protein interactions (Traynelis *et al.,* 2010). The variability in each NMDAR tetramer arises from the presence of its NR2 subunit, which differ in their expression profiles, desensitization kinetics, pharmacological properties, downstream signaling pathways and trafficking mechanisms (Gladding and Raymond, 2011). Additionally, although NR1 expression remains fairly constant throughout development, NMDAR composition changes with the maturation of neurons in the hippocampus and cortex. NR2B is highly expressed early in development and declines into adulthood, while NR2A is absent early and increases in expression with age (Cull-Candy *et al.,* 2001).

The functional activation of NMDARs is unique among other receptors for a variety of reasons. First, the activation of NMDARs is dependent on the simultaneous binding of two agonists: glycine and glutamate. The NR1 subunit provides the glycine-binding site while the NR2 subunit forms the glutamate binding site (Furukawa and Gouaux, 2003). However, co-binding of the two agonists does not allow for NMDAR activation, as the presence of a Mg^{2+} block in the channel pore requires release, which occurs with postsynaptic depolarization, prior to allowing for calcium influx (Gladding and Raymond, 2011).

The synaptic localization of NMDARs governs many of its signaling properties. The same NMDARs residing in a different location will have different signaling outcomes (Traynelis *et al.,* 2010). Typically, NMDARs are classified as existing within three distinct locations: synaptic, perisynaptic, and extrasynaptic (Gladding and Raymond, 2011). Synaptic NMDARs are those that exist within the postsynaptic density, a cytoskeletal protein-enriched interconnected network that acts as a scaffold to secure and anchor NMDARs for the efficient glutamate-induced activation of the receptor located immediately across the synapse from the presynaptic axon terminal (Newpher and Ehlers, 2009). This allows for the formation of large macromolecular NMDAR complexes containing various adaptor and effector proteins involved in downstream signaling cascades and membrane stability, ultimately effecting NMDAR function and trafficking (Sheng and Lee, 2000). Perisynaptic NMDARs are classified as located within 200-300 nm of the post-synaptic density, which is typically an area that contains mobile receptors in transit towards and away from the post-synaptic density (Gladding and Raymond, 2011). Extrasynaptic NMDARs are localized farther away from the post-synaptic density, residing on the dendritic spine neck, the dendritic shaft, or the soma (Newpher and Ehlers, 2009). Perisynaptic and extrasynaptic NMDARs are only activated by high concentrations of glutamate in the synaptic cleft, as low levels of glutamate release rarely results in glutamate-induced activation of the receptors at extrasynaptic locales. At low concentrations, glutamate is either first bound by synaptic glutamatergic receptors or taken out of the synapse by transporter activity before diffusion to the extrasynapse (Groc *et al*., 2009).

Initial observations found that calcium entry through synaptic NMDARs leads to the activation of the transcription factor cyclic-AMP response element binding protein (CREB), thereby promoting cell survival, while calcium entry from extrasynaptic

NMDAR activation dominates over synaptic NMDAR activation and inactivates CREB, thereby diminishing pro-survival signals (Hardingham *et al.,* 2002). Furthermore, it was also initially proposed that activation of synaptic NR2A subunits mediate pro-survival while activation of extrasynaptic NR2B subunits elicits cell death (Liu *et al*., 2007). However, such generalizations are not always necessarily true. Both NR2A and NR2B subunits have been reported to mediate either apoptosis or neuroprotection, not only at synaptic sites, but also at extrasynaptic locations. This suggests that downstream signaling responses of NMDARs depends more on the surrounding biochemical environment and the NMDAR associated signaling complexes than simply the subunit composition and synaptic location (Hardingham and Bading, 2010).

NMDAR localization and function is also regulated through posttranslational modifications of the intracellular C-terminus domain, particularly through protein-protein interactions (Gladding and Raymond, 2011). Scaffolding proteins known to be involved in the anchoring of NMDARs, as well as assembling the formation of a signaling meshwork, include the membrane associated guanylate kinase (MAGUK) family of proteins. These include post synaptic density protein-95 (PSD-95), post-synaptic density protein-93 (PSD-93), synapse associated protein-102 (SAP-102), and synapse associated protein 97 (SAP-97; Kim and Sheng, 2004). Among the four MAGUK family members, PSD-95 is the most thoroughly studied in synaptic function. PSD-95 is highly expressed in the post-synaptic density, and contains three Drosophila disc large tumor suppressor (DlgA), and zonula occludens-1 protein (zo-1) (PDZ) binding domains, one SRC homology 3 (SH3) domain, and one guanylate kinase-like (GK) domain (Xu, 2011). PSD-95 has been demonstrated to be important in NMDAR function through two mechanisms, by anchoring NMDARs in the post-synaptic density, and scaffolding NMDARs to intracellular signaling complexes composed of various kinases, phosphatases, other scaffolding proteins, and nitric oxide synthase into close proximity of NMDAR channels (Xu, 2011). One such important scaffolding protein that binds PSD-95 through PDZ domain interactions is Shank, which is believed to function as an actin scaffold, ultimately serving the purpose as a link between NMDA/PSD-95 complexes and regulation of the cytoskeleton (Naisbitt *et al*., 1999). Shank has also been demonstrated to interact through an EVH1 domain with Homer (Tu *et al.,* 1998), a membrane protein located on the periphery of the post-synapse that selectively binds mGluRs (Brakeman *et al*., 1997). This interaction between NMDAR/PSD-95/Shank and mGluR/Homer signaling complexes physically bridges the actin cytoskeletal proteins with ionotropic and metabotropic glutamate receptors. Other proteins included in the large NMDAR/PSD-signaling complex incluce G α-interacting protein (GAIP), G α-interacting protein C-terminus (GPIC) (Yi *et al.,* 2007) and other cytoskeletal proteins such as α-actinin, spectrin (Dunah *et al.,* 2000), and F-actin (Newpher and Ehlers, 2009), all which play a role in the surface expression of NMDARs. Taken together, the various assemblies and interactions of the numerous scaffolded proteins associated with NMDARs govern not only synaptic anchoring of the receptor, but also downstream signaling complexes and dendritic cytoskeletal morphology.

In addition to protein-protein interactions, NMDAR phosphorylation events also mediate synaptic localization and overall receptor function. In particular, tyrosine phosphorylation has been shown to be a key event in modulating NMDAR expression and function (Chen and Roche, 2007). Tyrosine phosphorylation of NR2A subunits promotes synaptic stability and the potentiation of NMDAR currents (Kalia *et al.,* 2004), while tyrosine phosphorylation of NR2B subunits can promote extrasynaptic migration of the receptor (Prybylowski *et al*., 2005). Kinases that are held in close proximity to NMDARs via interactions with structural cytoskeletal proteins and scaffolding proteins such as PSD-95 include the Src Family Kinases (SFK) members Src, Fyn, and Lyn (Gladding and Raymond, 2011). Phosphatases involved in regulating NMDAR tyrosine phosphorylation events include Striatal-Enriched tyrosine Phosphatase (STEP; Braithwaite et al., 2006) and protein tyrosine phosphatase (PTP; Goebel-Goody *et al.,* 2009). Serine phosphorylation has also been shown to play a role in NMDAR localization and function, accomplished via the activity of casein kinase II (CK2) (Chung *et al.,* 2004), cyclic AMP dependent protein kinase A (cAMP-PKA), and protein kinase C (PKC) (Crump *et al.,* 2001). CK2 mediated NR2B serine phosphorylation and PKC mediated NR1 serine phosphorylation has been demonstrated to enhance migration from the synapse (Tingley *et al.,* 1997), while cAMP-PKA mediated serine phosphorylation has been shown to mediate enhanced synaptic NMDAR expression (Crump *et al.,* 2001). Additionally, the phosphorylation of the scaffolding proteins themselves by Ca^{2+}/calmodulin-dependent protein kinase II (CaMKII; Gardoni et al., 2006) and cyclin-dependent kinase 5 (CdK5) not only affects NMDAR synaptic stability, but also the binding affinity of SFKs (Kalia *et al.* 2006).

Protein interactions and posttranslational modifications regulating NMDAR PM localization

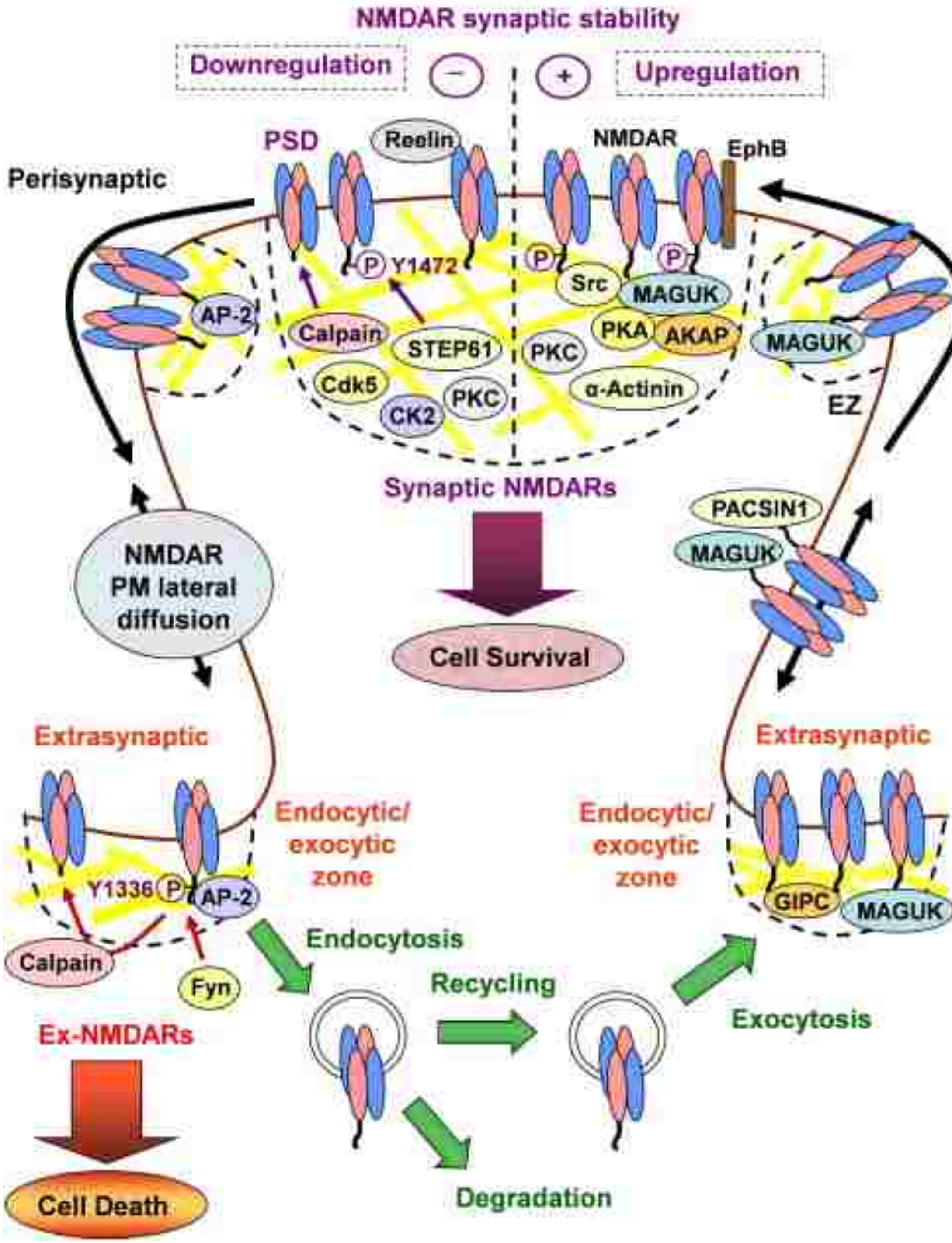

Diagram 4. The NMDAR location hypothesis and plasma membrane trafficking. Synaptic or extrasynaptic-NMDAR localization is linked to activation of cell survival or apoptotic signaling cascades, respectively. NMDAR stability in the PSD (purple arrows) is upregulated (right side of PSD in figure) and downregulated (left side of PSD in figure) by alterations in the surrounding actin cytoskeleton (yellow bars) and NMDAR interactions with scaffolding, anchoring and effector proteins, calpain cleavage of NMDARs or associated proteins and posttranslational modifications such as phosphorylation. STEP dephosphorylates the GluN2B Y1472 residue, allowing the adaptor protein AP-2 to bind, followed by lateral diffusion to endocytic zones (EZs) at perisynaptic and extrasynaptic sites (black arrows). Scaffolding proteins (membrane associated guanylate kinases (MAGUKs)) such as PSD-95 and SAP 102 are associated with both synaptic and extrasynaptic-NMDARs and may remain associated whilst receptors laterally diffuse along the plasma membrane (PM). Specific proteins such as GIPC, alterations in protein phosphorylation and enhanced calpain activity may also modulate extrasynaptic-NMDAR expression (red arrows). Fyn-mediated phosphorylation of the NR2B Y1336 residue is likely to promote extrasynaptic-NMDAR calpain cleavage, but cleaved receptors remain stable at the cell surface. Exocytosis and endocytosis occurs at extrasynaptic exocytic/endocytic zones and following the latter, receptors are targeted to either degradation or recycling pathways (green arrows). (From Gladding and Raymond, 2011).

In addition to protein-protein interactions and phosphorylation events, NMDAR localization and function is affected by palmitoylation, ubiqutination, and proteolytic cleavage (Gladding and Raymond, 2011). Palmitoylation of NMDARs is an important reversible posttranslational modification that enhances PSD-95 targeting and synaptic clustering (Christopherson *et al*. 2003). Additionally, altered palmitoylation of regulatory proteins such as SFKs affect their membrane targeting, ultimately effecting NMDAR phosphorylation state and its function and synaptic expression (Smotrys and Liner, 2004). Monoubiquitination of NMDARs regulates protein trafficking on the plasma membrane, while polyubiquitination of NMDARs targets the receptor for degradation via the proteasomal pathway (Glickman and Ciechanover, 2002). Also, the cleavage of the NMDAR subunits C-terminal region by the Ca^{2+} activated protease calpain diminishes PSD-95 scaffolding, thereby promoting extrasynaptic migration while ultimately not affecting the ion channel function of Ca^{2+} influx (Guttman *et al.,* 2001).

Taken together, NMDAR expression, function, and localization is a complex yet tightly regulated process involving differential subunit composition, expression patterns, synaptic localization, the formation of downstream signaling complexes via interactions with scaffolding proteins, as well as posttranslational modifications such as phosphorylation, palmitolyation, and ubiquitination.

NMDARs in Ischemia/Reperfusion

While calcium influx from NMDARs receptors is critical for normal synaptic function, the uncontrolled overstimulation of these receptors also plays a central role in a number of neurodegenerative pathologies (Arudine and Tymianski, 2003). Early microdialysis studies demonstrated a significant rise in extracellular glutamate concentrations in response to ischemia in the striatum, hippocampus, cortex, and thalamus. Interestingly, only the hippocampus was significantly damaged by a mild global ischemic event (Globus *et al*., 1990). More specifically, CA1 pyramidal neurons of the hippocampus are the most vulnerable subpopulation of the brain in response to ischemic insults (Mitani *et al.,* 1998). NMDAR receptors mediate cellular damage in response to these elevated glutamate concentrations. Both competitive and non-competitive NMDAR antagonism reduces neuronal injury following ischemia, albeit at varying efficacy depending on stroke modalities, drug administration patterns, and neuroanatomical locations (Lau and Tymianski, 2010). However, while NMDAR-mediated excitotoxicity has long been established as a primary factor in mediating neuronal death following ischemia, selective compounds involved in NMDAR antagonism are not clinically feasible in humans due to their lack of efficacy, harmful side effects, and relatively short therapeutic window (Gladstone *et al.,* 2002). Nonetheless, significant research in the past decade has been devoted to further understanding the mechanisms mediating NMDAR-induced cell death following ischemia with the hope of leading to novel NMDAR-based therapeutics.

Further complicating full elucidation of NMDA function, particularly in ischemia, is the fact that NMDARs often modulate opposing functions, particularly neuronal survival and death. In recent years however, two hypotheses have been put forward to unify these contrasting ideas: the location hypothesis and the subtype hypothesis (Lai *et al.,* 2011). The location hypothesis revolves around ideas of differential function depending on extrasynaptic or synaptic NMDAR localization. As discussed previously, preferential activation of synaptic NMDARs following ischemia has been reported to be involved in pro-survival pathways due to the downstream activation of CREB. In contrast, selective activation of extrasynaptic NMDARs has been reported to mediate pro-death effects by diminishing CREB signaling (Hardingham *et al.,* 2002). Contrary to these findings however, it has also been demonstrated that the synapse-specific protein PSD-95 is required for NMDAR-mediated excitotoxic neuronal death (Aarts *et al.,* 2002), and synaptic NMDAR activation is important in ischemic-induced neuronal death (Lai *et al*., 2011).

Another hypothesis for differential NMDAR mediated neuronal death following ischemia is based on differential subtype activation. Because of distinct protein-protein interactions and differential signaling complexes, NR2B may mediate cellular death through either direct or indirect protein-protein interactions with pro-death signals (Martin and Wang, 2010). In support of this theory, selective antagonists for NR2A and NR2B demonstrated that NR2A subunits mediate pro-survival and NR2B subunits mediate neuronal death following stroke (Liu *et al.,* 2007). However, such a broad characterization is not without conflicting reports, as it has also been reported that NR2A subunits can contribute to neuronal death (von Engelhardt *et al.,* 2007) and that NR2B subunits can mediate neuronal survival (Martel *et al.,* 2009). Additionally, questions have risen about the selectivity of the subtype-specific NR2A and NR2B antagonists (Lai *et* *al.,* 2011), as well as the role of heterotrimeric NMDARs containing both NR2A and NR2B subunits (Traynelis *et al.,* 2010). Taken together, it appears that neither subtype-specific downstream signals nor subtype-specific localization clearly mediate specific NMDAR functional outputs alone, but rather the combination of the location, subunit composition, temporal and spatial distributions, protein-protein interactions, and other posttranslational modifications are responsible for the NMDAR mediated excitotoxic-induced neuronal death during stroke.

One of the better-studied posttranslational modifications of NMDARs known to affect receptor function following ischemia is receptor phosphorylation. More specifically, numerous studies have been conducted on the role of tyrosine phosphorylation of NMDA receptor subunits following ischemia. Functionally, NMDAR tyrosine phosphorylation results in the potentiation of NMDAR currents (Yu *et. al.* 1997), thereby facilitating calcium entry and exacerbating calcium cytotoxicity. While there have been no identified tyrosine phosphorylation sites on NR1 subunits, three tyrosine phosphorylation sites have been identified on both NR2A subunits (Y1292, Y1325, and Y1387) and NR2B subunits (Y1252, Y1336, Y1472) (Chen and Roche, 2007). One of the key molecular kinases shown to affect NMDAR tyrosine phosphorylation and NMDAR function following stroke has been SFKs (particularly Src, and Fyn), which are up-regulated in activity following ischemia (Jian *et al.,* 2008). Pharmacologic inhibition of SFKs provides neuroprotection following ischemia by preventing NR2A tyrosine phosphorylation (Hou *et al.,* 2007). Furthermore, suppression of PSD-95 expression levels, which have been shown to be important in SFK-mediated tyrosine phosphorylation of NR2A subunits, also attenuated NR2A tyrosine phosphorylation levels and diminished neuronal death following ischemia (Hou *et al.,* 2003). Additionally, mGluR1 antagonism following ischemia diminishes SFK activation and prevents NR2A tyrosine phosphorylation, ultimately attenuating infarct size (Murotomi *et al.,* 2008). The NMDAR NR2B subunit has also been reported to increase in SFK-mediated tyrosine phosphorylation status following ischemia, leading to both an enhanced extrasynaptic migration and potentiated calcium current (Jian *et al.,* 2008).

While tyrosine phosphorylation of NMDAR subunits has perhaps been the most thoroughly studied phosphorylation events following ischemia, serine/threonine phosphorylation is also involved in NMDAR-induced pathogenesis. Numerous serine phosphorylation sites exist on NR1 subunits, with S890 and S896 being identified as targets for PKC phosphorylation, negatively affecting NR1 synaptic clustering (Chen and Roche, 2007). Phosphorylation of S897 has been identified as a PKA mediated phosphorylation event, shown to be involved in intracellular NMDAR trafficking (Chen and Roche, 2007). Ischemia induces PKC gamma (PKCγ) mediated phosphorylation of NR1 at S890, which when prevented by mGluR5 antagonism, reduced S890 phosphorylation and cell death in the hippocampal CA1 region (Takagi *et al.,* 2010). NR2A subunits also have multiple serine phosphorylation sites, with PKC-mediated phosphorylation of NR2A on S1219 and S1312 being involved in the potentiation of NMDA currents (Grant *et al.,* 2001). Additionally, Cdk5 mediated serine phosphorylation of S1232 on NR2A subunits increases following ischemia, and when blocked with a Cdk5 inhibitor, blunts NMDA-evoked currents and attenuated neuronal death in CA1 hippocampal neurons (Li *et al.,* 2001). NMDAR NR2B subunits are also serine phosphorylated, at PKC sites S1303 and S1323, events involved in the potentiation of

NR1/NR2B receptor currents (Chen and Roche, 2007). Also, CKII-mediated serine phosphorylation at S1480 regulates the PDZ binding of NMDARs to PSD-95, ultimately affecting surface expression (Chen and Roche, 2007). However, the importance of these sites in ischemic pathology has yet to be investigated.

The dysregulation of NMDAR function, expression, and signaling following ischemia is a complex process involving many factors, including but not limited to subunit composition, subunit localization, receptor trafficking, protein-protein interactions, phosphorylation events, and kinase/phosphatase activity. The breakdown or dysfunction of any or all of these points of regulation involved in the proper fine-tuning of NMDAR function contribute to the ischemic-induced NMDAR-mediated neuronal death observed in stroke pathology.

AMPA Receptor Structure and Function

A crucial mechanism in governing synaptic transmission lies in the regulation of the glutamatergic 2-amino-3-(3-hydroxy-5-methylisoazol-4-yl)propionic acid receptor (AMPARs). AMPARs arise from four genes (GLUR1-4) that encode four subunits, which combine in varying stoichiometries to form the primary excitatory ligand-gated ion channel in the brain (Shepherd and Huganir, 2007). Structurally, AMPARs exist as a "dimer of dimers," primarily composed of GluR1 and GluR2 hetero-tetramers (especially in the forebrain including the hippocampus), with low levels of GluR3 and GluR4, although subunit expression combinations are varied depending on neuroanatomical location (Passafaro *et al.,* 2001). Each subunit subtype structurally shares a large extracellular N-terminal region and a true transmembrane domain, followed by a re-entrant loop which does not traverse the membrane but rather dips into it from the cytosolic side, thereby creating a pore-forming domain (Bennett and Dingledine, 1995). The re-entrant loop is then followed by a second true transmembrane domain, an extracellular loop, a third transmembrane domain and a cytosolic C-terminal tail of varying length (Bennett and Dingledine, 1995). Each subunit contains an extracellular domain on the first and second true transmembrane domain that form the binding site for the neurotransmitter glutamate, termed the S1-S2 site (Borges and Dingledine, 1998). Additionally, each of the four AMPAR subunits occur in two alternatively spliced versions of the extracellular ligand-binding domain, termed "flip" and "flop", with splicing being regulated both developmentally ("flip" splice forms expressed in early postnatal mammalian life, followed by "flop" isoforms later in development) and regionally, ultimately effecting kinetic properties of the channel, as the "flop" version undergoes desensitization much more rapidly in response to glutamate stimulation than the “flip” version (Shepherd and Huganir, 2007).

However, while all AMPAR subunits share a large degree of homology, the presence or absence of a GluR2 subunit contained within the functional AMPAR tetramer is most important in determining channel properties and ionic permeability as a consequence of its amino acid makeup. Almost all GluR2 protein contains a positively charged arginine (R) residue within the channel pore region of the re-entrant membrane loop substituted from a neutral glutamine (Q) residue, thereby rendering GluR2-containing AMPARs impermeable to divalent cation (Ca^{2+} and Zn^{2+}) conductance, in addition to making the receptor insensitive to blockade by intracellular polyamines (Traynelis *et al*., 2010). The Q/R substitution is a result of hydrolytic RNA editing of a single adenosine base to inosine though the activity of the adenosine deaminase enzyme ADAR2 (Bass, 2002). The Q/R editing site is located within subunit interfaces as well, and is thought to affect receptor assembly in the endoplasmic reticulum (ER) by favoring heterodimerization with GluR1 over homodimerization with another GluR2 subunit (Mansour *et al.,* 2001). After ER exit and trafficking to the plasma membrane, the positive charge of the arginine in the pore region of the GluR2-containing AMPAR prevents divalent cation entry, exclusively promotes monovalent cation (Na^{+}) conductance, and repulses intracellular blockade by similarly charged polyamines at positive voltages (Koike *et al.,* 1997).

A.

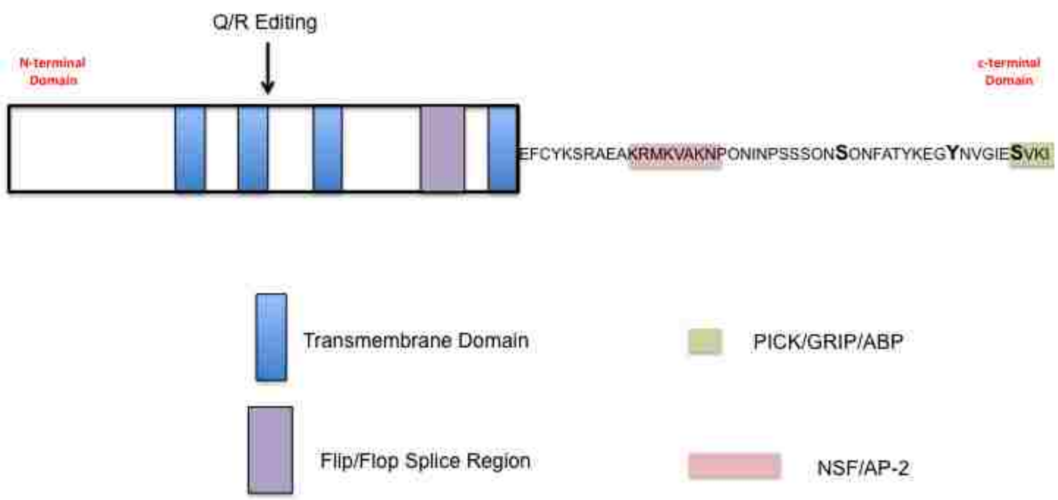

Sites reported to be phosphorylated *in vivo* are displayed in **bold**

B.

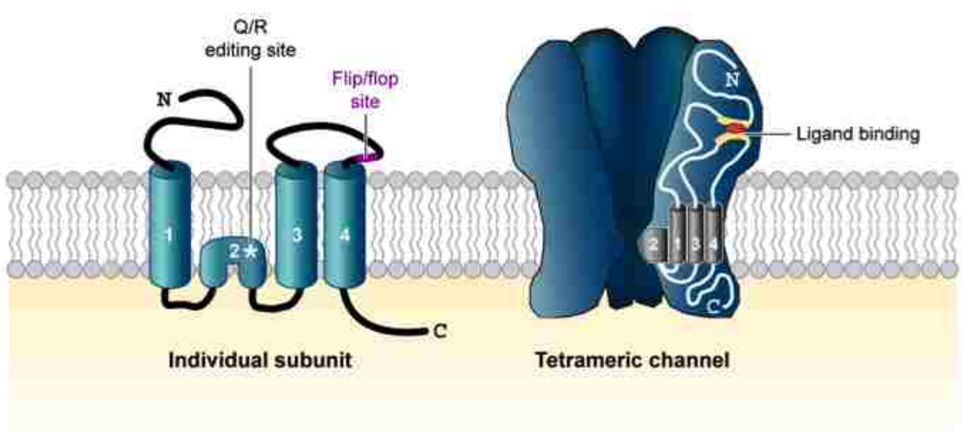

Diagram 5. GluR2 subunit domain structure, schematic subunit structure, and general structure of AMPAR complex. (A) GluR2 subunit domain structure with c-terminus sequence detailed for the GluR2-short splice isoform which is the predominant form in the brain. Transmembrane domains are depicted in blue, the flip/flop alternatively spliced region is illustrated in purple, and editing, phosphorylation, and protein interaction sites are as indicated. **(B)** Schematic Diagram of an AMPAR Subunit. All subunits have a similar structure and topology. Three of the four hydrophobic segments span the membrane, while one dips into the membrane from the cytoplasmic face and contributes to the channel pore. The alternatively spliced flip/flop region and the c-terminal PDZ binding domain are shown, as well as the GluR2-specific Q/R editing. Schematic of predicted 3D structure of the tetrameric AMPAR complex. (Diagram **(A)** was adapted from Isaac *et al.*, 2007). (Diagram **(B)** from Shepherd and Huganir, 2007).

However, neuronal inputs in both physiology and pathology modify the permeability of AMPARs to include conductance of divalent cations via GluR2 surface removal and expression changes, which is governed by highly complex processes including endocytosis/exocytosis, phosphorylation events, protein-protein interactions, and changes to mRNA editing as well as *de novo* synthesis of GluR2.

The surface removal of AMPARs occurs via the classically studied route of endocytosis through the action of clathrin-coated pits and dynamin (Shepherd and Huganir, 2007). The disruption of clathrin-dependent endocytosis through the expression of a dominant-negative form of dynamin, high concentrations of sucrose, or preventing the interaction of GluR2 with the clathrin adaptor protein AP-2 all inhibit AMPAR endocytosis (Carroll *et al*., 1999; *Man et al*. 2000; Lee *et al.,* 2003). Specific endocytic zones separate from the post-synaptic density on the lateral margins of excitatory synapse are believed to be the site for glutamate receptor internalization (Racz *et al.,* 2004). Once internalized, AMPARs are trafficked via the activity of Rab GTPases, and are sorted within early endosomes to recycling endosomes for reinsertion to the surface, or are sent to late endosome and ultimately to the lysosome for degradation (Ehlers, 2000).

Rab GTPases and AMPAR Trafficking

The Rab GTPase protein family makes up the largest branch of the Ras GTPase superfamily, with the existence of over 60 Rab genes in the human genome (Stenmark and Olkkonen, 2001). Similar to other GTPases involved in regulation, Rab proteins alternate between two differing conformations: an “inactive” GDP-bound state, and an “active” GTP-bound state, as the active GTP-bound conformation of Rab proteins enables them to interact with its downstream effectors (Stenmark and Olkkonen, 2001). The conformation state of Rab proteins is regulated by guanine nucleotide exchange factors (GEFs) and GTPase-activating proteins (GAPs; Novick *et al.,* 2006). GEF activity activates Rab proteins by triggering the binding of GTP, while GAP activity inactivates the Rab protein by accelerating the hydrolysis of bound GTP to GDP (Novick *et al.,* 2006).

The state of membrane attachment for Rab proteins is also regulated by undergoing changes between membrane insertion and extraction (Novick *et al.* 2006). This control is achieved through the actions of Rab escort protein (REP) and GDP dissociation inhibitor (GDI; Stenmark and Olkkonen, 2001). After inactivation through GAP activity, REP and GDI can extract GDP-bound Rab proteins from the membrane and recycle the Rab proteins back to the cytosol for further activity after GEF re-activation (Novick *et al.,* 2006). In clathrin-mediated endocytosis, which includes the endocytosis of AMPARs,

activated Rab5 is responsible for the cytoskeletal motility and homotypic fusion with the early endosome, and is also required for early endosomal fusion (Levey *et al.,* 2000). In contrast to Rab5 activity, Rab15 exhibits an inhibitory action to Rab5 by preventing early endocytic events (Wandinger-Ness *et al.,* 2000 and 2003). After fusion with the early endosome, the endocytosed cargo can be shuttled to three different pathways, regulated by two Rab proteins. Cargo destined towards recycling is directed to Rab4 containing micro-domains in the early endosome (Sonnichsen et al. 2000). From this domain, the cargo can travel directly back to the membrane to permit fast recycling. The cargo can also travel along a slower-recycling pathway, being transported to the perinuclear recycling endosome (Wandinger-Ness *et al,* 2003, Zerial *et al.* 2000). From the recycling endosome, Rab11 directs the transport back to the membrane. While it remains unclear weather Rab4 controls recycling along both pathways, it is clear that co-ordination between Rab5 and Rab4 is responsible for maintaining influx into and efflux out of the early endosome (Wandinger-Ness *et al.* 2000). The third pathway involved in transport from the early endosome does not lead to recycling, but rather degradation. Rab7 mediates the delivery of cargo to the late endosome, from which further Rab7 association is involved with lysosomal transport (Lefkowitz *et al.,* 2006). From the late endosome, cargo can be re-directed from the lysosome and transported to the trans Golgi network via Rab9 (Wandinger-Ness *et al.,* 2003). AMPARs have been demonstrated to co-localize with Rab5, Rab4, Rab7, and Rab11 throughout the course of endocytic trafficking towards the lysosome or recycling to the plasma membrane (Ehlers, 2000).

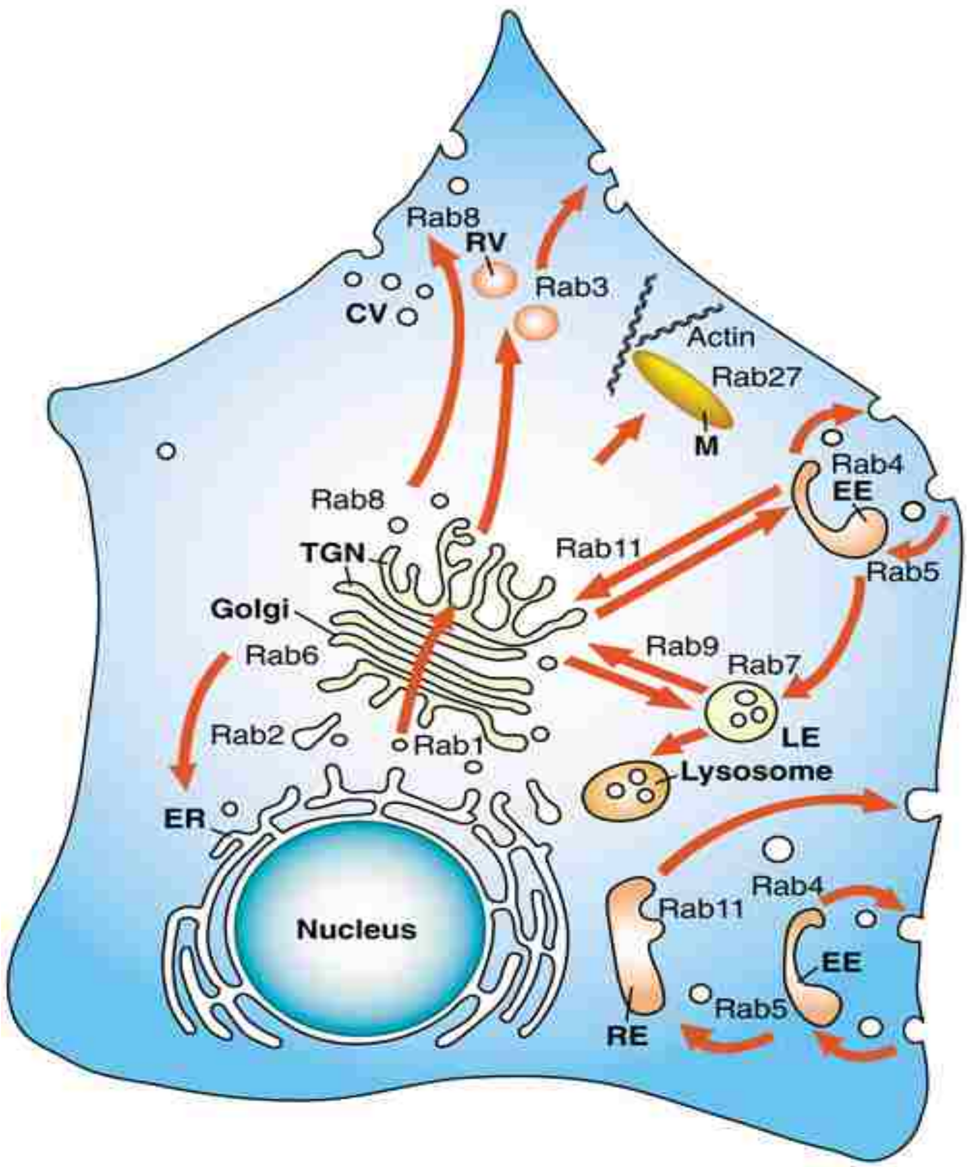
Rab8
RV
Rab3
CV
Actin
Rab27
M
Rab4
EE
Rab5
Rab8
TGN
Rab11
Golgi
Rab6
Rab9
Rab7
Rab2
Rab1
LE
Lysosome
ER
Rab4
Rab11
Nucleus
EE
Rab5
RE

Diagram 6. Schematic illustration of the Rab-regulated endocytotic and exocytotic pathways. The biosynthetic pathway transports proteins from the endoplasmic reticulum (ER) through the Golgi complex to the cell surface. In the *trans*-Golgi network (TGN), molecules can enter either constitutive secretory vesicles (CV) or regulated secretory granules/vesicles (RV). Surface proteins internalized from outside the cell reaches the early endosomes (EE) first and can be recycled back to the surface, either directly or via a perinuclear recycling endosome (RE) compartment, or transported to late endosomes (LE) and lysosomes. The biosynthetic and endocytic circuits (arrows) exchange material at the level of the Golgi apparatus and the endosomal elements. The localization of selected mammalian Rab proteins in the membrane compartments participating in these transport processes is indicated. (Stenmark and Olkkonen, 2001).

Opposing the activity of surface removal of AMPARs is the exocytosis and plasma membrane insertion of AMPARs. While the exact localized site of AMPAR insertion remains controversial, with reports of receptor insertion into the somatic plasma membrane and lateral diffusion to the synapse (Adesnik *et al.,* 2005) and other reports of insertion of AMPARs into the dendritic PSD directly via cytoskeleton-associated motors (Gerges *et al.,* 2006). It is clear however that AMPAR insertion is accomplished through SNARE-dependent exocytosis (Lu *et al.,* 2001). However, differential trafficking rates occur depending on subunit composition. Surface insertion of GluR1 has been demonstrated to occur slowly under basal conditions and rapidly speed up upon increased neuronal activity and NMDAR activation (Hayashi *et al*., 2001). GluR2 insertion however occurs constitutively without the need for increased synaptic activity (Passafaro *et al.,* 2001). Interestingly, when GluR1/GluR2 heteromers are expressed, the activity-dependent trafficking of GluR1 dominates, but when GluR2/GluR3 heteromers are expressed, the constitutive trafficking pattern of GluR2 dominates (Shepherd and Huganir, 2007). The differential trafficking mechanisms are dependent on the C-terminal tail interactions, as the C-terminus of GluR2 has been demonstrated to bind N-ethylmaleimide-sensitive fusion protein (NSF; Nishimune *et al.,* 1998), which regulates exocytosis of GluR2 at synaptic sites, either by its classical role in membrane fusion, or by dissociating the GluR2-protein-interacting with kinase C alpha 1 (PICK1) complex, an association known to prevent AMPAR recycling (Hanley *et al.,* 2002).

Synaptic strength is dictated almost entirely on the density of AMPARs that accumulate at dendritic synapses (Borges and Dingledine, 1998). During LTP, AMPARs are rapidly inserted at the plasma membrane to strengthen the connectivity of the synapse, and conversely, are removed from the membrane and either sent to recycling/sorting pools or trafficked over towards degradation during LTD (Shepherd and Huganir, 2007). It is the delicate balance between the processes of AMPAR plasma membrane insertion or removal, in combination with other receptor inputs (NMDARs, mGluRs, and others) that compose the most accepted models as the molecular correlate for the cellular mechanism of learning and memory. Activity of mitogen-activated protein kinase (MAPK) family is involved in the fine tuning of Rab-regulated AMPAR trafficking, surface removal, and plasma membrane insertion. Studies have demonstrated that p38 MAPK activity is responsible for accelerating AMPAR endocytosis and promoting LTD by enhancing Rab5 activity (Cavalli *et al.,* 2001; Huang *et al.,* 2004; Zhong *et al*., 2008). Further studies have linked p38 MAPK activation with a decreased AMPAR surface expression, while inactivation of p38 MAPK was shown to increase AMPAR surface clusters under physiological conditions (Zhu *et al.,* 2002; Rumbaugh *et al.,* 2006). Opposing the activity of p38 MAPK in AMPAR trafficking is extracellular signal-regulated kinase 1/2 (ERK1/2), which under LTP conditions is responsible for the exocytosis and surface insertion of AMPARs, thereby strengthening the synapse (Patterson *et al*., 2010).

AMPAR Phosphorylation and Protein-Protein Interactions

Phosphorylation events on AMPAR subunits govern many of the protein-protein interactions involved in AMPAR stabilization at the synapse. Each phosphorylation event either promotes an increased or decreased association with various proteins demonstrated to be involved in receptor anchoring, endocytosis, recycling, and exocytosis.

Dephosphorylation of GluR1 on serine 845, a PKA site, and serine 831, a CaMKII site is important in AMPAR surface removal. Mutations in these sites prevent AMPAR internalization induced by NMDAR activation (Lee *et al.,* 2003). However, the exact mechanisms of how these de-phosphorylation events regulated AMPAR surface removal have yet to be fully resolved.

Phosphorylation of GluR2 at serine 880 (Ser880) has been shown to be PKCα dependent (Xia *et al.,* 2000) and is important in the internalization of AMPARs, ultimately resulting in a decrease in surface GluR2-containing receptors in hippocampal neurons (Chung *et al.,* 2000). Three proteins, glutamate receptor interacting protein 1 (GRIP1), AMPA receptor binding protein (ABP also known as GRIP2) and PICK1 all interact with GluR2 at the extreme C-terminal PDZ site (Dong *et al*., 1997; Srivastava *et al.,* 1998) where the Ser800 residue resides. Phosphorylation of GluR2 at Ser800 disrupts the GluR2-GRIP interaction, an interaction that is important in anchoring AMPARs to the PSD (Matsuda *et al.,* 2000), thereby promoting the binding of PICK1 (Chung *et al.,* 2000), which decreases surface GluR2 levels via increased endocytosis and delayed recycling (Terashima *et al.,* 2004; Lu and Ziff 2005; Terashima *et al.,* 2008). However, other reports have indicated through the use of PICK1 knock-out mice that PICK1 is not required for NMDA induced GluR2 internalization in hippocampal neurons, but is involved in affecting GluR2 membrane expression, as demonstrated by the accelerated GluR2 recycling that occurs in the same knock-out mice (Lin and Huganir, 2007). The precise mechanisms though which PICK1 accomplishes decreased GluR2 surface expression remains unresolved, with reports indicating a role in promoting internalization, preventing recycling, or a combination of both. However, the notion that PICK1 is intimately involved in effecting GluR2 surface expression is agreed upon in the published literature.

The interaction of GluR2 with PICK1 is preceded by activation of PKC alpha (PKCα), which upon calcium-induced activation, undergoes a comformational change that exposes a PDZ site for binding with the PDZ domain of PICK1 (Perez *et al.,* 2001). Phosphorylation of GluR2 Ser880 is dependent on the trafficking of PKC alpha to the plasma membrane via PICK1, which interacts with a Bin-Amphiphysin-Rvs (BAR) domain on GRIP1, thereby bringing the complex in close proximity to the c-terminal tail of GluR2 (Lu and Ziff, 2005). After Ser880 phosphorylation of GluR2, the GluR2-GRIP interaction is disrupted, the GluR2-PICK1 interaction is favored, and the surface removal of GluR2 occurs, a process that is thought to be an important mechanism in which neurons increase their basal excitability through increasing their calcium permeability via GluR2-lacking AMPARs.

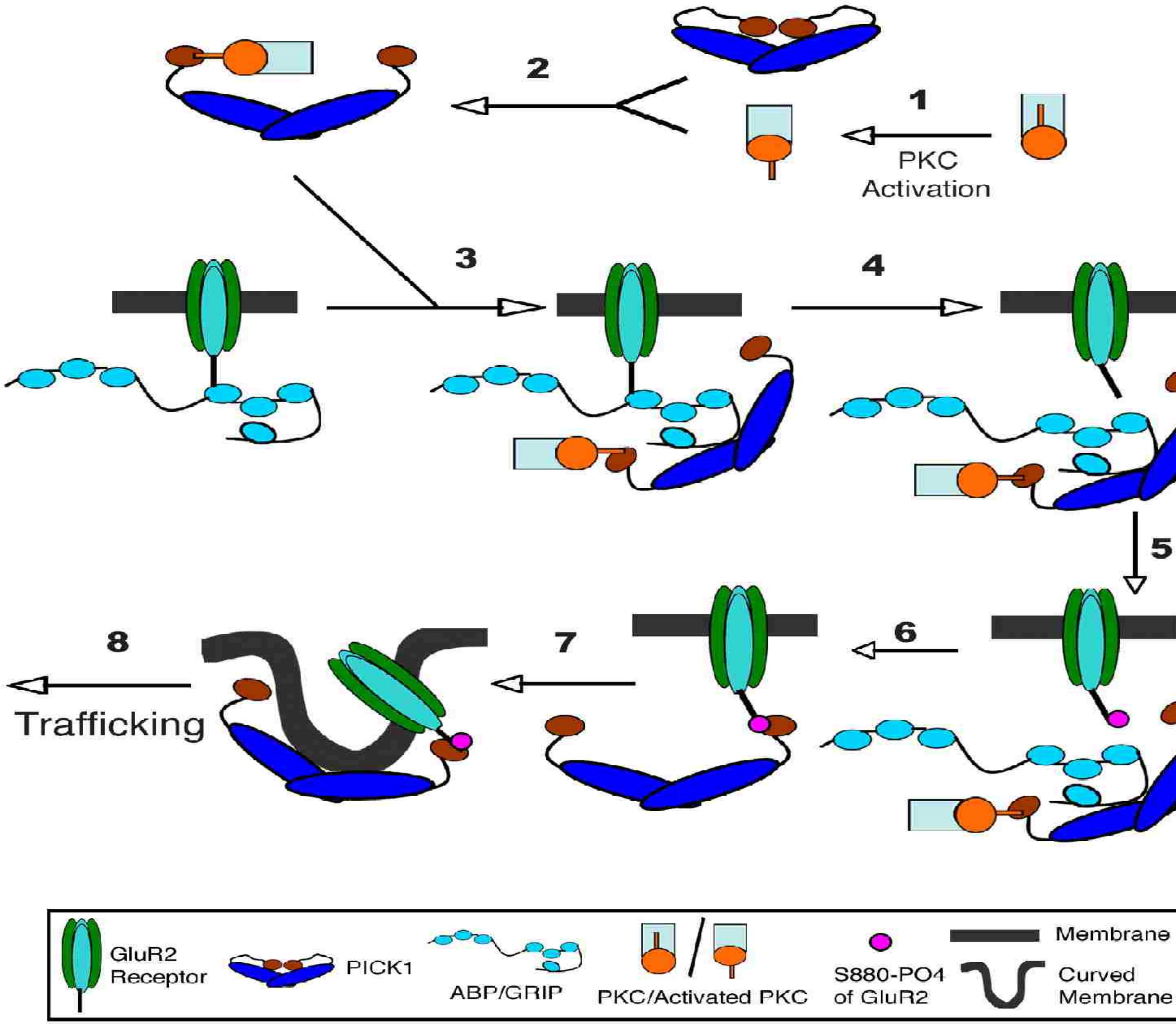

1
PKC
Activation
2
3
4
5
6
7
8
Trafficking
GluR2
Receptor
PICK1
ABP/GRIP
PKC/Activated PKC
S880-PO4
of GluR2
Membrane
Curved
Membrane

Diagram 7. Model for the Role of the PICK1-ABP/GRIP Interaction in AMPAR Trafficking. GluR2 receptors are anchored at synaptic and intracellular membranes by ABP/GRIP but undergo cycling between these membranes in association with PICK1. Trafficking of GluR2 receptors from ABP/GRIP anchorage requires the PICK1-ABP/GRIP interaction. Activation of PKCα (1) causes PKCα to bind to the PICK1 PDZ domain, which disrupts the PICK1 PDZ-BAR domain interaction and leads to the exposure of the PICK1 BAR domain (2). The PICK1-PKCα complex is targeted to the ABP/GRIP-GluR2 complex through the interaction of the exposed BAR domain with the Br sequence of ABP/GRIP (3). PICK1 competes with ABP/GRIP for the GluR2 interaction (4). PKCα phosphorylates Ser880 of GluR2. GluR2 phosphorylated at Ser880 cannot bind back to ABP/GRIP (5) but is able to bind to PICK1 (6). The PICK1 BAR domain directs the PICK1-GluR2 complex to curved membranes (7), where GluR2 receptors bud from the plasma membrane and internalize or bud from an internal membrane prior to reinsertion into synapses (8). (From Lu and Ziff, 2005).

Tyrosine phosphorylation of GluR2 is also important in mediating AMPAR internalization. Tyrosine phosphorylation at residue 876 (Tyr876) disrupts the interaction of GluR2 with GRIP and ABP, although phosphorylation at Tyr876 did not influence the interaction with PICK1 (Hayashi and Huganir, 2004). The phosphorylation was dependent on the activity of SFKs, but not other protein tyrosine kinases such as Fak and Pyk2, which is consistent with other findings that shown the importance of SFK regulation in excitatory synaptic transmission (Soderling and Derkach, 2000).

While surface expression levels of AMPARs are an important mechanism effecting changes in AMPAR function, transcriptional modifications also influence AMPAR function. Total GluR2 protein levels can also be altered by the action of repressor element-1 silencing transcription factor (REST), a transcriptional repressor that diminishes *de novo* synthesis of GluR2 via the binding with the GluR2 promoter site (Gorter *et al.,* 1997). GluR2 Q/R mRNA editing, the site important for rendering GluR2-containing AMPARs calcium impermeable, can also be inhibited by diminished CREB signaling, which is responsible for ADAR2 expression, thereby leading to the expression of calcium permeable AMPARs, thereby strengthening synaptic signaling (Peng *et al*., 2006).

Taken together, the mechanisms of AMPAR synaptic delivery and removal is a process governed by much complexity, with many inputs including subunit composition, phosphorylation events, protein-protein interactions, and transcriptional alterations, which are all involved in the mechanism that form the foundation of basal neuronal function and synaptic plasticity.

AMPA Receptors in Ischemia/Reperfusion

Initial reports of ischemia-induced glutamate-dependent excitotoxicity suggested that NMDARs were primarily responsible for mediating the majority of calcium overload observed following stroke. However, more recently, it has been shown that the over-activation of calcium-permeable AMPARs, when expressed, result in similar levels of intracellular calcium as NMDAR activation (Lu *et al.,* 1997). While the vast majority of AMPARs in the CNS exhibit low permeability to Ca^{2+} and Zn^{2+} due to the presence of the edited form of the GluR2 subunit, and short-lived changes in the expression of GluR2-lacking AMPARs have been reported to be an important mediator of neuronal signaling in the induction of LTP (Terashima *et al.,* 2008). However, long-lasting switches in AMPAR subunit composition to GluR2-lacking AMPARs have been implicated in a number of neurological pathologies. These include drug abuse (Conrad *et al.,* 2007), epilepsy (Rakhade et al., 2008), Alzheimer's disease (AD; Shepherd and Hugnair, 2007), amyotrophic lateral sclerosis (ALS; Kwak and Weiss, 2006), and stroke (Noh *et al*., 2005).

Following transient global ischemia induced in hippocampal pyramidal neurons, an increased number of calcium-permeable AMPAR channels in the CA1 region results, correlating with an increased vulnerability to neuronal death (Anzai *et al.,* 2003). Furthermore, increasing GluR2 protein levels (Liu *et al.,* 2004) or pharmacologic blockade of calcium-permeable AMPARs (Noh *et al.,* 2005) afforded neuroprotection following ischemia. Additionally, blockade of calcium permeable AMPARs resulted in decreased Zn^{2+} accumulation following ischemia (Yin *et al.,* 2002), which also afforded neuroprotection, and along with other studies involving chelators (Calderone *et al.,* 2004), suggest a role for ischemic-induced Zn^{2+} toxicity through the action of GluR2-lacking AMPARs.

Many of the mechanisms involved in physiologic LTD-induced GluR2 surface occur with ischemia/reperfusion. PKC mediated Ser880 phosphorylation of GluR2 (Liu *et al.,* 2006) has been implicated following ischemia, resulting in decreased surface GluR2 levels. Furthermore, ischemia promotes GluR2 dissociation from GRIP1, PICK1 association with ABP (Liu *et al*., 2006), and GluR2 association with PICK1, a potentially necessary step involved in GluR2 endocytosis (Dixon *et al*., 2009). Additionally, peptides that interfere with PICK1 PDZ domain interactions block the ischemia-induced GluR2 subunit composition switch, ultimately resulting in neuroprotection (Dixon *et al.,* 2009). To date, no studies have investigated the role of Tyr876 phosphorylation in mediating GluR2 surface removal following ischemia, although SFKs, which mediates GluR2 Tyr876 phosphorylation (Hayashi and Huganir, 2004), have been well documented to increase in activity in post-ischemic neurons (Hou *et al.,* 2007; Jian *et al.,* 2008). Interestingly, GluR1 protein levels are not affected by ischemia, thereby, the selective degradation of GluR2 ultimately promotes a rise in the number of Ca^{2+}/Zn^{2+}-conducting AMPARs (Soundarapandian *et al.,* 2005).

In addition to the surface membrane loss of GluR2-containing AMPARs, translational and transcriptional dysregulation also contributes to the decreased number of GluR2-containing AMPARs. Following ischemia, particularly in the vulnerable CA1 hippocampal region, GluR2 mRNA is markedly and selectively reduced (Pelligrini-Giampietro *et al.,* 1997). More specifically, the transcriptional repressor REST mediates cell death in post-ischemic neurons by suppressing GluR2 protein transcription, and genetic knockdown of REST rescues GluR2 levels and provides neuroprotection (Calderone *et al.,* 2004). Additionally, ADAR2, the nuclear enzyme responsible for GluR2 pre-mRNA Q/R editing, is selectively reduced following ischemia (Peng *et al.,* 2006). Furthermore, exogenous ADAR2 gene delivery or expression of a constitutively active CREB, which induces ADAR2 expression, was also shown to restore GluR2 Q/R editing and protect neurons from ischemic-induced cellular death (Peng *et al.,* 2006). Interestingly, direct delivery of the Q/R site edited GluR2 gene rescued ADAR2 degradation (Peng *et al.*, 2006), thereby linking the loss of GluR2 with the selective loss of ADAR2.

In summary, alterations at multiple levels, including receptor trafficking and transcriptional/translational regulation all contribute to the ischemic-induced loss of GluR2-containing Ca^{2+}/Zn^{2+} impermeable AMPARs, thereby resulting in the surface expression of AMPARs that are important in mediating excitotoxic ischemic-induced neuronal death.

SPECIFIC AIMS

- **Aim 1:** To test the hypothesis that generation of superoxide from NADPH oxidase following oxygen-glucose deprivation/reperfusion underlies the signaling mechanism responsible for the increase in NMDAR NR2A subunit tyrosine phosphorylation.

    - *Sub-Aim 1.1* To determine if NADPH oxidase mediates the tyrosine phosphorylation of NMDAR subunits following oxygen-glucose deprivation/reperfusion.

    - *Sub-Aim 1.2* To determine if NADPH oxidase inhibition dampens the excitotoxic effect of NMDA stimulation following oxygen-glucose deprivation/reperfusion.

- **Aim 2:** To test the hypothesis that increased NADPH oxidase activity following oxygen-glucose deprivation/reperfusion is responsible for the acceleration of endocytosis of AMPAR subunits.

    - *Sub-Aim 2.1* To determine if inhibition of NADPH oxidase prevents the decrease in surface GluR2-containing AMPARs following exposure to oxygen-glucose deprivation/reperfusion.

    - *Sub-Aim 2.2* To determine if oxygen-glucose deprivation results in an increased p38 MAPK activity and is mediated by NADPH oxidase activity

    - *Sub-Aim 2.3* To determine if NADPH oxidase activity mediates p38 MAPK activation following oxygen-glucose deprivation/reperfusion results in the formation of the Rab5-GDI complex.

- **Aim 3:** To test the hypothesis that the oxygen-glucose deprivation/reperfusion-induced increase in NADPH oxidase activity is involved in the sustained serine phosphorylation of the GluR2 AMPAR subunit.

    - *Sub-Aim 3.1* To determine if inhibition of NADPH oxidase prevents the OGD/R-induced increase in Ser880 phosphorylation of the GluR2 subunit.

    - *Sub-Aim 3.2* To determine if NADPH oxidase prevents the OGD/R-induced dissociation of GRIP1 and the increased association with PICK1.

CHAPTER 1

Inhibition of NADPH Oxidase Prevents the Oxygen-Glucose Deprivation/Reperfusion Induced Increase in Tyrosine Phosphorylation of the NMDA Receptor NR2A subunit.

Abstract

Evidence exists that oxidative stress promotes the tyrosine phosphorylation of NMDA receptor (NMDAR) subunits during reperfusion of post-ischemic brain tissue. We have now identified the reactive oxygen species (ROS) generator in cultured retinoic acid differentiated SH-SY5Y neuroblastoma cells that mediates the increase in tyrosine phosphorylation of the NR2A subunit in response to oxygen-glucose deprivation and reperfusion (OGD/R). Inhibition of the ROS generator, NADPH oxidase, attenuated the increased tyrosine phosphorylation of the NR2A subunit, as well as the interaction of activated Src Family Kinases (SFKs) with PSD-95 induced by OGD/R. In contrast, inhibition of ROS production from mitochondrial or xanthine oxidase sources failed to dampen the OGD/R-induced increase in tyrosine phosphorylation of the NR2A subunit. In addition to attenuating tyrosine phosphorylation of the NR2A subunit, inhibition of NADPH oxidase also markedly reduced cellular death in SH-SY5Y cells stimulated by NMDA following OGD. These data suggest that NADPH oxidase has a key role in facilitating NR2A tyrosine phosphorylation via SFK activation during post-ischemic reperfusion.

Materials and Methods

Materials

Ethidium homodimer was bought from Molecular Probes (Eugene, OR, USA). HALT protease inhibitor cocktail was bought from Pierce (Rockford, IL, USA). All other chemicals used in the study were purchased from Sigma (St. Louis, MO, USA).

Methods

Cell Culture and differentiation

Human SH-SY5Y neuroblastoma cells were used throughout the study. SH-SY5Y cells were cultured in Dulbecco's Modified Eagle's Medium: Ham's Nutrient Mixture F-12, 1:1 (D-MEM/F-12) purchased from ATCC (Manassas, VA, USA) supplemented with 10% fetal bovine serum (Gibco, Grand Island, NY, USA) and Penicillin (100 µg/mL) / Streptomycin (100 U/mL). For immunoprecipation and lysate preparation, SH-SY5Y cells were seeded onto 10 cm dishes at a density of approximately 4×10^6 cells per dish. Approximately 24 hours later, cells were differentiated by treatment with complete D-MEM/F-12 supplemented with 10 µM retinoic acid for 6 days and fresh media containing retinoic acid was changed every 48 hours (Nitti *et al.*, 2007).

Oxygen-Glucose Deprivation/Reperfusion

Anoxia was achieved by incubating the cultures in a controlled humidified hypoxic glove box (Coy Laboratories, Grass Lake, MI, USA) for 40 minutes at 37°C. The gas mixture in the incubator was 0% O_2, 5% CO_2, and 95% N_2. Anoxia was verified using an oxygen meter with an O_2 microelectrode (OM-4; Microelectrodes Inc., Bedford, MA, USA). Glucose free DMEM without serum was placed in the hypoxic glove box overnight at 0% O_2 at 37°C to de-oxygenate the media. Prior to oxygen-glucose deprivation/reperfusion (OGD/R), cells were serum starved for 4 hours. Cells were then rinsed 3 times with phosphate buffered saline (PBS) prior to placement in the hypoxic glove box at 37°C. The de-oxygenated glucose and serum free media was then added to the dishes in the glove box and the cultures were incubated for 40 minutes. Following OGD, the anoxic glucose free media was removed and cultures were returned to a normoxic (ambient air O_2 levels; 18-21% O_2) tissue culture incubator with serum free media containing glucose (± drug treatment) for the various incubation periods as described per individual experiments.

Detection of Reactive Oxygen Species Generation

Dihydroethidium (DHE) experiments were modified and adapted from the method described by Abramov *et al.* (2007). Briefly, SH-SY5Y cells were plated at 1 x 10^5 onto nitric acid washed glass coverslips in 35 mm dishes. Approximately 24 hours after seeding, cells were differentiated as previously described. OGD/R experiments were performed with 5 µM DHE present in the media throughout the entire experiment and no pre-loading period was performed. Following treatment, cells were washed 3 times with cold PBS (4ºC, pH 7.4) and fixed with cold 4% paraformaldehyde/PBS (4ºC, pH 7.4). Cells were visualized using an Olympus 1X71 inverted microscope equipped with a 60X oil immersion objective. Images were obtained with Olympus Image Manager. For the nitrobluetetrazolium (NBT) assay, methods were adapted from Aukrust *et al.* (1994). Briefly, 5 x 10^4 cells were plated onto 12-wells plates and differentiated with retinoic acid as described above. After 4 hours of serum starvation, media containing 0.1% (w/v) NBT was added to each well and incubated for 1 hour. After loading, excess NBT was washed away 3 times with warmed PBS (37ºC, pH 7.4) and the OGD/R treatments were performed along with time-matched normoxic controls. Following treatments, cells were fixed with absolute methanol (-20ºC) and washed twice with room temperature 70% methanol. Plates were allowed to air dry before dissolving the formazan deposits by the addition of 2 M KOH and 100% DMSO to each well. The absorbance was then measured at 630 nm with a Spectra Max Gemini M2 plate reader (Molecular Devices, Sunnyvale, CA, USA).

Immunoprecipitation of NR2A and PSD-95

SH-SY5Y cells were plated onto 10 cm tissue culture dishes at a density of 4 x 10^6 cells per dish as previously described. Approximately 24 hours later, cultures were differentiated with retinoic acid as previously described. Prior to treatment, the cultures were serum starved for 4 hours. Immediately following treatment, two 10 cm dishes of cells were washed twice with cold PBS (4ºC, pH 7.4), and were pooled to ensure adequate protein yield after harvesting in HEPES lysis buffer (50 mM HEPES, pH 7.5, 0.5% NP-40, 250 mM NaCl, 2 mM EDTA, 10% Glycerol, 1 mM sodium orthovanadate, 1 mM sodium fluoride, 1 μg/mL benzamidine, 2 μl/mL Halt Protease Inhibitor Cocktail Kit). Cells were briefly sonicated for a 5 second burst at 25% power output with a VirTis Ultrasonic Cell Disrupter 100 (Gardiner, NY, USA). Cell lysates were spun at 1,000 x *g* to remove nuclei and cell debris. Protein concentration was determined using a bicinchoninic acid assay (BCA), and lysates (500 μg/sample) were then pre-cleared using Protein-A/G 50/50 mix of agarose beads for 1 hour at 4°C followed by incubation with primary antibody overnight (affinity-purified rabbit-polyclonal NR2A, Sigma, St. Louis, MO, USA or an affinity-purified rabbit-monoclonal PSD-95, Cell Signal, Beverley, MA, USA) at 4°C. The immunocomplex was then incubated for 4 hours with 50 μL Protein-

A/G beads at 4°C with rotation before being washed 3 times with 500 μL of HEPES lysis buffer. Samples were eluted from the agarose beads by treatment with Laemmli buffer and heat (100°C) and then subjected to 7.5% sodium dodecyl sulfate polyacrylamide gel electrophoresis (SDS-PAGE). After transfer to nitrocellulose membranes (Bio-Rad, Berkeley, CA, USA), blots were blocked for 1 hour at room temperature with 5% BSA in Tris Buffered Saline, 0.1% Tween 20 (TBS-T) and incubated with an affinity-purifed phospho-tyrosine (1:2000, Sigma, St. Louis, MO, USA) or phospho-Src Family Kinase (Tyr416) (1:1000, Cell Signaling Technology, Beverly, MA, USA). Immunoreactive bands were then visualized and captured with a Fuji imaging system using enhanced chemiluminescence after adding HRP conjugated secondary antibodies (1:2000) of Goat anti-Mouse-HRP or Mouse anti-Rabbit-HRP (IgG Light chain specific) both purchased from Jackson ImmunoResearch (West Grove, PA, USA). Bands were analyzed using Image-Gauge software.

Immunoblotting

Samples for direct immunoblotting were subjected to 7.5% SDS-PAGE, transferred to nitrocellulose membranes and blocked with 5% BSA/TBS-T as previously described. Blots were incubated with primary antibody overnight at 4°C at the concentration indicated. The affinity purified NR2A rabbit polyclonal antibody (1:2000) was purchased from Sigma (St. Louis, MO, USA). The affinity purified rabbit-polyclonal p67*phox* antibody (1:1000) was purchased from Millipore (Billerica, MA, USA). The affinity purified rabbit-monoclonal Src Family Kinase (1:1000) antibody was purchased for Cell Signaling Technology (Beverly, MA, USA). The affinity-purified mouse-monoclonal ß-actin (1:5000) antibody was purchased from CalBiochem/EMD

(Darmstadt, Germany). Goat anti-Mouse-HRP and Goat-anti-Rabbit-HRP secondary antibodies (1:2000) were purchased from Jackson ImmunoResearch (West Grove, PA, USA). Immunoreactive bands were visualized and captured with a Fuji imaging system using enhanced chemiluminescence after adding HRP conjugated secondary antibodies. Bands were analyzed using Image-Gauge software.

Quantification of cell death

Cell viability was determined using an ethidium homodimer exclusion test as described by Jackson *et al.* (2006). Briefly, approximately 5 x 10^4 cells were plated onto 12 well plates and 24 hours later cells were differentiated with retinoic acid as previously indicated. Prior to treatments, cells were serum starved for 4 hours. Following OGD, cultures were incubated in serum free D-MEM/F-12 containing 5 mM N-methyl-D-aspartic acid (NMDA). After 6 hours, cultured media was replaced with 300 μL of warm PBS (37ºC, pH 7.4) and background fluorescence was determined (*Fmin*). Cultures were then provided with 6 μM ethidium homodimer and incubated for 30 minutes at 37°C after which fluorescence was measured (*F*). Wells were then incubated with 0.03% saponin for 60 minutes at 37°C at which time a final measurement of fluorescence was taken (*Fmax*). Fluorescence data was collected using a Spectra Max Gemini M2 plate reader (Molecular Devices, Sunnyvale, CA, USA) at excitation/emission wavelengths of 530/620 with a cutoff of 610 nm. The percentage of dead cells was calculated using the following formula for each well:

$$\%\ cell\ death = [(F-Fmin)/(Fmax-Fmin)] \times 100$$

Introduction

N-methyl *D*-aspartate receptor (NMDAR) activation is one of the many important steps necessary to elicit long-term potentiation (LTP). This is accomplished by NMDARs not only through calcium entry, but also through the initiation of several downstream effectors, notably the production of superoxide. NMDAR activation has been shown to lead to the activation NADPH oxidase, resulting in superoxide production (Brennan *et. al.* 2009). The generation of superoxide anions in the central nervous system (CNS) plays an intriguing dual role, delicately balancing normal function and the potential to cause cellular damage. Under normal physiologic conditions, superoxide has been shown to be necessary for LTP in the hippocampus (Klann *et al.* 1998). Recent studies have demonstrated that upon activation of NMDARs, a resulting superoxide burst arises from NADPH oxidase (Brennan *et al.*, 2009, Girouard *et al.,* 2009), which when blocked with pharmacological inhibition of NADPH oxidase prevents LTP in the hippocampus (Kishida *et al.,* 2006). Spatial localization of NADPH oxidase subunits revealed immunohistochemical staining of a membrane bound subunit of NADPH oxidase, gp91^{phox}, as well as the cytosolic components of NADPH oxidase, p67^{phox} and p47^{phox}*,* in the soma and dendrites of mouse hippocampal slices (Tejada-Simon *et al.,* 2005). This localization is consistent with previous studies that have demonstrated a similar spatial expression of NMDARs (Spruston *et al.,* 1995). Since superoxide is short lived due to its highly reactive properties, its generation needs to be in close proximity to its protein targets to serve as a possible signaling molecule. Given the proximity of NADPH oxidase to the synapse, the localized production of superoxide can serve as a signaling molecule to affect NMDAR function.

However, while ROS may be necessary for the processes of LTP, its un-controlled overproduction leads the cell into a state of oxidative stress. Abramov *et al.* (2007) demonstrated that superoxide anions are generated in a tri-phasic manner in neurons following 40 minutes oxygen-glucose deprivation/reperfusion (OGD/R). The three superoxide bursts were identified sequentially originating from mitochondrial, xanthine oxidase, and NADPH oxidase through pharmacological inhibition as well as knock out studies, with the tertiary superoxide burst from NADPH oxidase occurring during reperfusion. Since NADPH oxidase reduces molecular oxygen to superoxide, the lack of available oxygen during OGD limits the reaction. However, upon re-introduction of oxygen, a rapid and sustained burst of superoxide from NADPH oxidase occurs. Furthermore, this superoxide burst is involved in the processes of cellular death, as pharmacological inhibition of NADPH oxidase during ischemia/reperfusion (I/R) with the NADPH oxidase inhibitor apocynin is highly neuroprotective (Wang *et al.,* 2006).

NMDARs play a key role in the mechanisms of excitotoxic neuronal death following I/R. The massive increase in extracellular glutamate known to occur during I/R injury leads to an over-stimulation of NMDARs, a key factor in neuronal death accomplished via intercellular calcium overload and increased ROS production. In addition to excessive glutamate stimulation, NMDARs also undergo phosphorylation mediated conformational changes following I/R that potentiates the effect of glutamate NMDAR stimulation. In particular, a rapid and sustained increase in tyrosine phosphorylation of the NMDAR NR2A subunit has been reported following I/R (Takagi *et al.,* 1997, Pei *et al.* 2000, Liu *et al.,* 2001, Jiang *et al*., 2008, Murotomi *et. al.,* 2008). Increased tyrosine phosphorylation of the NR2A subunit functionally potentiates

NMDAR currents by increasing the likelihood of the receptor being in an open conformation, and decreases the probability of the receptor being in an inactive state (Yu *et. al.*, 1997).

In recent years, evidence has documented the role of Src Family Kinases (SFKs) in upregulating the activity of NMDARs (Kalia *et. al.,* 2004) via tyrosine phosphorylation of residues located on the C-terminus of NR2 subunits (Chen *et. al*., 1996). Through inhibition of SFK activity, phosphorylation of NR2 subunits is prevented and the elicitation of LTP is blocked (Kalia *et. al.,* 2004). While this process is important for synaptic plasticity, an enhancement of the effect of glutamate during an excitotoxic event only exacerbates the damage. The SFKs have been implicated in modulating NMDAR function following I/R (Jian X *et al.,* 2008). Direct inhibition of SFKs with PP2 was shown to provide neuroprotection following ischemic insult (Hou *et al.,* 2007, Jian *et al.,* 2008). Additionally, the interaction of SFKs with postsynaptic density protein 95 (PSD-95), a scaffolding protein that concentrates NMDARs at the post-synaptic density, is an important mechanism underlying I/R-induced increases in the tyrosine phosphorylation of NR2A and NR2B subunits. Suppression of PSD-95 expression diminishes tyrosine phosphorylation of both subunits following I/R (Hou *et. al.,* 2003). Furthermore, inhibiting Src interaction with PSD-95 prevents the I/R-induced increase in tyrosine phosphorylation of the NMDAR NR2A subunit (Hou *et. al.,* 2003). Taken together, the process of SFKs interacting with PSD-95 facilitates the tyrosine phosphorylation of NMDAR NR2 subunits, thereby enhancing calcium entry through the receptor.

While SFKs become active following I/R (Hou *et al.,* 2007; Jian *et al.,* 2008), the upstream signals leading to its activation remain largely unresolved. SFKs have been reported to be redox sensitive in nature (Li *et al.,* 2008, Giannoni *et. al.,* 2010), although the ROS source responsible for its redox-induced activation during I/R remains unknown. In this study, we sought to determine whether superoxide production from NADPH oxidase was involved in the activation of SFKs associated with PSD-95, thereby mediating the tyrosine phosphorylation of the NMDAR NR2A subunit.

Results

Increased NADPH oxidase activity following oxygen glucose deprivation in retinoic acid differentiated SH-SY5Y cells

To examine whether SH-SY5Y cells served as an appropriate cell model to study the effects of NADPH oxidase activity on NMDAR NR2A subunits following OGD/R, we examined the expression of NADPH oxidase cytosolic subunit p67*phox* in retinoic differentiated and non-retinoic acid differentiated SH-SY5Y cells. Consistent with previous findings (Nitti *et. al.*, 2007), protein expression of the NADPH oxidase cellular component $p67^{phox}$ in retinoic acid differentiated SH-SY5Y increased 4-fold as compared to non-differentiated SH-SY5Y cells (data not shown). Therefore, differentiated SH-SY5Y cells were used throughout this study to examine whether NADPH oxidase was involved in the OGD/R-induced increase in tyrosine phosphorylation of the NR2A subunit. To determine whether activation of NADPH oxidase activity occurred during OGD incubation or during the subsequent reperfusion, as previously reported in cortical neuronal cells (Abramov *et al.*, 2007), we subjected 6-day retinoic acid differentiated SH-SY5Y neuroblastoma cells to 40-minutes of OGD followed by reperfusion of cultures for various incubation times in the presence of dihydroethidium (DHE). There was no observable increase in superoxide generation in cultures subjected to 40-minutes of OGD alone (Fig. 1A). Reperfusion of OGD cultures, however, did lead to superoxide generation that was maximal between 15- and 30-minutes (Fig. 1A and 1B). Treatment of cultures with the NADPH oxidase inhibitor DPI (100 nM) during reperfusion drastically decreased DHE fluorescence, suggesting that NADPH oxidase may be responsible for superoxide production during reperfusion of OGD subjected cultures. Treatment of cultures with 1μM phorbol 12-myristate 13-acetate (PMA) for 15 minutes, a known positive control for NADPH oxidase activity, yielded a strong fluorescent signal. As anticipated based upon Western blot results showing a low level of p67*phox*, an increase in ROS production during reperfusion following 40 minutes of OGD in non-differentiated SH-SY5Y cells was not observed (data not shown). We also observed an increase in the reduced product of nitroblue tetrazolium chloride (NBT) in differentiated SH-SY5Y cultures subjected to OGD/R (Fig. 1B), which was similar to the time course to ROS production observed with DHE. Treatment of OGD cultures with DPI during reperfusion blunted NBT reduction (Fig. 1B), suggesting that NADPH oxidase activation underlies the ROS production during reperfusion of OGD cultures.

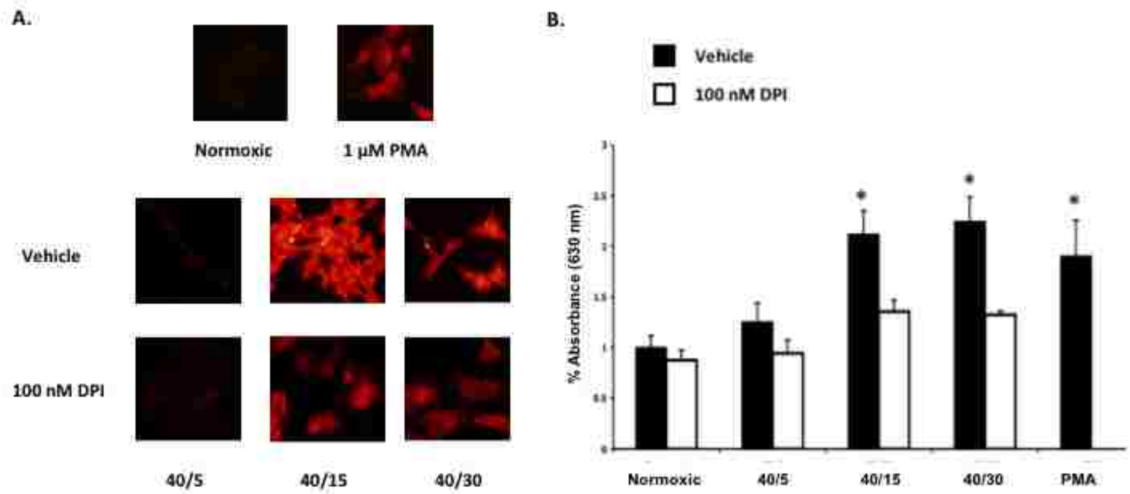

Figure 1. Increased ROS generation during reperfusion of OGD treated cultures of retinoic acid differentiated SH-SY5Y involves NADPH oxidase activity.

Representative fluorescent images from three independent experiments of reactive oxygen species production following OGD (A) with vehicle (1:1000 DMSO) or DPI (100 nM) detected using dihydroethidium (DHE). Spectrophotometric quantification of reactive oxygen species following OGD (B) with vehicle (1:1000 DMSO) or DPI (100 nM) utilizing nitrobluetetrazolium chloride (NBT). Data represent mean ± S.E.M from three separate experiments that consisted of at least 6 determinents (askteriks * indicates a $p < 0.05$ from vehicle treated normoxic control; ANOVA with *post hoc* Bonferroni test). Phorbol 12-myristate 13-acetate (PMA; 1µM for 15 minutes) was used as a positive control for NADPH oxidase activity in both the DHE and NBT assays.

OGD/Reperfusion-induced Increased tyrosine phosphorylation of NMDAR NR2A subunit

Previous studies have demonstrated that there is a rapid and sustained increase in tyrosine phosphorylation of the NMDAR NR2A subunit during post-ischemic reperfusion (Takagi *et al*., 1997). Therefore, experiments were performed to examine whether OGD or subsequent reperfusion of OGD subjected cultures would lead to an increase in tyrosine phosphorylation of the NMDAR NR2A subunit. In non-differentiated SH-SY5Y cells subjected to OGD/R, there was no observable increase in tyrosine phosphorylation of the NR2A subunit as compared to time-matched normoxic control (data not shown). In contrast, we found a significant increase in tyrosine phosphorylation of the NR2A subunit at 30-minutes of reperfusion in differentiated SH-SY5Y cells subjected to OGD incubation (Fig. 2A and 2B). This increase in tyrosine phosphorylation coincided with the time course in which we observed maximal ROS generation (Fig. 1). Collectively, these results indicate that NMDAR NR2A subunit undergoes an increase in tyrosine phosphorylation during reperfusion of OGD subjected differentiated SH-SY5Y cells. This increase in tyrosine phosphorylation of the NR2A subunit coincided with increased ROS production.

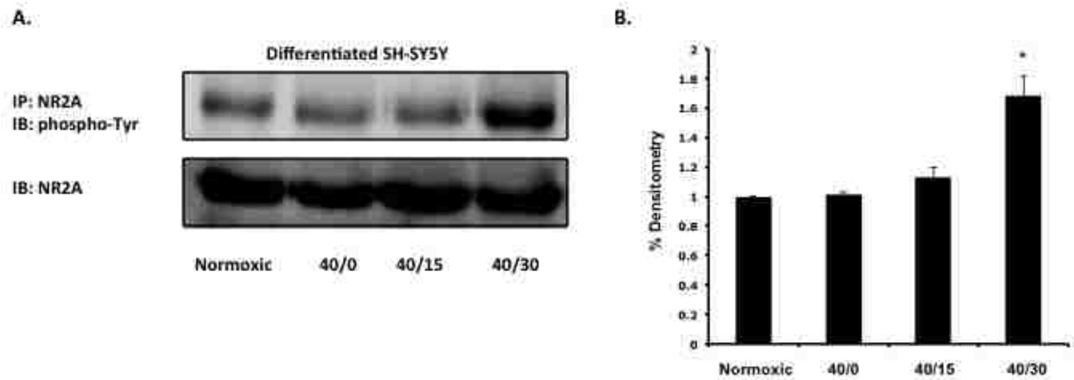

Figure 2. OGD/R promotes the increase in tyrosine phosphorylation of the NMDAR NR2A subunit in differentiated SH-SY5Y cells. Immunoprecipitation and immunoblotting of lysates prepared from differentiated SH-SY5Y cells exposed to OGD/R reveals a significant increase in tyrosine phosphorylation of the NR2A subunit. (A) Western blot shown is representative of three independent experiments. (B) Quantification of the relative densitometry of the phospho-Tyr-NR2A immunoreactive band. Data represent mean ± S.E.M from three separate experiments. (askteriks * indicates a p <0.01 from normoxic control; ANOVA with *post hoc* Bonferroni test).

Inhibition of NADPH oxidase attenuates OGD/Reperfusion-induced increase in NR2A tyrosine phosphorylation

To examine whether mitochondrial, xanthine oxidase, or NADPH oxidase is the ROS generator that mediates the oxidative stress signaling cascade responsible for the increase in tyrosine phosphorylation of the NR2A subunit in differentiated SH-SY5Y cells, cultures were treated during reperfusion with 0.5 μM of the mitochondrial depolarization uncoupler carbonyl cyanide 4-(trifluoromethoxy)phenylhydrazone (FCCP), the xanthine oxidase inhibitor oxypurinol (1 μM), or the NADPH oxidase inhibitor DPI (100 nM). Treatment of cultures with FCCP or oxypurinol failed to prevent increase in tyrosine phosphorylation of the NR2A subunit during 30-minutes of reperfusion of OGD treated SH-SY5Y cultures (Fig. 3B). However, inhibition of NADPH oxidase activity with DPI prevented the increase in tyrosine phosphorylation of the NR2A subunit at 30 minutes of reperfusion following OGD. There were no changes in total protein levels of NR2A in cultures treated with DPI, oxypurinol, or FCCP. These results indicate that NADPH oxidase underlies the oxidative stress-signaling cascade responsible for the OGD/R-induced increase in NR2A tyrosine phosphorylation.

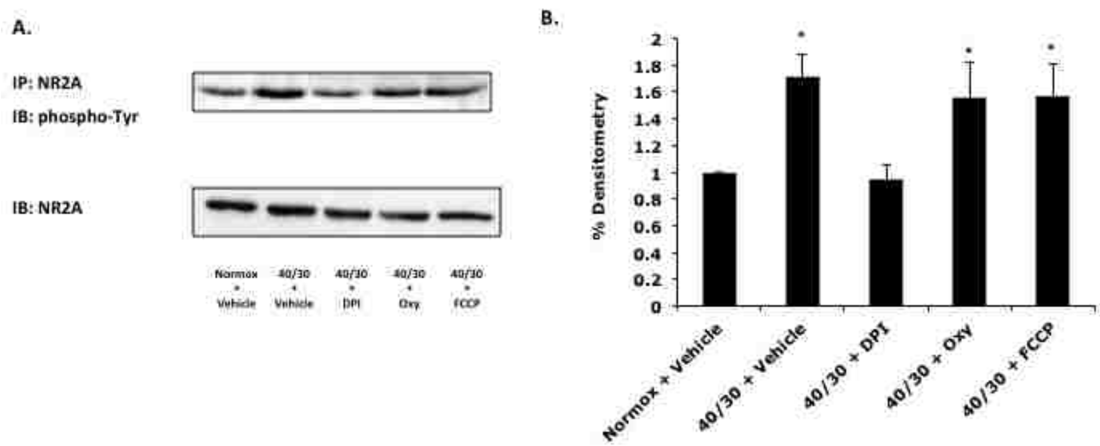

Figure 3. Inhibition of NADPH Oxidase activity blocks the OGD/R-induced increase in tyrosine phosphorylation of the NMDAR NR2A. Inhibition of superoxide generation from xanthine oxidase with oxypurinol (1 μM) and mitochondria with FCCP (0.5 μM) failed to prevent the OGD/R-induced increase in tyrosine phosphorylation of the NMDAR NR2A subunit. However, inhibition of NADPH Oxidase with DPI (100 nM) was found to block the increase in tyrosine phosphorylation of the NR2A subunit. Representative Western blot (A) of three independent experiments of phospho-Tyr-NR2A with vehicle (1:1000 DMSO), DPI, oxypurinol, and FCCP. (B) Quantification of the density of the phospho-Tyr-NR2A band. Data represent mean ± S.E.M from three separate experiments. (askteriks * indicates a p <0.05 from normoxic control; ANOVA with *post hoc* Bonferroni test).

OGD/Reperfusion-induced association between Src-family kinase and PSD-95 is prevented with inhibition of NADPH oxidase activity

SFKs have been shown to mediate increases in tyrosine phosphorylation of NMDAR subunits after transient cerebral ischemia (Takagi *et al*., 1997; Pei *et al*., 2000; Liu *et al*., 2001; Hou *et al.,* 2007; Jiang *et al.,* 2008). To determine whether SFKs were involved in mediating OGD/R-induced increase in tyrosine phosphorylation of the NR2A subunit in differentiated SH-SY5Y cells, cultures were treated with the potent SFK inhibitor PP2. Administration of PP2 (1 μM) immediately following OGD blunted the increase in tyrosine phosphorylation of the NR2A subunit (Fig. 4B). In a previous study, it was reported that suppression of PSD-95 expression reduced the increase in tyrosine phosphorylation of the NR2A subunit after transient brain ischemia in the hippocampus (Hou *et. al.* 2003). Therefore, to determine whether activation of NADPH oxidase facilitated the interaction of activated SFKs associating with the scaffolding postsynaptic density protein 95 (PSD-95), we performed an immunoprecipitation of PSD-95 combined with immunoblotting for activated SFKs. We found that the active form of SFKs (phospho-Tyr416) associated with PSD-95 during reperfusion of OGD cultures (Fig. 5A), as early as 5 minutes of reperfusion and sustained for at least 30 minutes of reperfusion. Inhibition of NADPH oxidase significantly reduced the association of activated SFKs with PSD-95 during reperfusion of OGD cultures (Fig. 5C). These results indicate that the OGD/R-induced activation of NADPH oxidase facilitates the interaction of activated SFKs with PSD-95 thereby facilitating the tyrosine phosphorylation of the NR2A subunit.

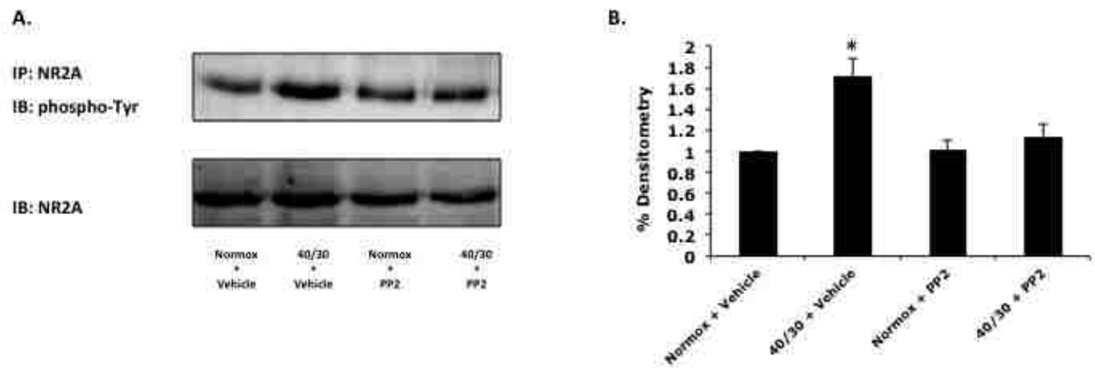

Figure 4. The OGD/R-induced increase in tyrosine phosphorylation of the NMDAR NR2A subunit is attenuated by treatment with the Src Inhibitor PP2. Inhibition of Src Family Kinase activity with the selective inhibitor PP2 rescued the increase in tyrosine phosphorylation of the NMDAR NR2A subunit. (A) Representative Western blot from 3 independent experiments illustrates the dampened tyrosine phosphorylation of NR2A with direct inhibition of Src Family Kinases during reperfusion following OGD with PP2 (1 μM). (B) Quantification of the density of the phospho-Tyr-NR2A band. Data represent mean ± S.E.M from three separate experiments. (askteriks * indicates a $p < 0.05$ from normoxic control; ANOVA with *post hoc* Bonferroni test).

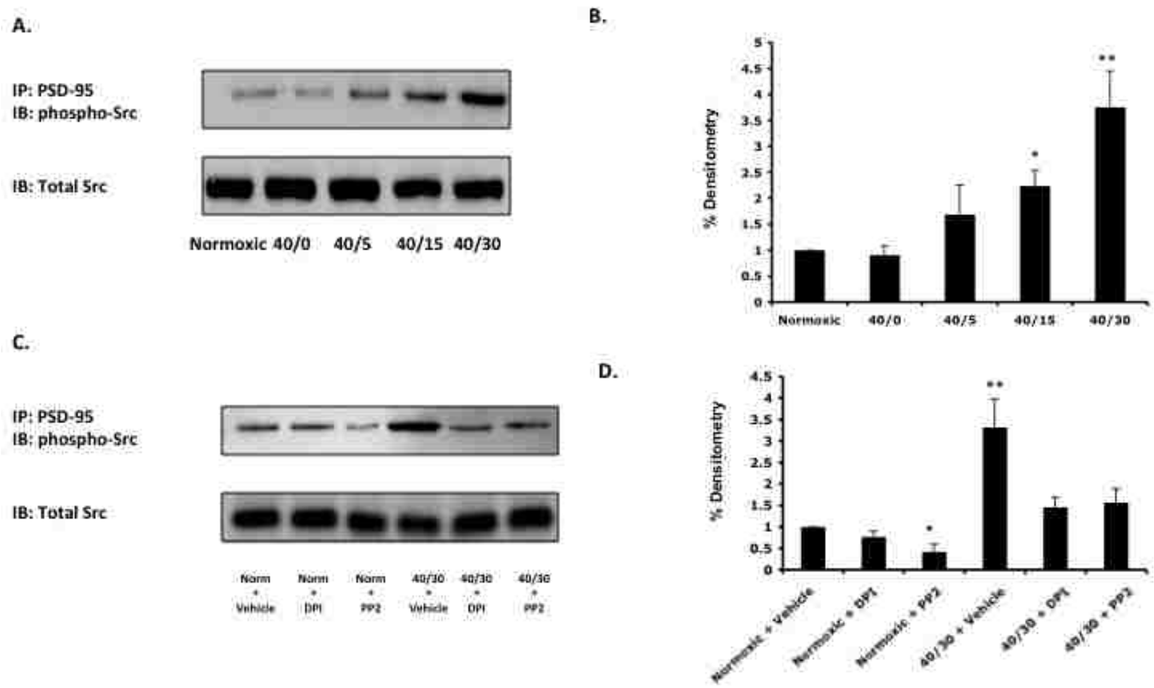

Figure 5. OGD/R promotes the interaction between activated Src Family Kinases and PSD-95, which is reduced with NADPH oxidase inhibition differentiated SH-SY5Y cells. (A) Immunoprecipitation of PSD-95 and immunoblotting with phospho-SFK(Tyr416) shows the increase in the active form (phospho-Tyr416) of SFKs bound to PSD-95 with treatment of OGD/R compared to normoxic controls (Norm). Western blot is representative of three independent experiments. (B) Quantification of the density of the phospho-SFK(Tyr416) band after PSD-95 immunoprecipitation. (C) Representative western blot from Immunopreciptation of PSD-95 from three independent experiments illustrates the dampening of activated SFKs bound to PSD-95 with DPI (100nM) or PP2 (1 μM) treatment during reperfusion following 40 minutes of OGD. (D) Quantification of the density of the phospho-SFK(Tyr416) band after PSD-95 immunoprecipitation. For both (B) and (D), data represent mean ± S.E.M from three separate experiments. (askteriks * indicates a p <0.05 from normoxic control; ** indicates a p <0.001; ANOVA with *post hoc* Bonferroni test).

Inhibition of NADPH oxidase following OGD/R dampens the exacerbated effect of NMDA induced cellular death.

One of the functional consequences of NMDAR NR2A tyrosine phosphorylation is a potentiation of NMDAR currents (Yu et. al. 1997). Through an increased permeability to calcium, the effect of glutamate stimulation of NMDARs is amplified, thereby exacerbating calcium overload and subsequent cellular death. Previous studies have demonstrated a marked decrease in cellular viability of SH-SY5Y cells when exposed to NMDA stimulation (0.25-5 mM, Corasanitl *et al.,* 2007). To determine if the OGD/R-induced activation of NADPH oxidase contributed to NMDAR mediated cellular death, we used an ethidium homodimer exclusion assay as a marker for cellular viability. We found that following 40 minutes of OGD, treatment of differentiated SH-SY5Y cells with NMDA (5 mM) elicited an increased susceptibility to cellular death after 6 hours as compared to normoxic NMDA stimulated controls (Fig. 6). However, inhibiting NADPH oxidase during the 6 hours of NMDA treatment with DPI (100 nM) following the 40 minutes of OGD, significantly reduced susceptibility to NMDA mediated cellular death. These results indicate that the NMDAR mediated cell death in post-ischemic differentiated SH-SY5Y cells involves NADPH oxidase.

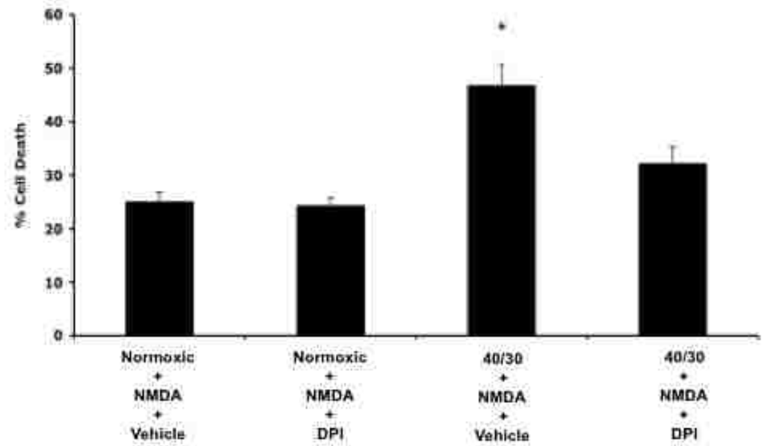

Figure 6. Inhibition of NADPH Oxidase activity decreases NMDA-mediated cell death following exposure to OGD. Differentiated SH-SY5Y cells exhibit an increased susceptibility to cell death after 6 hours of NMDA (5 mM) stimulation following 40 minutes of OGD as assessed by the ethidium homodimer exclusion assay. This enhanced NMDA-induced cell death is diminished with NADPH oxidase inhibition using DPI (100 nM). Data represent mean ± S.E.M from three independent experiments consisting of 10-12 determinents (askteriks * indicates a $p < 0.05$ from normoxic control; ANOVA with *post hoc* Bonferroni test).

Discussion

There are several lines of evidence that indicate that oxidative stress signaling cascades strongly contribute to synaptic glutamatergic excitotoxicity following post-ischemic neuronal injury. While numerous studies have identified changes in NMDAR subunit function following ischemia (Liu *et al.,* 2001, Jiang *et al*., 2008), as well as the downstream signaling cascades leading to cellular death (Arundine and Tymianski 2003, Forder and Tymianski 2008), upstream mechanisms leading to these changes remain largely unresolved. Therefore, experiments were conducted to identify the source of ROS generation involved in the oxidative stress-signaling cascade responsible for the increase in tyrosine phosphorylation of the NMDAR NR2A subunit. Additionally, we performed experiments to establish the mechanism in which the OGD/R-induced activation of NADPH oxidase leads to this increase in tyrosine phosphorylation of the NR2A subunit, as well as to demonstrate a functional consequence of NADPH oxidase activity on enhanced NMDAR-induced cellular death following OGD/R.

Superoxide, which can serve as a signaling molecule to alter NMDAR function, can be produced during ischemia/reperfusion from numerous sources. Abramov *et al*. (2007) demonstrated that in cortical neuronal cultures, both during OGD and the subsequent reperfusion, superoxide is generated in a tri-phasic manner from distinct sources. The primary and secondary burst arise from the mitochondria and the enzyme xanthine oxidase during the OGD phase. During the reperfusion following OGD, a tertiary burst of superoxide was observed which was shown to be a result of NADPH oxidase activity. Further studies have also reported that NADPH oxidase activity results in the production of superoxide *in vivo* in the hippocampus of adult mice subjected to ischemia/reperfusion (Suh *et al.,* 2008).

We therefore sought to determine the temporal pattern of ROS production following exposure to OGD/R in retinoic acid differentiated SH-SY5Y cells utilizing DHE fluorescence as well as NBT reduction. ROS production, while observed to be minimal during 40 minutes of OGD, was maximally increased by 15 minutes of reperfusion and was drastically blunted when NADPH oxidase was inhibited with DPI, both in the DHE and NBT assays (Fig. 1A and 1B). In contrast, ROS generation during reperfusion following OGD was minimal in non-differentiated SH-SY5Y cells (data not shown), which may be due to the decrease in NADPH oxidase subunit protein expression levels seen reported by Nitti *et al.* (2007), and confirmed by our study. While superoxide production from NADPH oxidase has been shown to contribute to neuronal death (Wang *et al.,* 2006, Suh *et al.,* 2008) following stroke, its basal activity under physiologic conditions is thought to be critical in the processes of LTP as demonstrated by an inhibition of LTP in knock-out studies of mice lacking a functional NADPH oxidase holoenzyme (Kishada *et al.,* 2006). Therefore, under pathologic conditions such as ischemia/reperfusion, we sought to determine if superoxide produced from NADPH oxidase played a role in mediating the increased tyrosine phosphorylation of the NMDAR NR2A subunit following OGD/R.

Modifications on the C-terminal regions of NMDAR subunits in the brain via phosphorylation are thought to play a key role in neuronal development, synaptic plasticity, and a variety of pathologic conditions (Lau and Huganir, 1995). While increases in both serine and threonine phosphorylation does occur on NR1 and NR2 subunits, potentiation of NMDA currents seems to be accomplished via direct tyrosine phosphorylation of NR2 subunits by protein tyrosine kinases (Chen *et al.*, 1996). Tyrosine phosphorylation of the NR2A increases the probability that the receptor will enter a long-lived open conformation, as well as decrease the likelihood of the receptor entering a long-lasting closed state (Yu *et al*., 1997). This increase in tyrosine phosphorylation ultimately affects the amount of calcium that is able to enter through the receptor, resulting in an increased effect of glutamate upon NMDAR stimulation. While this is an important phenomenon for synaptic plasticity under physiologic conditions, the increased entry of calcium through NMDAR during pathologic insults only exacerbates neuronal death via calcium overload. We found that a significant increase in tyrosine phosphorylation of the NMDAR NR2A subunit occurred during reperfusion of OGD subjected in retinoic acid differentiated SH-SY5Y cells. As indicated previously, ROS generation by NADPH oxidase occurs during post-ischemic reperfusion (Abramov *et. al.* 2007). While numerous reports have established that ischemic insult results in an increase of NMDAR tyrosine phosphorylation (Takagi *et al.,* 1997; Pei *et al.* 2000), oxidative stress signaling pathways leading to the increases in phosphorylation status still remained largely unresolved. We found that inhibition of NADPH oxidase activity with DPI significantly attenuated the OGD/R-induced increase in NR2A tyrosine phosphorylation. Inhibition of mitochondrial ROS production with FCCP or xanthine oxidase ROS production with oxypurinol had no significant effect on reducing NR2A tyrosine phosphorylation, suggesting that the key superoxide source for signaling for changes in NMDAR NR2A tyrosine phosphorylation is NADPH oxidase. These findings are consistent with previous studies by Murotomi *et al.* (2008 and 2010), as inhibition of

NADPH oxidase with mGluR1 antagonism reduced the increase in tyrosine phosphorylation of the NR2A subunit following I/R, ultimately decreasing infarct size *in vivo*. However, these studies did not report underlying mechanisms between NADPH oxidase activation and an increase in NMDAR NR2 subunit phosphorylation status.

SFKs, originally discovered as a proto-ocongene yet later found to be highly expressed in fully differentiated mature neurons (Cotton and Brugge, 1983), are important in mediating NMDAR tyrosine phosphorylation (Yu *et al.,* 1997; Liu *et al.,* 2001). SFKs have also been shown to be activated and form interactions with NMDARs during ischemia (Jian *et al.,* 2008). We demonstrated that OGD/R-induced tyrosine phosphorylation of the NR2A subunit involves the activity of SFKs. This SFK mediated tyrosine phosphorylation of the NR2A subunit appears to also involve interaction with PSD-95. This is consistent with the findings of Hou *et al.* (2003) that reported I/R-induced increase in NR2 subunit phosphorylation requires activated Src to bind to PSD-95 prior to phosphorylating NR2 subunits. We have extended this finding by demonstrating that inhibition of NADPH oxidase leads to a diminished SFK interaction with PSD-95. Additionally, the OGD/R-induced increase in tyrosine phosphorylation of the NMDAR NR2A subunit is diminished by inhibiting NADPH oxidase activity. Therefore, this result suggests that OGD/R-induced increase in NR2A tyrosine phosphorylation involves the NADPH oxidase mediated SFK interaction with PSD-95. SFKs have been shown to play a role in mediating cellular death during stroke, as treatment with the inhibitor PP2 has been demonstrated to be neuroprotective (Hou *et al.,* 2007, Jian *et al.,* 2008). In retinoic acid differentiated SH-SY5Y cells, we demonstrated that treatment with PP2 significantly reduced the OGD/R-induced tyrosine phosphorylation of the NR2A subunit, further indicating the importance of SFKs in mediating the tyrosine phosphorylation of NMDARs. A possible explanation of SFK activation during OGD/R lies in the redox sensitive nature of SFK activity (Li *et al.,* 2008), which would explain the large increase in SFK activation observed when in a state of oxidative stress such as stroke.

Lastly, we sought to determine if inhibition of NADPH oxidase could protect against the exacerbated excitotoxic effect of NMDA stimulation following OGD/R. Wang and others (2006) had previously showed the neuroprotective effect of NADPH oxidase inhibition *in vivo* following I/R. However, the mechanism providing this neuroprotection was not fully investigated. Physiologic LTP studies have demonstrated that pharmacologic inhibition of NADPH oxidase diminishes the ability of receptor signaling to potentiate synaptic currents (Kishida *et. al.* 2006). While necessary for LTP under physiologic conditions, the dampening of excitatory receptor signaling could be beneficial in pathologic conditions leading to calcium overload via excitotoxcicity as during I/R. Through inhibition of NADPH oxidase activity with DPI, enchanced cell death after NMDA stimulation following OGD/R was significantly rescued. A plausible mechanism for such protection could be explained by the prevention of the increase in tyrosine phosphorylation of the NMDAR NR2A subunit with NADPH oxidase inhibition, thereby diminishing the enhanced excitotoxic effect of NMDAR stimulation.

In summary, we have demonstrated that NADPH oxidase is activated and is a major source of ROS generation during reperfusion following OGD in retinoic acid differentiated SH-SY5Y cells. This ROS burst from NADPH oxidase is important in mediating the activation of SFKs and its interaction with PSD-95, which consequently are responsible for the observed increase in the tyrosine phosphorylation of the NMDAR NR2A subunit. Collectively, this data indicates an upstream mechanism leading to changes in the phosphorylation of NMDAR NR2A subunit, thereby ultimately affecting the potentiated properties of the receptor in post-ischemic tissue.

ISCHEMIA/REPERUSION

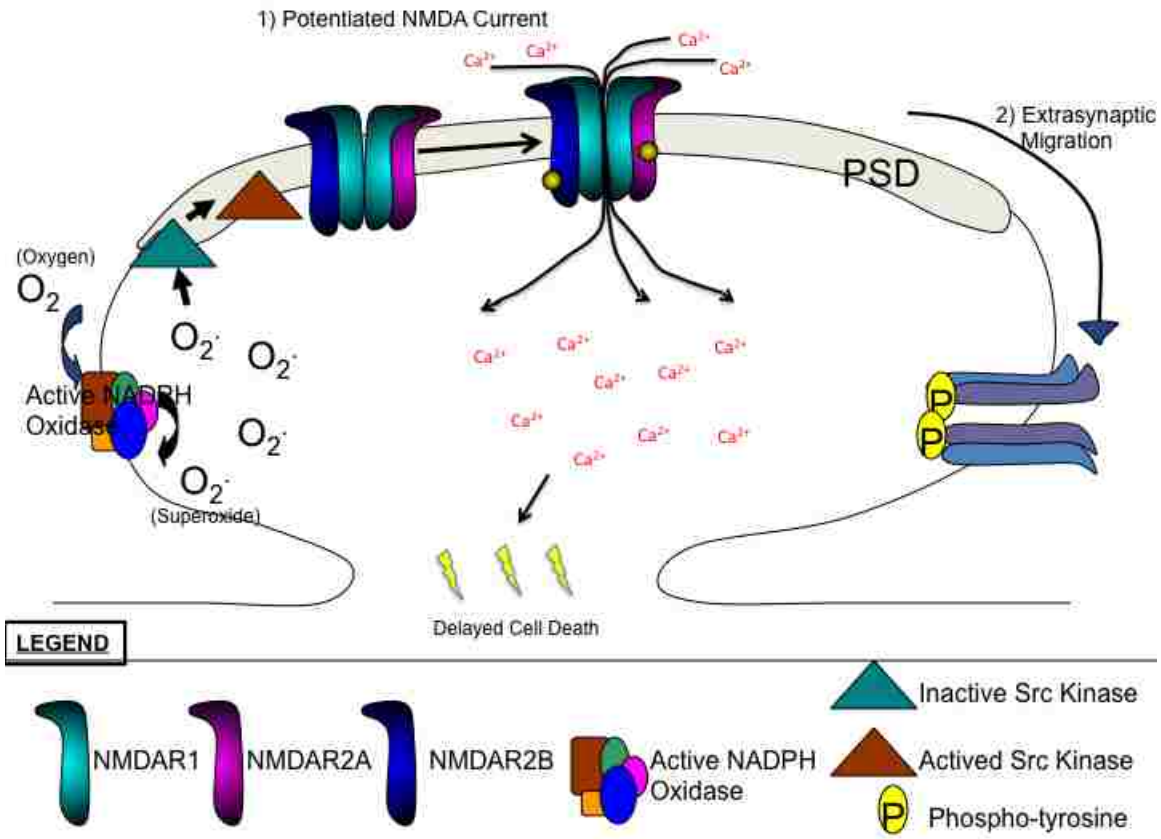

Diagram 8. Proposed model for CHAPTER 1. NADPH oxidase signaling following OGD/R leads to the activation of SFKs, which tyrosine phosphorylate NR2A and NR2B subunits, leading to an enhanced calcium entry via potentiation of NMDAR channels (1) and possible extrasynaptic migration (2).

CHAPTER 2

Oxygen-Glucose Deprivation/Reperfusion-Induced Degradation of the GluR2 AMPA Receptor Subunit Involves NADPH Oxidase and p38 MAPK.

Abstract

Following a stroke, the pathological increase in intracellular calcium arising from the over-activation of post-synaptic glutamatergic receptors has long been established as a key contributor to neuronal death. More recently, calcium and zinc permeable 2-amino-3-(3-hydroxy-5-methylisoazol-4-yl)propionic acid receptors (AMPARs) have been shown to contribute to neuronal death following ischemic-reperfusion injury via an unusual subunit composition change to GluR2-lacking AMPARs that renders the receptor permeable to divalent cations. In this study, we investigated the effect of superoxide production from NADPH oxidase in contributing to an oxidative stress-signaling cascade involved in the accelerated endocytosis and degradation, resulting in the AMPAR subunit switch in post-ischemic tissue. Inhibition of NADPH oxidase with apocynin attenuated the oxygen-glucose deprivation/reperfusion-induced (OGD/R) degradation of the AMPAR GluR2 subunit, as well as damped the OGD/R-induced increase in p38 MAPK activation, thereby affecting early endocytic machineries by decreasing the GDI:Rab5 complex formation. Direct inhibition of p38 MAPK with SB202190 also rescued GluR2 degradation following OGD/R through preventing the surface removal of GluR2 by decreasing the Rab5-GDI interaction. Furthermore, inhibition of clathrin-mediated endocytosis prevented the surface removal of GluR2 and subsequent degradation. Collectively, these data suggest that NADPH oxidase has an important role in mediating GluR2 degradation in hippocampal slices following exposure to OGD/R.

Materials and Methods

Preparation of acute rat hippocampal slices

Adult male (6-8 week) Sprague-Dawley rats (Charles River Labs, Wilmington, MA, USA) were anesthetized with isoflurane and rapidly decapitated. The entire brain was then removed and placed in an ice-cold cutting solution (75mm Sucrose, 80mm NaCl, 2.5 mM KCl, 1.25 mM NaH_2PO_4, 24 mM $NaHCO_3$, 25 mM Glucose, 4mM $MgCl_2$, 1mM L-Ascorbic Acid, 3mM Na Pyruvate, 0.5 mM $CaCl_2$, pH 7.4). Both hippocampi were then quickly dissected away from the brain and coronal 400 micron thick slices were made using a tissue chopper. Slices were then subsequently equilibrated in oxygenated (95% O_2, 5% CO_2) artificial cerebrospinal fluid (aCSF; 124 mM NaCl, 2.5 mM KCl, 1.25 mM KH_2PO_4, 26 mM NaHCO3, 10 mM Glucose, 1.5 mM $MgCl_2$, 2.5 mM $CaCl_2$, pH 7.4) for 90 minutes prior to treatment with OGD/R, with fresh aCSF being replaced every 15-30 minutes during the equilibration phase. Pre-treatment with 30 µM apocynin (Sigma, St. Louis, MO, USA) or 1:1000 vehicle (DMSO) occurred during the final 30 minutes of the equilibration process and was present throughout the duration of the experiment, either during time matched normoxia treated controls or OGD and subsequent reperfusion. Treatment with 10 µM of the selective p38 MAPK inhibitor SB202190 (Sigma, St. Louis, MO, USA) occurred immediately following OGD and was left in for the duration of reperfusion or time matched normoxia treated controls.

Oxygen-Glucose Deprivation/Reperfusion of hippocampal slices

Following equilibration in oxygenated aCSF, slices to be subjected to OGD/R were rinsed with aCSF without glucose (aCSF with 10 mM Mannitol substituted for 10 mM Glucose, pH 7.4), to remove glucose from the slices, and incubated for 40 minutes in a hypoxic glove box (Coy Laboratories, Grass Lake, MI, USA) containing a gas mixture of 0% O_2, 95% N_2, 5% CO_2 with aCSF minus glucose. The aCSF minus glucose media used for OGD was placed in 0% O_2 overnight to ensure complete anoxia. Following OGD, slices were removed from the hypoxic glove box and transferred back to oxygenated aCSF containing glucose for the time periods indicated. Normoxic controls were left in aCSF containing glucose throughout the entire experiment and were time matched to the last of the OGD/R time points.

Detection of ROS using nitro-bluetetrazolium chloride

Slices were incubated in oxygenated aCSF with nitro-bluetetrazolium chloride (NBT; 0.5 mg/mL; Sigma, St. Louis, MO, USA) for 10 minutes prior to OGD/R. Excess NBT was then rinsed away with aCSF minus glucose and OGD/R treatment proceeded as previously described. At the indicated time point, the reaction was stopped with 0.25 M HCl. Slices were visualized via phase contrast microscopy (Olympus SZX16, 4X air objective), then lysed via sonication in DMSO containing a protease inhibitor cocktail. The lysate was then aliquoted into a 96 well plate and absorbance was read at 550 nM on a spectrophotometric microplate reader (VersaMax plate reader, Molecular Devices, Sunnyvale, CA, USA).

Propidium Iodide Staining

Following dissection and equilibration, hippocampal slices were treated with either 40 minutes of OGD alone, OGD plus reperfusion time points, or time matched normoxia. Slices were incubated with propidium iodide (4 mg/mL, Sigma) in aCSF for the final 30 minutes of treatment. Slices were then rinsed 3 times in PBS to remove excess propidium iodide and visualized in triplicates for each time point using a fluorescent dissecting microscope (Olympus). Staurosporine (10 μM, 30 minutes) was used a positive control for cell death.

Lysate Preparation

Slices were removed from aCSF at the indicated time point and rinsed with ice cold PBS. For total protein level detection, slices were places in tubes containing lysis buffer (250 mM Sucrose, 20 mM HEPES, 2 mM EDTA, 5 mM $MgCl_2$, 1 mM dithiothreitol, 1 mM AEBSF, 1% protease and phosphatase inhibitor cocktail (Thermo, Rockland, IL, USA), 1% Triton X-100, 0.01% saponin, pH 7.4) and lysed immediately via sonication for a 3 separate 5 second bursts at 25% power output with a VirTis Ultrasonic Cell Disrupter 100 (Gardiner, NY, USA). Samples were then spun at 1,000 x g to remove nuclei and cellular debris and a BCA assay was performed to determine protein content. Samples were then denatured in Laemmli buffer and heat (100°C) for 10 minutes and resolved via sodium dodecyl sulfate polyacrylamide gel electrophoresis (SDS-PAGE). For cellular and membrane fractionations, slices were placed in lysis buffer without Triton X-100 or saponin, lysed via sonication, and then spun at 1,000 x g for 10 minutes to remove the nuclei and cellular debris. The supernatant was then collected and spun in a swinging bucket rotor at 100,000 x g for 30 minutes. The resulting supernatant yielded a clean cytosolic fraction. The membrane fraction pellet was then extracted on ice using lysis buffer containing Triton X-100 and saponin, disrupted via sonication, and spun at 1,000 x g to remove any insoluable proteins. Protein levels were determined using a bicinchoninic acid assay (BCA; Thermo), and samples were heated with Laemmli buffer as previously described and resolved via SDS-PAGE. Samples were then transferred to a nitrocellulose membrane (Bio-Rad, Berkeley, CA, USA) for subsequent detection via immunoblotting.

Immunoblotting

Blots were blocked for 1 hour at room temp with either 5% BSA (for phospho-antibody detection) or 5% non-fat dry milk in Tris Buffered Saline, 0.1% Tween 20, pH 7.5 (TBS-T). After blocking, blots were incubated with primary antibody overnight at 4°C at the concentration indicated. The affinity purified GluR1 rabbit-polyclonal antibody (1:1000) was purchased from AbCam (Cambridge, MA, USA). The affinity purified rabbit-monoclonal GluR2 antibody (1:2000) was purchased from Epitomics (Burlingame, CA, USA). The affinity purified rabbit-polyclonal p38 MAP Kinase (1:1000) antibody and the affinity purified rabbit-monoclonal phospho-p38 MAP Kinase (Thr180/Tyr182) (1:500) were purchased from Cell Signaling Technology (Beverly, MA, USA). Goat anti-Mouse-HRP and Goat-anti-Rabbit-HRP secondary antibodies (1:2000) were purchased from Jackson ImmunoResearch (West Grove, PA, USA). The affinity purified mouse monoclonal Rab5 (1:250) antibody and the affinity purified goat polyclonal p67*phox* (1:250), gp91*phox* (1:250), and phosphoglycerate kinase 1 (PGK;

1:250) antibodies were purchased from Santa Cruz Biotechnologies (Santa Cruz, CA, USA). The donkey anti-Goat-HRP secondary antibody was also purchased from Santa Cruz. Immunoreactive bands were visualized and captured with a Fuji imaging system using enhanced chemiluminescence after adding HRP conjugated secondary antibodies. Bands were analyzed using Fuji Image-Gauge software. Blots were stripped and re-probed up to 4 times using Restore Plus Western Blotting Stripping Buffer (Thermo).

Immunoprecipitation

To visualize the Rab5-GDI protein complex, rat hippocampal slices were lysed in a buffer containing 50 mM Tris-HCl, 100 mM NaCl, 5 mM EGTA, 5 mM EDTA, 1 mM phenylmethylsulfonyl fluoride, 0.5% Triton X-100, and 1% protease and phosphatase inhibitor cocktail. Protein concentration was then determined using a BCA assay, and lysates (500 μg/sample in 500 μl) were then pre-cleared using Protein-A/G 50/50 mix of agarose beads for 1 hour at 4°C followed by incubation with a Rab5 antibody overnight at 4°C. The immunocomplex was then incubated for 4 hours with 50 μL Protein-A/G beads at 4°C with rotation before being washed 3 times with lysis buffer. Samples were eluted from the agarose beads by treatment with Laemmli buffer and heat (100°C) for 10 minutes and then subjected to SDS-PAGE. After transfer to nitrocellulose membranes, blots were blocked as previously described and incubated overnight at 4°C with a mouse affinity-purifed Rab-GDI anti-body (1:1000; Synaptic Systems, Goettingen, Germany). Immunoreactive bands were analyzed using Fuji Image-Gauge software.

Immunostaining of hippocampal slices

Slices were treated to either normoxia or OGD/R as previously described, washed with PBS, and fixed using 4% paraformaldehyde. Slices were then cryoprotected (30% sucrose/PBS) overnight before resectioning on a sliding Microtome to produce 60 micron thick slices. The slices were then permeablized (0.4% Triton X-100), blocked (20% BSA/PBS), and then stained with primary antibodies for Rab5 (1:200) or Rab-GDI (1:200). Slices were then rinsed three times with PBS and treated with pre-immune serum for 30 minutes at room temperature prior to being stained with fluorescent secondary antibodies. The slices were then rinsed three times with PBS prior to being stained with a NeuroTrace fluorsecent Nissl stain (Invitrogen, Carlsbad, CA, USA) for 20 minutes at room temperature. Slices were then rinsed three times with PBS and mounted on to slides for visualization via fluorescent confocal microscopy (Olympus FV1000, 40X oil objective).

Biotinylation of hippocampal slices

Acute adult rat hippocampal slices were prepared and treated to OGD/R or time matched normoxia as previously described, washed with ice cold Buffer A (25 mM HEPES, 119 mM NaCl, 5 mM KCL, 2 mM $CaCl_2$, 2 mM $MgCl_2$, 30 mM glucose, pH 7.4), and incubated at 4°C in Buffer A containing 0.5 mg/ml of sulfo-NHS-SS-biotin (Thermo) for 30 minutes with gentle agitation. After biotin labeling, slices were washed three times in ice cold Buffer A. For cleaved controls, slices were treated to two 15 minute incubations in Glutathione Buffer (75 mM glutathione, 75 mM NaCl, 10 mM EDTA, 1 % bovine serum albumin, pH 7.4) and rinsed 3 times in ice cold Buffer A.

Slices were then lysed via sonication with 3 separate 5 second bursts at 25% power output in Buffer A containing 1% protease and phosphatase inhibitor cocktail, and then spun at 1,000 x g to remove the nuclei and cellular debris. The supernatant was then collected and spun in a swinging bucket rotor at 100,000 x g. The biotin labeled membrane fraction was then solubilized on ice for 10 minutes using Solubilization Buffer (10 mM Tris, 150 mM Nacl, 1% protease and phosphatase inhibitor cocktail, 1 % Triton X-100, pH 8). The biotin labeled membrane pellet was then collected and sonicated with 2 separate 5 second bursts at 25% power output and a BCA assay was performed to determine protein content. Biotin labeled membrane proteins (500µg sample/500µl of Solubilization buffer) were then incubated overnight with gentle agitation at 4°C with 60 µl 50% streptavidin sepharose beads (GE Healthcare, Little Chalfont, UK). The streptavidin sepharose beads were then washed twice with High Salt Buffer (Solubilization Buffer containing 0.6 M NaCl, pH 8.0), followed by two washes with Solubilization Buffer. The streptavidin sepharose bead complex was then denatured with Laemmli and heat (80°C) for 10 minutes, subjected to SDS-PAGE, and transfered to nitrocellulose membranes for subsequent immunoblotting with GluR1 and GluR2 antibodies as previously described. Immunoreactive bands were analyzed using Fuji Image-Gauge software. For experiments using high sucrose concentrations to prevent clathrin-mediated endocytosis, 0.45 M sucrose was added to aCSF with/without glucose solutions. Slices were incubated in oxygenated aCSF with glucose containing 0.45 M sucrose for 30 minutes prior to OGD treatment in pre-anoxiated aCSF without glucose containing 0.45 M sucrose. Subsequent reperfusion of slices occurred in oxygenated aCSF with glucose containing 0.45 M sucrose or time matched normoxia.

Introduction

Annually in the United States, approximately 795,000 individuals suffer from a stroke, thereby making it the third leading cause of death and the leading cause of disability in the United States (Falluji *et al.,* 2011). Despite an enormous amount of research effort by both the scientific and pharmaceutical communities, efficacious therapeutic interventions for stroke patients has yet to reach the clinic. One of the well studied phenomena known to occur following stroke is the cytotoxic accumulation of intracellular calcium, resulting from the excessive release of the excitatory neurotransmitter glutamate, a process known as “excitotoxicity” (Szydlowska and Tymianski, 2010). While physiologic increases in calcium are a key event in regulating many cellular processes including synaptic plasticity, the over-activation of post-synaptic receptors in turn leads to the accumulation of high intracellular calcium, an event known to be responsible for much of the neuronal death associated with stroke (Arudine and Tymianski, 2003).

Excitatory synaptic transmission is therefore a tightly regulated process, mediated by both the total number and the temporal activation of the 2-amino-3-(3-hydroxy-5-methylisoazol-4-yl)propionic acid receptor (AMPAR). The co-ordination of N-methyl D-aspartate receptor (NMDAR) and AMPAR localization and activity govern the basic tenants of synaptic plasticity, with the extent of intracellular calcium concentration dictating the differential activation of downstream signaling cascades (Kullman and Lamsa, 2007). In its most basic form, AMPARs are inserted into the post-synaptic membrane during long term potentiation (LTP), or strengthening of the synapse, and removed from the surface during long term depression (LTD), or weakening of the synapse (Shepherd and Huganir, 2007). It is therefore this delicate balance between AMPAR trafficking, be it synaptic AMPAR delivery or synaptic AMPAR removal, in combination with numerous other receptor inputs, which composes the molecular basis for the cellular mechanisms of learning and memory.

However, the complexity of the process of AMPAR trafficking also involves numerous other inputs, including subunit composition, phosphorylation events, and protein-protein interactions. Specifically focusing on subunit composition, the presence or absence of the GluR2 subunit, one of four genes (GLUR1-4) which combine in various stochiometeries as a “dimer of dimers” to form the functional AMPAR tetramer, governs much of AMPAR channel properties and ionic permeability as a result of its amino acid makeup (Shepherd and Huganir, 2007). Hydrolytic RNA editing of the GluR2 transcript via the activity of the adenosine deaminase enzyme ADAR2 (Bass, 2002) substitutes a neutrally charged glutamine (Q) for a positively charged arginine (R) in the region which structurally composes the AMPAR channel pore, thereby making AMPARs that contain GluR2 (Q607R) impermeable to divalent cations (Ca^{2+} and Zn^{2+}), while AMPARs lacking GluR2 are able to conduct Ca^{2+} and Zn^{2+} (Traynelis *et al,* 2010). In the hippocampus, the majority of AMPARs are composed of GluR1 and GluR2 (Q607R) hetero-tetramers, with lower levels of GluR3 and GluR4, although subunit expression patterns are both activity dependent (Clem *et al*., 2010) and are vastly varied depending on neuroanatomical location (Passafaro *et al.,* 2001).

Surface removal of GluR2 containing AMPARs is a process thought to be important in increasing the basal excitability of neurons by increasing Ca^{2+} permeability via GluR2-lacking AMPARs (Lu and Ziff, 2005). While this short-lived change in promoting GluR2-lacking AMPAR subunit composition has been reported to be important in the induction of LTP (Terahsima et al., 2008), long-lasting changes in the switch of AMPAR subunit composition to Ca^{2+} and Zn^{2+} permeable AMPARs have been demonstrated to contribute to neuronal death in a number of Central Nervous System (CNS) pathologies, including Alzheimer's disease (Liu *et al.,* 2010), Parkinson's disease, Huntington's disease (Jayakar and Dikshit, 2004), and stroke (Noh *et al.,* 2005).

While initial reports of stroke-induced glutamate-dependent excitotoxicity demonstrated that excess activity of NMDARs was primarily responsible for mediating calcium cytotoxicity and subsequent neuronal death (Ford *et al,* 1989; Mcintosh *et al.,* 1989), more recently it has been documented that calcium permeable AMPARs also contribute to neuronal death following stroke (Yin *et al.*, 2002,; Anzai *et al*., 2003; Liu *et al.,* 2004; Noh *et al.,* 2005).

In this study, we show that the superoxide producing enzyme nicotinamide adenine dinucleotide phosphate oxidase (NADPH oxidase) is involved in mediating the removal of AMPARs from the surface of acute adult rat hippocampal slices subjected to oxygen-glucose deprivation/reperfusion (OGD/R) by enhancing the endocytic machineries responsible for AMPAR internalization. More specifically, we found that the OGD/R-induced activation of NADPH oxidase contributes to the activation of p38 mitogen-activated protein kinase (p38 MAPK), a kinase that has been demonstrated to be involved in AMPAR surface removal (Cavalli *et al.,* 2001; Huang *et al.,* 2005; Zhong *et al.* 2008). Furthermore, we show that total GluR2 protein levels are significantly reduced following OGD/R while total GluR1 protein levels are not affected. Inhibition of NADPH oxidase during OGD/R diminished p38 MAPK activation, reduced the activity of early endocytic machineries, decreased AMPAR surface removal, and rescued total and surface GluR2 protein levels. These results provide direct evidence of a NADPH oxidase-mediated oxidative stress-signaling cascade responsible for the AMPAR dysfunction observed following ischemia/reperfusion.

Results

NADPH oxidase contributes to oxidative stress in the adult rat hippocampus following exposure to OGD/R

To assess the contribution of NADPH oxidase in promoting the oxidative stress observed following OGD/R, a NBT test was performed in acute adult rat hippocampal slices treated to OGD/R or time matched normoxia in the presence or absence of the NADPH oxidase inhibitor apocynin (30 μM). NBT is reduced by superoxide or oxidant metabolites to form formazan, an insoluble dye which can be observed via colorimetry and quantified (Altman, 1977). Treatment of hippocampal slices to OGD/R increased formazan formation, illustrating a large increase in the oxidative environment, particularly during the reperfusion phase in slices subjected to OGD (Fig. 7A and 7B). It had previously been demonstrated that OGD/R results in a tri-phasic production of reactive oxygen species (ROS), sequentially identified as resulting from the mitochondria, xanthine oxidase, and a large tertiary burst resulting from NADPH oxidase during reperfusion (Abramov *et al.,* 2007). Consistent with these results, we found that pharmacologic inhibition of NADPH oxidase with apocynin significantly reduced formazan deposits following OGD/R, suggesting that NADPH oxidase significantly contributes to oxidative stress in the rat hippocampus during reperfusion following OGD exposure.

NADPH oxidase is composed of both catalytic and regulatory subunits that assemble at the plasma membrane to form a functional holoenzyme. NOX2, one of 7 NADPH oxidase family members to be identified (NOX 1-5, DUOX 1/2; Brown and Griendling, 2009), is most the highly expressed isoform in neurons of the CNS and requires the membrane bound gp91^{phox} catalytic subunit and translocation/assembly of the cytosolic activators p47^{phox} and p67^{phox} in order for superoxide-producing activity to occur (Bedard and Krause, 2007). Consistent with the NBT assay results, we found a significant and long lasting association of the cytosolic activator p67^{phox} with the membrane fraction following OGD/R treatment (Fig. 7C and 7D), with maximal membrane interaction at 30 minutes of reperfusion following OGD. Apocynin has been demonstrated to block Nox2 assembly (Stolk *et al.,* 1994), and consistent with these findings, we found that apocynin prevented the OGD/R-induced association of p67^{phox} with the membrane fraction at the 40/30 OGD/R time point (Fig. 7E and 7F). However, inhibition of NADPH oxidase activity with apocynin not only reduced oxidative stress, but also increased cellular viability in acute rat hippocampal slices treated to OGD/R as assessed by propidium iodide staining (Fig. 8) results that are in agreement with the findings Wang *et al.* (2006) in the gerbil hippocampus. Taken together, these results (Figs. 7 and 8) strongly support the view that NADPH oxidase is a major contributor to the oxidative stress environment observed following ischemia/reperfusion, in turn contributing to cellular death.

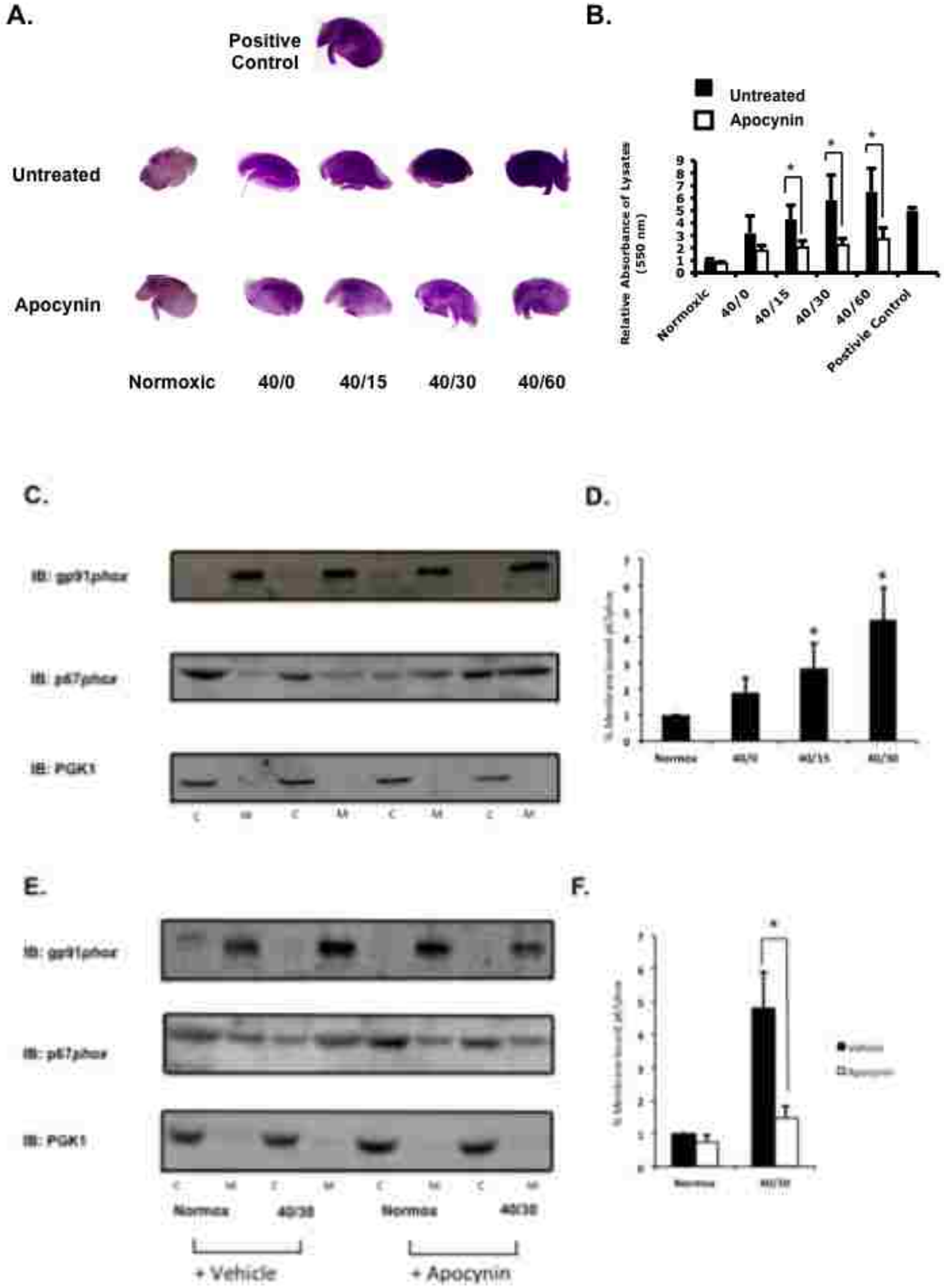
A.
Positive Control
Untreated
Apocynin
Normoxic
40/0
40/15
40/30
40/60
B.
Untreated
Apocynin
Relative Absorbance of Lysates (550 nm)
Normoxic
40/0
40/15
40/30
40/60
Postivie Control
C.
D.
IB: gp91phox
IB: p67phox
IB: PGK1
E.
F.
+ Vehicle
+ Apocynin

Figure 7. NADPH oxidase activity contributes to oxidative stress during reperfusion of OGD-treated hippocampal slices. Adult rat hippocampal slices were loaded with NBT and subjected to either time-matched normoxia, OGD alone, or OGD with various reperfusion time points. Phase contrast images (A) were collected on a dissecting scope. Reduced NBT was quantified (B) by cellular lysis in DMSO with the absorbance of the resultant supernatant being collected at 550 nM. Apocynin treatment (30 μM) dramatically decreased the amount of reduced NBT as compared to untreated slices, suggesting NADPH oxidase is a major contributor to the oxidative burst observed during reperfusion following exposure to OGD. Phorbol 12-myristate 13-acetate (PMA; 10 μM, 10 minutes) was used as a positive control for NADPH oxidase activity. Data are presented as the % mean of untreated controls ± S.D and is representative of three independent experiments with at least 5 individual hippocampal slices per group. (askteriks * indicates a p of at least <0.05; ANOVA with post hoc Bonferroni test). Lysates were prepared and resolved via centrifugation and detergent extraction in Figure 1C to yield cytosolic (C) and membrane (M) fractions, which illustrates the translocation of the cytosolic 67^{phox} to the plasma membrane. The cytosolic phosphoglycerate kinase (PGK) and the membrane bound component of NADPH oxidase, $gp91^{phox}$, were used as markers for cytosolic and membrane fractions. Data are expressed in (D and F) as relative mean densitometry of membrane bound $p67^{phox}$ as of ratio of $gp91^{phox}$ ± S.D (askteriks * indicates a p of at least <0.05 from normoxic controls; ANOVA with post hoc Bonferroni test).

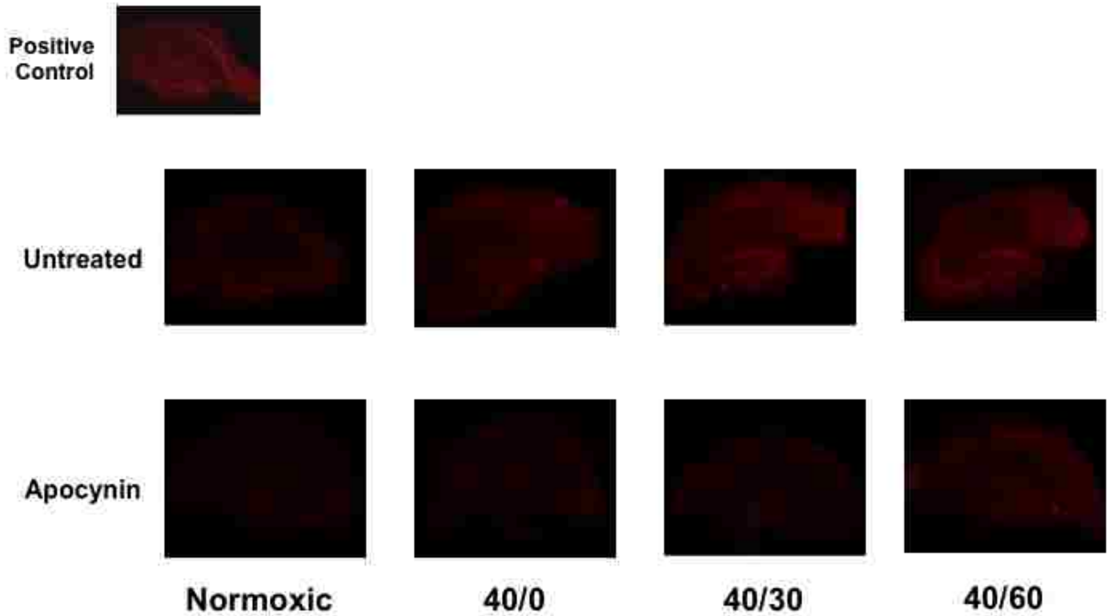

Figure 8. NADPH oxidase inhibition with apocynin is neuroprotective in adult rat hippocampal slices exposed to OGD/R. Adult rat hippocampal slices were subjected to time matched normoxia, OGD alone, or OGD with various reperfusion time points in the presence or absence of the NADPH oxidase inhibitor apocynin (30 μM). Cellular viability was assessed using propidium iodide staining (4 μg/mL, 30 minutes). Staurosporine (10 μM, 30 minutes) was used as a positive control for cell death. Images are representative of two independent experiments that were done in triplicate for each group.

OGD/R induces AMPAR surface removal and the selective degradation of GluR2, which is attenuated with NADPH oxidase inhibition

Numerous studies have demonstrated that ischemia/reperfusion results in a functional change in the subunit composition of AMPARs, from those containing GluR2 to those lacking the GluR2 subunit (Pellegrini-Giampietro *et al.,* 1992; Pellegrini-Giampietro *et al.* 1997; Optiz *et al.,* 2000; Liu *et al*., 2004), an event known to contribute to AMPAR-mediated cell death (Anzai *et al*., 2003; Noh *et al*., 2005; Soundarapandian *et al.,* 2005). To examine this phenomena in our model of acute adult rat hippocampal slices, time course experiments were performed to examine total protein levels of GluR1 and GluR2. While total protein levels of GluR1 were not significantly altered from normoxia treated controls, total GluR2 protein levels were significantly reduced after 40 minutes of OGD followed by 30 minutes of reperfusion (Fig. 9A and 9B). However, through the use of biotin surface protein labeling experiments, both GluR1 and GluR2 subunits are removed from the cell surface following exposure to OGD/R (Fig. 9C and 9D), while only GluR2 is degraded. These results indicate a differential trafficking event leading to the selective degradation of GluR2, thereby promoting AMPARs that are GluR2-lacking and consequently Ca^{2+}/Zn^{2+}-permeable following OGD/R.

However, inhibition of NADPH oxidase activity with apocynin during OGD/R significantly rescued the OGD/R-induced degradation of total/membrane bound GluR2 (Fig. 10 A-D). Furthermore, treatment of slices with apocynin during OGD/R also decreased the surface removal of GluR2, as well as GluR1 (Fig. 10E and 10F), suggesting an OGD/R-induced NADPH oxidase-dependent signaling cascade is involved in increased endocytic trafficking and subsequent selective GluR2 degradation.

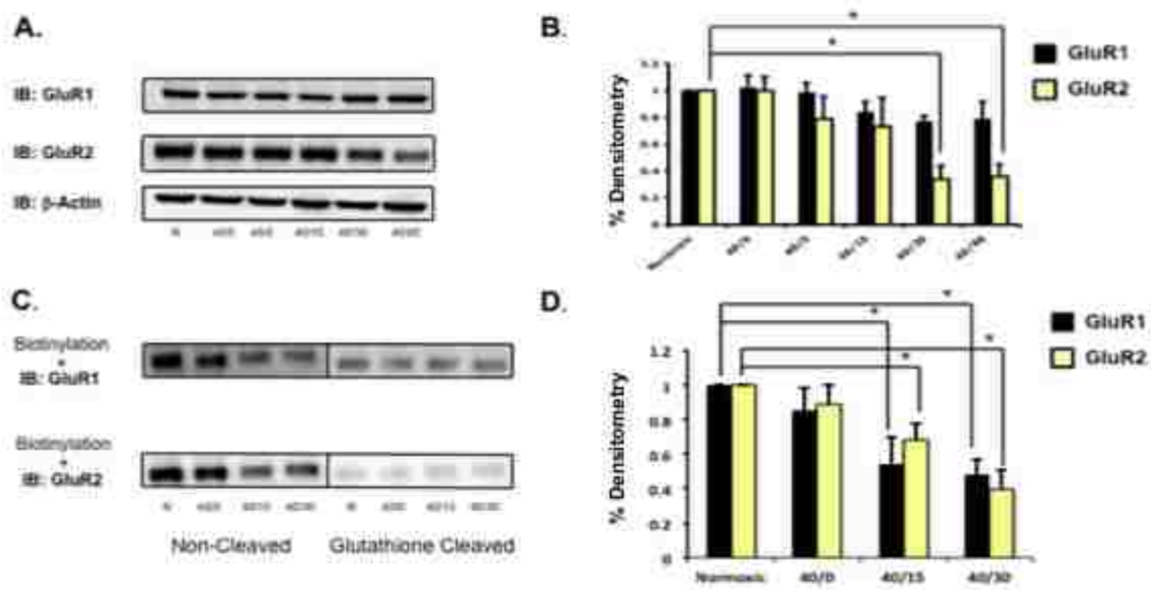

Figure 9. GluR2 is selectively degraded in the rat hippocampus following oxygen-glucose deprivation/reperfusion. Total lysates were prepared from hippocampal slices exposed to time-matched normoxia, OGD alone, or OGD/R time points. Representative Western blot (A) of four independent experiments illustrates the selective decrease in GluR2 protein levels. However, a representative Western blot (C) of three independent experiments reveals that after biotinylation of surface proteins, both GluR1 and GluR2 are decreased. Data are expressed in (B) and (D) as relative mean densitometry of normoxic controls (corrected to β-actin in the case of (B)) ± S.D (askteriks * indicates a p of at least <0.05 from normoxic (N) control; ANOVA with post hoc Bonferroni test).

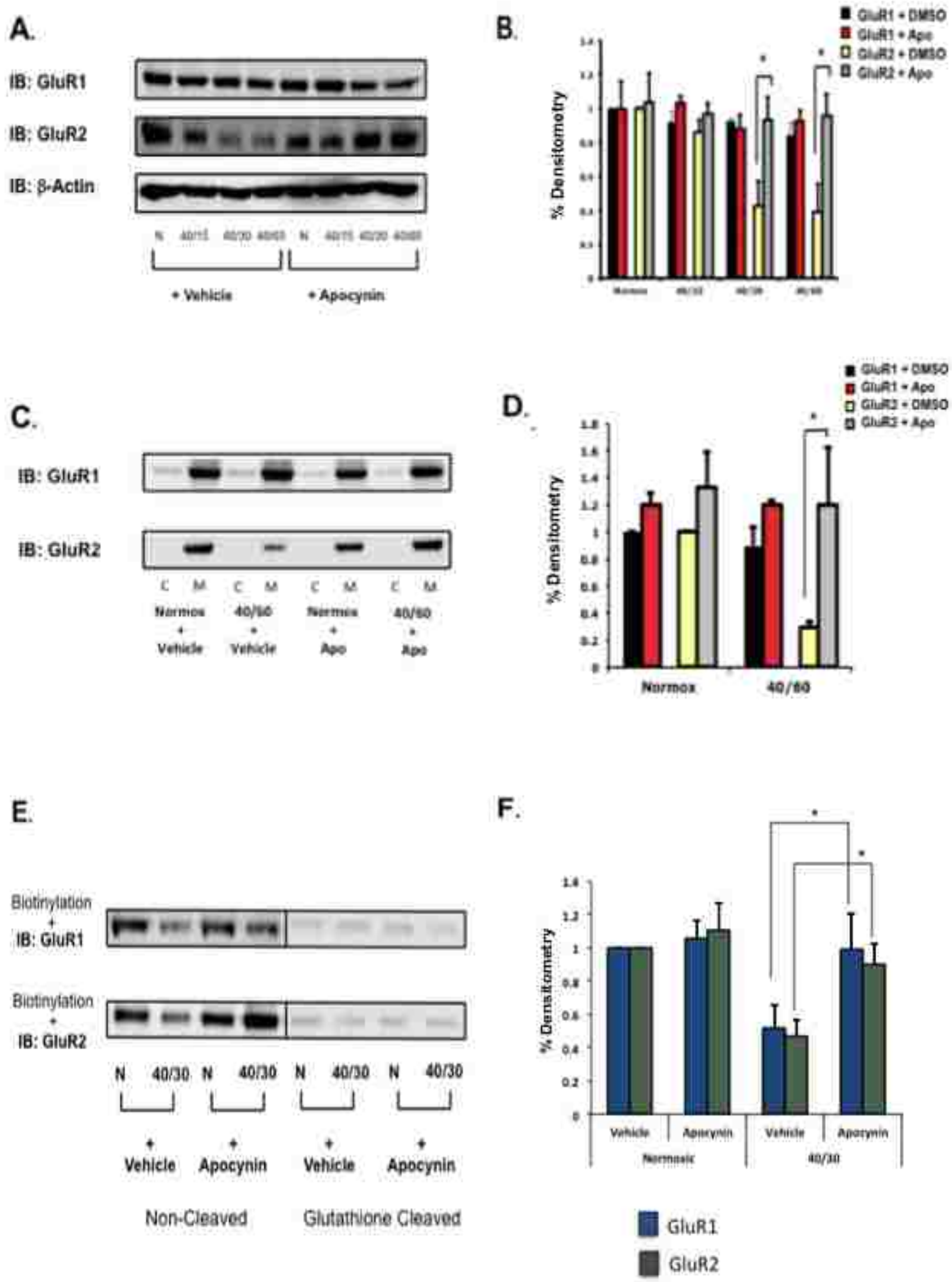

A.
IB: GluR1
IB: GluR2
IB: β-Actin
+ Vehicle
+ Apocynin
B.
GluR1 + DMSO
GluR1 + Apo
GluR2 + DMSO
GluR2 + Apo
% Densitometry
C.
IB: GluR1
IB: GluR2
C M C M C M C M
Normox + Vehicle
40/60 + Vehicle
Normox + Apo
40/60 + Apo
D.
GluR1 + DMSO
GluR1 + Apo
GluR2 + DMSO
GluR2 + Apo
% Densitometry
Normox
40/60
E.
Biotinylation + IB: GluR1
Biotinylation + IB: GluR2
N 40/30 N 40/30 N 40/30 N 40/30
+ Vehicle
+ Apocynin
+ Vehicle
+ Apocynin
Non-Cleaved
Glutathione Cleaved
F.
% Densitometry
Vehicle
Apocynin
Vehicle
Apocynin
Normoxic
40/30
GluR1
GluR2

Figure 10. Total/Membrane and surface bound GluR2 is degraded in the rat hippocampus following oxygen-glucose deprivation/reperfusion and is attenuated with inhibition of NADPH Oxidase activity. Lysates were prepared from rat hippocampal slices exposed to OGD/R with vehicle (1:000 DMSO) or 30 µm of the NADPH Oxidase inhibitor apocynin (Apo). Samples were prepared as either total lysates (A), resolved (Fig 3C) via centrifugation and detergent extraction to yield cytosolic (C) and membrane (M) fractions or surface biotin labeled proteins isolated with streptavidin beads (E) from 4 independent experiments. Glutathione cleavage (75 mM) following biotin labeling is also illustrated as an additional control. Data is expressed in (B), (D) and (F) as % mean densitometry of Normoxic vehicle treated control (corrected to β-actin in the case of (B)) ± S.D. (askteriks * indicates a $p < 0.05$; ANOVA with post hoc Bonferroni test).

OGD/R promotes the activation of p38 MAPK and the formation of the Rab5:GDI complex, which is diminished with NADPH oxidase inhibition

Increasing lines of evidence indicate an important role for p38 MAPK in promoting the endocytosis of AMPARs in neurons during LTD (Huang *et al.,* 2005; Shepherd and Huganir, 2007; Zhong *et al.,* 2008). Early endocytic membrane trafficking is primarily regulated through the action of the small GTPase Rab5 (Stenmark and Olkkonen, 2001), which is governed in part by the activity of guanyl nucleotide dissociation inhibitors (GDI) (Novick *et al.,* 2006). GDI extracts inactive GDP-bound Rab5 from membranes to form the cytosolic GDI:Rab5 complex, which is subsequently delivered to the appropriate membrane target for further activity (Novick and Zerial, 1997). Serine phosphorylation of GDI, mediated by p38 MAPK, enhances its ability to extract Rab5 and form the GDI:Rab5 complex, thereby increasing endocytic trafficking (Cavalli *et al.,* 2001).

Oxidative stress is well documented to induce the activation of p38 MAPK (Robinson and Cobb, 1997, Ogura and Kitamura 1998, Blair *et al.,* 1999), including oxidative stress generated by ischemia (Lu *et al.,* 2011). Therefore, experiments were performed to examine if the oxidative stress observed in adult rat hippocampal slices exposed to OGD/R resulted in the activation of p38 MAPK. Consistent with the NBT data illustrating the oxidative environment within the hippocampal slices, our data revealed a significant increase in the amount of activated p38 MAPK (phospho-Thr180/Tyr182) after 40 minutes of OGD and 15 minutes of reperfusion (Fig. 11A and 11B). Additionally, by diminishing oxidative stress during OGD/R through the inhibition of NADPH oxidase activity with apocynin, the activated levels of p38 MAPK were significantly reduced at all OGD/R time points (Fig. 11C and 11D).

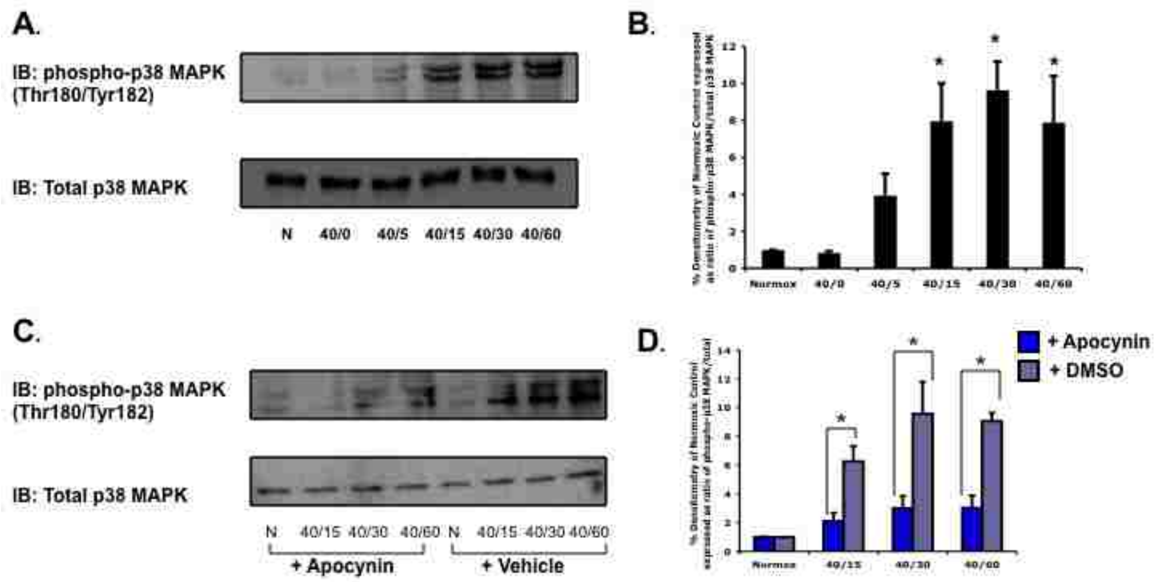

Figure 11. Increased p38 MAPK activity in adult rat hippocampal slices following exposure to oxygen-glucose deprivation/reperfusion is blunted with NADPH oxidase inhibition. (A) Representative Western blot from 3 independent experiments of hippocampal slices illustrates the time course of p38 MAPK activation (phospho-Thr180/Tyr182) during reperfusion following 40 minutes of OGD. (C) Representative Western blot of the OGD/R-induced increase in p38 MAPK activation illustrating the decrease in phospho-p38 MAPK levels with apocynin (30 μM) treatment compared to vehicle (1:1000 DMSO). Quantification (B) and (D) of the density of the phospho-p38MAPK immunoreactive band expressed as a ratio of the phosphorylated form of p38 MAPK to total p38 MAPK protein levels. Data represent % densitometry mean (of normoxic control) ± S.D from three separate experiments. (askteriks * in (B) indicates a p <0.01 from normoxic controls or between groups shown in (D); ANOVA with post hoc Bonferroni test).

Next, the formation of the GDI:Rab5 complex, an association enhanced by p38 mediated phosphorylation of GDI, was examined following OGD/R. Consistent with the time-course of p38 MAPK activation following OGD/R, immunohistochemical staining (Fig. 12A) and immunoprecipitation assays (Fig. 12B and 12C) revealed that Rab5 and GDI form a complex during reperfusion following 40 minutes of OGD. However, inhibition of NADPH oxidase during OGD/R, which was demonstrated to attenuate p38 MAPK activation (Fig. 11C and 11D), significantly reduced the OGD/R-induced increase in the GDI:Rab5 complex formation (Fig. 13A and 13B). Additionally, direct inhibition of p38 MAPK with the selective inhibitor SB202190 (10 μM) during reperfusion of OGD-treated slices also prevented the formation of the GDI:Rab5 complex (Fig. 13A and 13B), further illustrating the importance of p38 MAPK activity in promoting the GDI:Rab5 complex, a result in agreement with the findings of others (Cavalli *et al.,* 2001, Huang *et al.,* 2005).

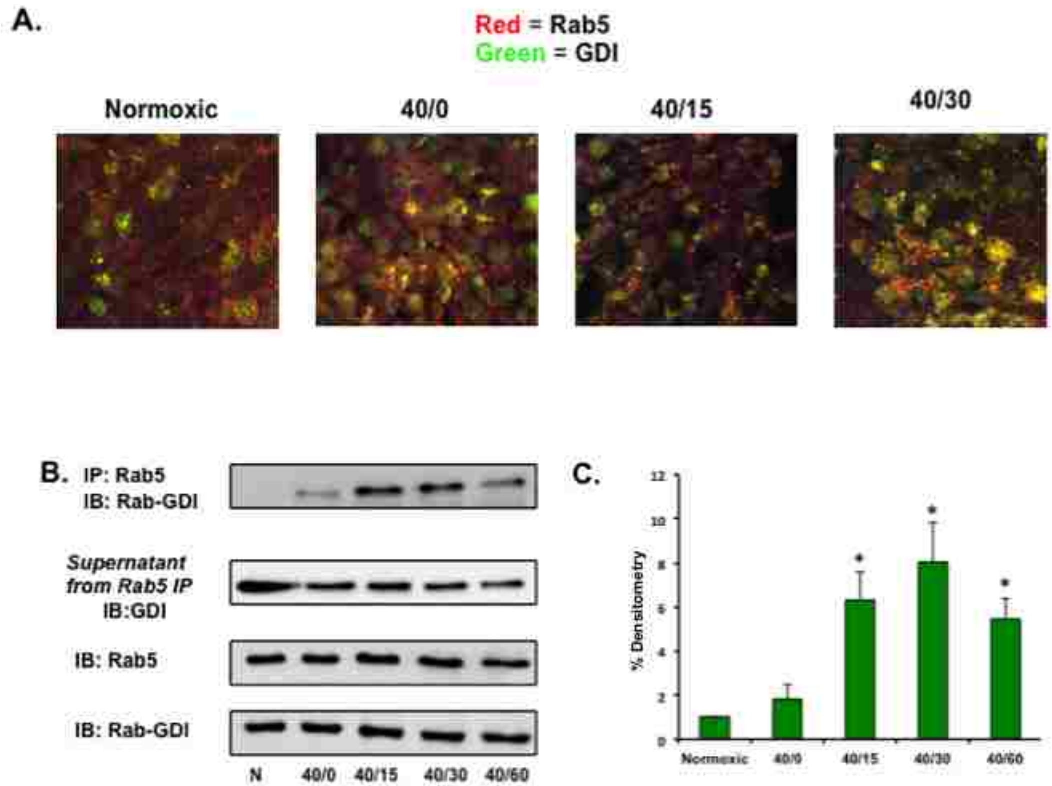

Figure 12. OGD/R promotes the formation of the Rab5-GDI complex. Hippocampal slices subjected to time matched normoxia, OGD alone, or OGD with reperfusion time points were immunostained (A) for Rab5 (Texas Red) and GDI (FITC), which reveals co-localization during reperfusion following exposure to OGD. Images were collected via confocal microscopy (40X) and are representative of three independent experiments done in triplicates. (B) Immunoprecipitation of Rab5 from total lysates prepared from adult male rat hippocampal slices treated to OGD/R show an increase in the formation of the Rab5:GDI complex. Also illustrated in (B) is the GDI immunoreactive band resulting

from the supernatant following immunoprecipitation of Rab5, in addition to total levels of both Rab5 and GDI. Quantification (C) of the density of the Rab5-GDI immunocomplex band are expressed as a % densitometry mean of normoxic controls ± S.D from three separate experiments. (asterisk * in (C) indicates a $p < 0.05$ from normoxic controls or between groups shown; ANOVA with post hoc Bonferroni test).

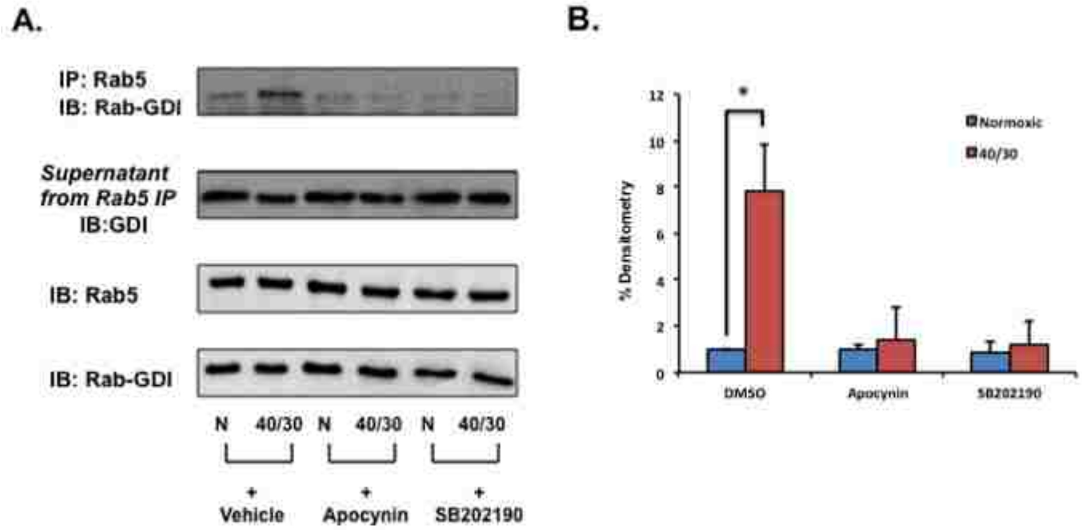

Figure 13. Inhibition of NADPH oxidase and p38 MAPK prevents the OGD/R-induced formation of the Rab5-GDI complex. Immunoprecipitated lysates (A) prepared from hippocampal slices subjected to time matched normoxia or OGD/R with either vehicle (1:1000 DMSO), 30 μM apocynin, or 10 μM of the selective p38 MAPK inhibitor SB202190 attenuates the formation of the Rab5-GDI complex. Quantification (B) of the density of the Rab5-GDI immunocomplex band are expressed as a % densitometry mean of normoxic controls ± S.D from three separate experiments. (askteriks * in (B) indicates a $p < 0.01$ from normoxic controls or between groups shown; ANOVA with post hoc Bonferroni test). Also illustrated in (A) is the GDI immunoreactive band resulting from the supernatant following immunoprecipitation of Rab5, in addition to total levels of both Rab5 and GDI.

Direct inhibition of p38 MAPK or clathrin-dependent endocytosis rescues the OGD/R-induced AMPAR surface removal and selective degradation of GluR2

As previously mentioned, p38 MAPK activation has been reported to mediate AMPAR surface removal (Zhong *et al.,* 2008; Xiong *et al*., 2006; Huang *et al*., 2005). Experiments were performed on OGD/R-treated adult rat hippocampal slices in the presence or absence of the selective p38 MAPK inhibitor SB202190 (10 μM) to examine the effect on GluR1 and GluR2 protein levels and surface expression. The addition of the selective p38 MAPK inhibitor SB202190 (10 μM) did not have any significant effect on the membrane translocation of $p67^{phox}$ (data not shown), indicating that SB202190 does not affect the OGD/R-induced increase in NADPH oxidase activity. However, inhibition of p38 MAPK prevented the OGD/R-induced decrease in total/membrane GluR2 protein levels (Fig. 14A-14D). In addition to rescuing the loss of GluR2 protein following OGD/R, treatment of SB202190 during reperfusion of OGD-treated slices also prevented the surface membrane removal of GluR1 and GluR2 (Fig. 14E and 14F), as assessed by biotin labeling of surface proteins and subsequent streptavidin bead pulldown. These observations demonstrate that p38 MAPK activity is involved in the rapid loss of surface AMPARs in rat hippocampal slices following exposure to OGD/R, presumably through the p38 MAPK-mediated stimulation of endocytic machineries. Through p38 MAPK mediated phosphorylation of GDI (Cavalli *et al.,* 2001), the activity of GDI in extracting GDP-bound Rab5 in increased, consequently forming the cytosolic GDI-Rab5 complex and allowing Rab5 to once again become GTP-bound for further Rab5 mediated endocytosis.

To further confirm the importance of endocytosis in the processes of the OGD/R-induced degradation of GluR2, slices were treated with hypertonic sucrose (0.45 M) to prevent clathrin coated pit formation (Heuser and Anderson, 1989). Studies have demonstrated that the formation of the clathrin coat is a necessary step for AMPAR internalization (Carroll *et al*., 1999). In agreement with previous findings, we found that hypertonic sucrose treatment prevented the surface removal of GluR2 as assessed by surface biotin labeling (Fig. 15C and 15D) of sucrose hypertonic OGD/R-treated slices, ultimately rescuing the selective degradation of GluR2 (Fig. 15A and 15B). These experiments further illustrate the importance of early endocytic trafficking in the OGD/R-induced loss of Glur2.

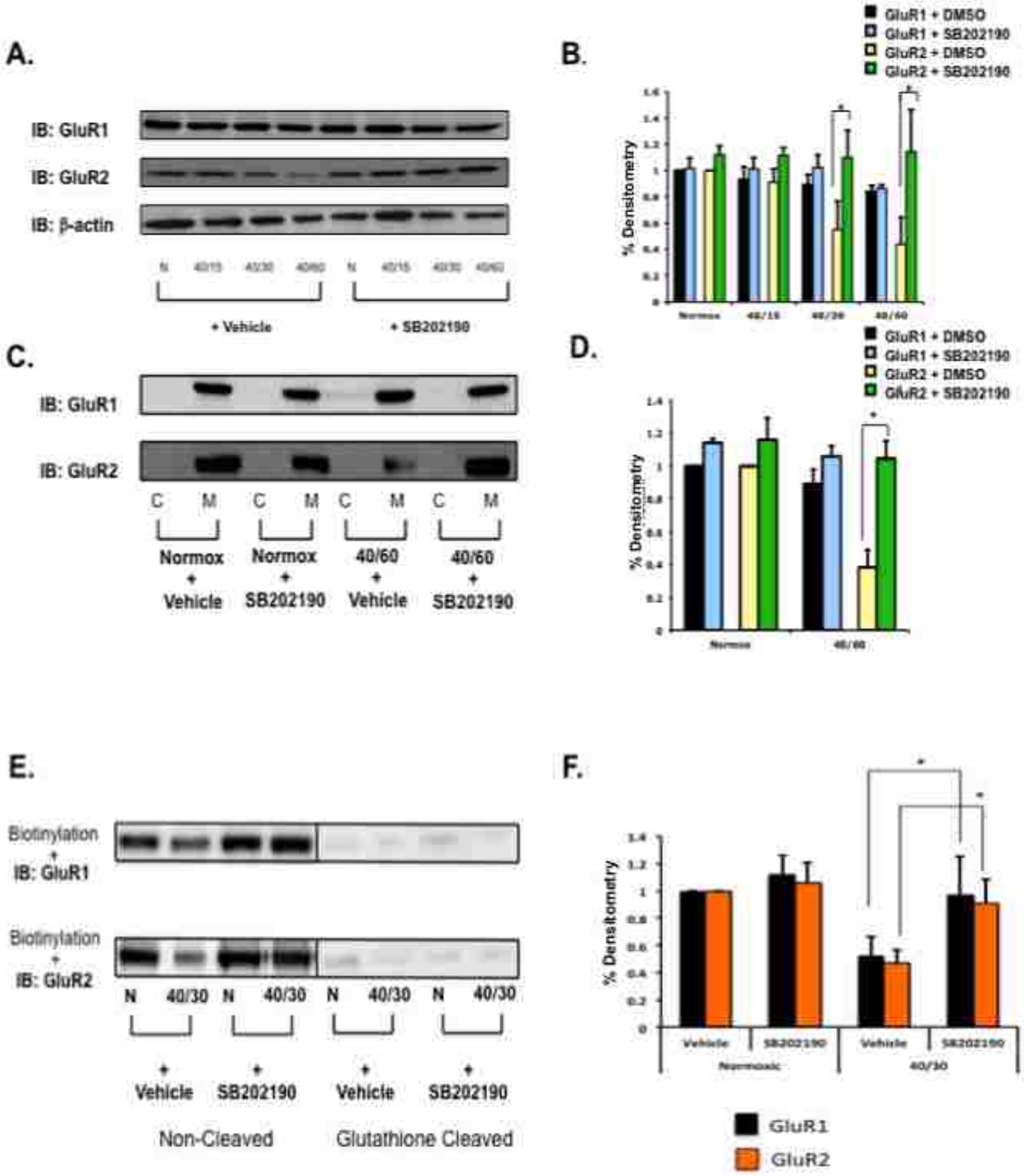
A.
IB: GluR1
IB: GluR2
IB: β-actin
+ Vehicle
+ SB202190
B.
GluR1 + DMSO
GluR1 + SB202190
GluR2 + DMSO
GluR2 + SB202190
% Densitometry
C.
IB: GluR1
IB: GluR2
C
M
Normox + Vehicle
Normox + SB202190
40/60 + Vehicle
40/60 + SB202190
D.
GluR1 + DMSO
GluR1 + SB202190
GluR2 + DMSO
GluR2 + SB202190
% Densitometry
E.
Biotinylation + IB: GluR1
Biotinylation + IB: GluR2
N
40/30
+ Vehicle
+ SB202190
Non-Cleaved
Glutathione Cleaved
F.
% Densitometry
GluR1
GluR2

Figure 14. Inhibition of p38 MAPK rescues GluR2 degradation following exposure to OGD/R. Lysates were prepared from hippocampal slices exposed to OGD/R with either vehicle (1:000 DMSO) or 10 μM of the p38 MAPK inhibitor SB202190. Representative western blots of total lysates (A), fractionated lysates (C) (cytosolic = C and membrane = M) or surface biotin labeled proteins isolated with streptavidin beads (E) from 4 independent experiments. Glutathione cleavage (75 mM) following biotin labeling is also illustrated as an additional control. Data is expressed in (B)**,** (D) and (F) as % mean densitometry of Normoxic vehicle treated control (corrected to β-actin in the case of (B)) ± S.D. (askterik * indicates a $p < 0.05$; ANOVA with post hoc Bonferroni test).

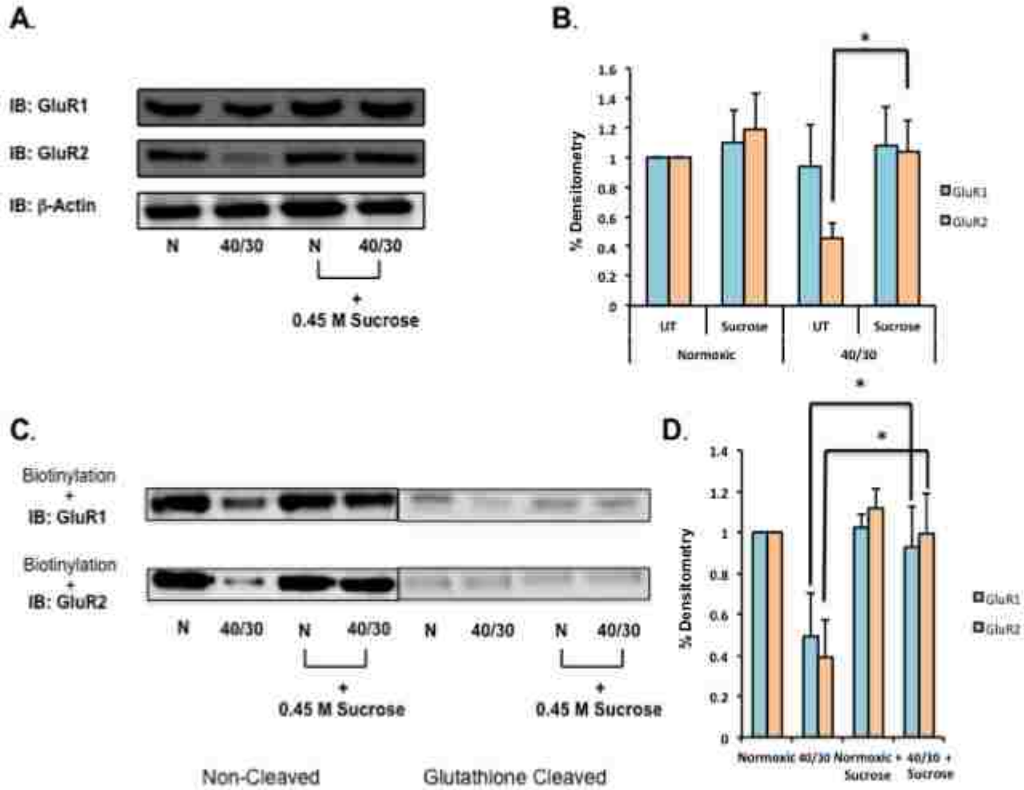

Figure 15. Inhibition of clathrin-dependent endocytosis rescues GluR2 degradation following exposure to OGD/R. Lysates were prepared from hippocampal slices exposed to OGD/R with or without hypertonic sucrose (0.45 M) added to aCSF. Representative western blots of total lysates (A) or surface biotin labeled proteins isolated with streptavidin beads (C) from 4 independent experiments. Glutathione cleavage (75 mM) following biotin labeling is also illustrated as an additional control. Data is expressed in (B) and (C) as % mean densitometry of Normoxic vehicle treated control (corrected to β-actin in the case of (B)) ± S.D. (askterik * indicates a $p < 0.05$; ANOVA with post hoc Bonferroni test).

Discussion

Following ischemia/reperfusion, the loss of surface GluR2-containing Ca^{2+}/Zn^{2+}-impermeable AMPARs correlates with areas of the brain most susceptible to delayed neuronal death (Liu *et al.,* 2004). This switch from Ca^{2+}/Zn^{2+}-impermeable to Ca^{2+}/Zn^{2+}-permeable AMPARs occurs through the surface removal and degradation of the GluR2 subunit (Dixon *et al*., 2009), the insertion of GluR2-lacking AMPARs to the plasma membrane (Liu *et al.,* 2006), in addition to transcriptional and translational downregulation of GluR2 transcript (Pelligrini-Giampietro *et al.,* 1997) and the RNA editing proteins involved in rendering GluR2 (Q607R) impermeable to divalent cation conductance (Peng *et al*., 2006).

In this study, we found that the OGD/R-induced activation of NADPH oxidase resulted in an increase in the endocytic machineries responsible for the internalization of AMPAR subunits. The data in this study indicate that ROS arising from NADPH oxidase activity during the reperfusion of OGD treated acute rat hippocampal slices are involved in the activation of p38 MAPK, which enhances Rab5/GDI complex formation and presumably accelerates Rab5 early endocytic trafficking by increasing the activity of GDI in extracting Rab5 from endosomal membranes, ultimately facilitating further endocytic traffic. Furthermore, the results from this study indicate a differential trafficking of the two AMPAR subunits GluR1 and GluR2, as OGD/R promoted the selective degradation of GluR2 while GluR1 protein levels remained largely unaffected, despite equal levels of GluR1 surface removal as GluR2. Inhibition of NADPH oxidase during OGD/R dampened p38 MAPK activation, decreased Rab5-GDI complex formation, and maintained significantly more GluR1 and GluR2 at the plasma membrane when compared to vehicle treated controls. Direct inhibition of p38 MAPK activity with the selective inhibitor SB202190 also maintained surface levels of GluR1 and GluR2, presumably through the inability of p38 MAPK to enhance endocytosis. Additionally, both p38 MAPK and NADPH oxidase inhibition during OGD/R also prevented the selective decrease in total GluR2 protein levels, thereby potentially rescuing the divalent cation impermeability of AMPARs in the hippocampus.

The activation of p38 MAPK has been established by previous studies to be both redox sensitive (Robinson and Cobb, 1997; Ogura and Kitamura 1998; Blair *et al.,* 1999) and activated by ischemia/reperfusion (Ozawa *et al.*, 1999; Sugino *et al.* 2000; Liu *et al*., 2009; Lu *et al*., 2011). While p38 MAPK activation has been clearly demonstrated to occur following ischemia/reperfusion, the exact upstream mechanisms that potentially modulate p38 MAPK activity are not yet fully resolved. One study has identified Nitric oxide (NO) as the upstream signal of p38 MAPK activation following hypoxia/re-oxygenation (Chen *et al*., 2009), while others have indicated a role for NADPH oxidase-derived ROS (Jian *et al*., 2011). Consistent with the findings of others (Abramov *et al*., 2007), we found that NADPH oxidase was the main contributor to the oxidative stress environment observed during the reperfusion of OGD subjected hippocampal slices. The data presented in this study strongly suggests that ROS derived from NADPH oxidase activity is an important mediator of p38 MAPK activity, but the contribution of nitric oxide synthase and other sources of ROS cannot be discounted.

Additionally, the data presented does not fully elucidate the mechanisms of how NADPH oxidase-derived ROS results in a sustained OGD/R-induced p38 MAPK activation. The activity of p38 MAPK pathways is tightly regulated and opposed by a family of dual-specificity MAPK phosphatases (Camps *et al*. 2000; Farooq and Zhou, 2004), which have been shown to become inactivated by ROS at low micromolar concentrations (Denu and Tanner, 1998; Seth and Rudolph, 2006). Furthermore, studies have shown that ROS-mediated inactivation of dual-specificity MAPK phosphatase activity potentially mediates enhanced MAPK activity under oxidative stress conditions (Hou *et al*., 2008). The inactivation of phosphatases involved in turning off p38 MAPK by ROS originating from the OGD/R-induced increase in NADPH oxidase activity must also therefore be considered as a potential target mechanism involved in the sustained p38 MAPK activation following OGD/R.

Various p38 MAPK inhibitors have been obviously demonstrated to afford neuroprotection following ischemia (Mackay and Mochly-Rosen, 1999; Barone *et al*., 2001; Legos *et al.,* 2001), primarily attributed towards shutting off pro-apoptotic signals and minimizing inflammation. Interestingly however, p38 MAPK inhibitors have also been demonstrated to provide neuronal protection in models of excitotoxic injury, specifically those demonstrated to be independent of affecting NMDAR electrophysiological currents or having any affect on NMDA agonist induced cell death (Legos *et al*., 2002), suggesting alternative pathways outside of the classic NMDAR excitotoxic induced caspase activation.

One such NMDA-independent alternative neuroprotective mechanism for p38 MAPK inhibition could be through the maintenance of surface levels of GluR2-containing AMPARs. Recent studies have demonstrated that the internalization of AMPARs is dependent on the p38 MAPK/Rab5-mediated endocytosis in a clathrin/dynamin-dependent manner (Cavalli *et al.,* 2001; Huang *et al.,* 2005; Zhong *et* *al.,* 2008). Rab5 serves as a key mediator of early endocytic trafficking events including early endosomal fusion (Gorvel *et al.,* 1991), internalization (Bucci *et al.* 1992), and clathrin-coated vesicle formation (McLauchlan *et al.,* 1999). GDI, when activated by p38 MAPK, extracts inactive GDP-bound Rab5 from endosomal membranes to form the cytosolic GDI-Rab5 complex (Cavalli *et al.,* 2001), eventually leading to Rab5 delivery to the plasma membrane where upon re-activation it can mediate endocytosis by triggering the formation of clathrin-coated pits, internalization, and subsequent sorting of receptors and other membrane protein into early endosome (McLauchlan *et al.,* 1999).

Given this important role of p38 MAPK/Rab5 in regulating endocytosis, the data from this study suggests that the large and sustained increase in activation of p38 MAPK is in part responsible for the accelerated surface removal of both the GluR1 and GluR2 AMPAR subunits following exposure to OGD/R. Our data supports that this is accomplished through the increase in the p38 MAPK-dependent GDI-Rab5 complex formation. Consistent with this notion, through inhibition of NADPH oxidase activity during OGD/R, our data show the OGD/R-induced p38 MAPK-mediated GDI-Rab5 complex formation is diminished. Similar inhibition of GDI-Rab5 complex formation during OGD/R is also seen with direct p38 MAPK inhibition using the selective p38 MAPK inhibitor SB202190. In line with these findings, through dampening the activity of the endocytic machinery involved in AMPAR surface removal following OGD/R with inhibition of NADPH oxidase or p38 MAPK, the data presented in this study showed that GluR1 and GluR2 surface protein levels were significantly increased compared to vehicle treated controls. Experiments performed with hypertonic sucrose to inhibit clathrin-mediated endocytosis also illustrate the importance of early endocytic steps in the surface removal and differential trafficking towards GluR2 degradation. Further studies need be done to fully understand the selective trafficking of GluR2 subunits towards degradative pathways, while GluR1 subunits protein levels remain intact. Additionally, the impact of OGD/R on endocytic recycling pathways needs to be studied, as dysregulation of the pathways involved in AMPAR re-insertion after surface removal may also serve as a critical event in the sustained loss of GluR2-containing AMPARs. Importantly however, the data indicates that through the attenuation of the OGD/R-induced acceleration of endocytic trafficking, the selective GluR2 trafficking towards degradation is prevented.

Collectively, this study provides compelling evidence for a NADPH oxidase-dependent oxidative stress signaling cascade involved in the OGD/R-induced surface removal of AMPAR subunits, ultimately leading to the subsequent selective degradation of GluR2.

CHAPTER 3

NADPH Oxidase Activity is involved in the Oxygen-Glucose Deprivation/Reperfusion-induced Serine880 phosphorylation of the AMPA Receptor GluR2 Subunit.

Abstract

Following ischemia/reperfusion, an interesting subunit composition switch occurs in which GluR2-subunit containing Ca^{2+}/Zn^{2+}- impermeable AMPA receptors change to GluR2-lacking Ca^{2+}/Zn^{2+}-permeable AMPA receptors, an event known to exacerbate delayed cellular death following stroke. In the present study, we investigated the early phosphorylation events leading to GluR2 surface removal in rat hippocampal slices following treatment with oxygen-glucose deprivation/reperfusion (OGD/R). We found that OGD/R results in a sustained phosphorylation of the GluR2 C-terminal serine residue 880 (Ser880), leading to the dissociation of GluR2 from the scaffolding proteins glutamate receptor interacting protein-1 (GRIP1) and AMPA receptor binding protein (ABP), thus favoring the association of GluR2 with protein interacting with C kinase-1 (PICK1), a protein known to be involved in diminishing surface expression of GluR2. Additionally, we found that inhibition of NADPH oxidase prevented the OGD/R-induced increase in Ser880 phosphorylation of GluR2, ultimately attenuating the loss of GRIP1/ABP-GluR2 interaction and diminishing the GluR2/PICK1 complex formation. Furthermore, inhibition of NADPH oxidase dampened the increase in activity of protein kinase C α (PCKα) following OGD/R and its subsequent association with PICK1, a necessary step prior to phosphorylation of Ser880 of GluR2. While the exact mechanisms of NADPH oxidase mediated GluR2 Ser880 phosphorylation have yet to be elucidated, outside of either directly or indirectly enhancing PKCα activity, this study provides some

of the first evidence in which NADPH oxidase dependent signaling may be involved in the surface signal of GluR2 subunit removal and subsequent degradation.

Materials and Methods

Preparation of acute rat hippocampal slices

Adult male (6-8 week) Sprague-Dawley rats (Charles River Labs, Wilmington, MA, USA) were anesthetized with isoflurane and rapidly decapitated. The entire brain was then removed and placed in an ice-cold cutting solution (75mM Sucrose, 80mM NaCl, 2.5 mM KCl, 1.25 mM NaH_2PO_4, 24 mM $NaHCO_3$, 25 mM Glucose, 4 mM $MgCl_2$, 1mM L-Ascorbic Acid, 3 mM Na Pyruvate, 0.5 mM $CaCl_2$, pH 7.4). Both hippocampi were then quickly dissected away from the brain and coronal 400 micron thick slices were made using a vibratome tissue chopper (McIlwain, Schwalbach, Germany). Slices were then subsequently equilibrated in oxygenated (95% O_2, 5% CO_2) artificial cerebrospinal fluid (aCSF; 124 mM NaCl, 2.5 mM KCl, 1.25 mM KH_2PO_4, 26 mM $NaHCO_3$, 10 mM Glucose, 1.5 mM $MgCl_2$, 2.5 mM $CaCl_2$, pH 7.4) for 90 minutes prior to treatment with OGD/R. Fresh aCSF was switched out every 30 minutes during equilibration. Pre-treatment with 30 µM apocynin (Sigma, St. Louis, MO, USA) or 1:1000 vehicle (DMSO) occurred during the final 30 minutes of the equilibration process and was present throughout the duration of the experiment, either during time matched normoxia treated controls or OGD and subsequent reperfusion.

Oxygen-Glucose Deprivation/Reperfusion of hippocampal slices

Following equilibration in oxygenated aCSF, slices to be treated with OGD/R were rinsed with aCSF without glucose (aCSF with 10 mM Mannitol substituted for 10 mM Glucose, pH 7.4) to remove glucose from the slices, and incubated for 40 minutes in a hypoxic glove box (Coy Laboratories, Grass Lake, MI, USA) containing a gas mixture of 0% O_2, 95% N_2, 5% CO_2 with aCSF minus glucose. The aCSF minus glucose media used for OGD was placed in 0% O_2 overnight to ensure complete anoxia. Following OGD, slices were removed from the hypoxic glove box and transferred back to oxygenated aCSF containing glucose for the time points indicated. Normoxic controls were left in aCSF containing glucose throughout the entire experiment and were time matched to the last of the OGD/R time points.

Lysate Preparation

Slices were removed from aCSF at the indicated time point and rinsed with ice cold PBS (pH 7.4). For total protein level detection, slices were places in tubes containing lysis buffer (250 mM Sucrose, 20 mM HEPES, 2 mM EDTA, 5 mM $MgCl_2$, 1 mM dithiothreitol, 1 mM AEBSF, 1% protease and phosphatase inhibitor cocktail (Thermo, Rockland, IL, USA), 1% Triton X-100, 0.01% saponin, pH 7.4) and lysed immediately via sonication for a 3 separate 5 second bursts at 25% power output with a VirTis Ultrasonic Cell Disrupter 100 (Gardiner, NY, USA). Samples were then spun at 1,000 x g to remove nuclei and cellular debris and a bicinchoninic acid assay (BCA, Thermo) assay was performed to determine protein content. Samples were then denatured in Laemmli buffer and heat (100°C) and resolved via sodium dodecyl sulfate polyacrylamide gel electrophoresis (SDS-PAGE). Samples were then transferred to a nitrocellulose membrane (Bio-Rad, Berkeley, CA, USA) for subsequent detection via immunoblotting.

Immunoblotting

Blots were blocked for 1 hour at room temp with either 5% BSA (for phospho-antibody detection) or 5% non-fat dry milk (for all others) in Tris Buffered Saline, 0.1% Tween 20, pH 7.5 (TBS-T). After blocking, blots were incubated with primary antibody overnight at 4°C at the concentration indicated. The affinity purified rabbit-monoclonal GluR2 antibody (1:2000), Protein Kinase C α (1:2000), and phospho-Protein Kinase C α (Thr497) (1:2000) were purchased from Epitomics (Burlingame, CA, USA). The affinity purified goat polyclonal PICK1 antibody was purchase from Santa Cruz Biotechnologies (Santa Cruz, CA, USA). The affinity purified rabbit polyclonal GRIP1 (1:1000) and ABP (1:1000) antibodies were purchased from Chemicon (Billerica, MA, USA). Goat anti-Mouse-HRP and Goat-anti-Rabbit-HRP secondary antibodies (1:2000) were purchased from Jackson ImmunoResearch (West Grove, PA, USA). The Donkey anti-Goat-HRP secondary antibody was purchased from Santa Cruz. Immunoreactive bands were visualized and captured with a Fuji imaging system using enhanced chemiluminescence after adding HRP conjugated secondary antibodies. Bands were analyzed using Fuji Image-Gauge software. Blots were stripped and re-probed up to 4 times using Restore Plus Western Blotting Stripping Buffer (Thermo).

Immunoprecipitation

To visualize the PICK1-PKCα and PICK1-GluR2 protein complex, rat hippocampal slices were lysed in a buffer containing 50 mM Tris-HCl, 150 mM NaCl, 1 mM EDTA, 1 mM phenylmethylsulfonyl fluoride, 1% NP-40, and 1% protease and phosphatase inhibitor cocktail, pH = 7.5. To immunoprecipitate GluR2-GRIP1, GluR2-ABP, and GluR2-PICK1, rat hippocampal slices were lysed in "GluR2 complex lysis Buffer" containing 20 mM HEPES, 2mM EDTA, 2 mM EGTA, 0.1 mM DTT, 100 mM KCl, 1% Triton X-100 and 1% protease and phosphatase inhibitor cocktail, pH = 7.2. Protein concentration was then determined using a BCA assay, and lysates (500 μg/sample in 500 μl) were then pre-cleared using Protein-A/G 50/50 mix of agarose beads for 1 hour at 4°C followed by incubation with either a PICK1 (1:50) or GluR2 (1:200) antibody overnight at 4°C. The immunocomplex was then incubated for 4 hours with 50 μL Protein-A/G beads at 4°C with rotation before being washed 3 times with lysis buffer. Samples were then eluted from the agarose beads by treatment with Laemmli buffer and heat (100°C) and subjected to 7.5% SDS-PAGE. After transfer to nitrocellulose membranes, blots were blocked as and incubated overnight at 4°C as previously described. Immunoreactive bands were analyzed using Fuji Image-Gauge software.

Introduction

Ischemic/reperfusion injury (stroke) is the leading cause of disability in the United States and Europe and the second leading cause of death in the world (Feigin, 2005), with effective therapeutics as yet to be discovered. At the cellular level, excessive stimulation of glutamatergic NMDARs and AMPARs have been demonstrated to play an important role in mediating excitotoxic ischemic/reperfusion-induced neuronal death (Arudine and Tymianski, 2003). When under proper physiologic control, AMPARs, which arise from 4 genes (GLUR1-GLUR4) to form a function receptor tetramer, mediate the majority of fast excitatory synaptic transmission in the CNS (Borges and Dingledine, 1998). AMPAR subunit composition varies depending on neuroanatomical location, but most areas tend to express AMPARs expressing the GluR2 subunit, especially in the hippocampus (Passafaro *et al.,* 2001). Following ischemia/reperfusion however, AMPARs undergo a subunit composition switch from GluR2 containing Ca^{2+}/Zn^{2+}- impermeable AMPA receptors to GluR2-lacking Ca^{2+}/Zn^{2+}-permeable AMPARs, thus allowing the AMPAR to excessively conduct calcium, an event in combination with overactive NMDAR stimulation exacerbates cellular death (Kwak *et al.,* 2006).

Under physiologic conditions, GluR2 endocytosis has been demonstrated to be mediated by protein kinase C alpha (PKCα) dependent phosphorylation of serine residue 880 (Ser880) (Chung *et al*., 2000). PKCα, when activated by calcium influx, is trafficked to the plasma membrane by protein interacting with C kinase 1 (PICK1) (Perez *et al.,* 2001), where it binds the GluR2 scaffolding protein AMPA receptor binding protein (ABP) and subsequently phosphorylates GluR2 at Ser880 (Lu and Ziff, 2005).

Phosphorylation of GluR2 at Ser880 promotes the dissociation of GluR2 with the scaffolding protein glutamate receptor interacting protein 1 (GRIP1), an interaction that is important in anchoring AMPARs to the plasma membrane (Matsuda *et al*., 2000). Additionally, Ser880 phosphorylation of GluR2 enables the increased binding of the subunit to PICK1 (Chung *et al.,* 2000), an interaction that has been shown to be important in decreasing surface GluR2 levels (Terashima *et al.,* 2004; Terashima *et al.,* 2008). As a result, the population of GluR2 containing AMPARs is reduced, ultimately allowing for an increase in calcium permeable GluR2-lacking AMPARs, an event important for synaptic strengthening under physiologic conditions (Seidenman *et al*., 2003), but ultimately deleterious if uncontrolled under pathologic conditions such as stroke (Noh *et al*., 2005).

Previous studies have demonstrated that ischemia/reperfusion leads to GluR2 dissociation from GRIP1, PICK1 association with ABP (Liu *et al*., 2006), and GluR2 association with PICK1, a step thought to be important in GluR2 endocytosis. Additionally, peptides interfering with PICK1 PDZ domain interactions have been shown to block the ischemia-induced AMPAR subunit composition switch, ultimately resulting in neuroprotection (Dixon *et al.,* 2009). However, the exact mechanisms beyond PKCα mediated signaling (Liu *et al.,* 2006) have not been fully described.

In this study, we show that oxygen-glucose deprivation/reperfusion (OGD/R) exposure of acute adult rat hippocampal slices results in an increase in Ser880 phosphorylation of the GluR2 subunit. Additionally, OGD/R results in an increase in activated PKCα-PICK1 interaction, a decrease in GluR2-GRIP1/ABP association, and an increase in GluR2-PICK1 interaction. Interestingly, the reactive oxygen species (ROS) generator NADPH oxidase, an enzyme known to contribute to oxidative stress (Abramov *et al.,* 2007) and cellular death following ischemia (Wang *et al.,* 2006), was found to be involved in the OGD/R-induced increase in Ser880 GluR2 phosphorylation. Inhibition of NADPH oxidase with apocynin not only reduced the OGD/R-induced increase in GluR2 Ser880 phosphorylation, but also prevented the decrease in GluR2-GRIP1/ABP association and attenuated GluR2-PICK1 interaction, ultimately rescuing the selective decrease in GluR2 protein levels. We therefore suggest that oxidative stress arising from increased NADPH oxidase activity contributes to GluR2 surface removal, ultimately increasing neuronal vulnerability to injury following ischemia/reperfusion.

Results

Oxygen-glucose deprivation/reperfusion results in an increase in activated PKCα-PICK association and GluR2 Ser880 phosphorylation

The endocytosis of GluR2 has been demonstrated to be both preceded and dependent on PKCα mediated Ser880 phosphorylation of the GluR2 subunit (Chung *et al.,* 2003). We therefore set to determine if exposure of acute adult rat hippocampal slices to OGD/R resulted in an increase in activated PKCα. In both total lysates and samples resolved via centrifugation and detergent extraction to yield cytosolic and membrane fractions, we found an overall increase in phospho-PKCα(Thr497) and a significant increase in phospho-PKCα(Thr497)-PICK1 association (data not shown), an event known to be an important step for GluR2 Ser880 phosphorylation (Lu and Ziff, 2005). Interestingly, OGD alone did not result in a significant PKCα-PICK1 association, but the reperfusion of OGD-treated slices did, ultimately resulting in a rapid and sustained phospho-PKCα-PICK1 interaction upon reperfusion. We also performed a time response experiment to determine a time course of the GluR2 Ser880 phosphorylation status in rat hippocampal slices treated to OGD/R and found that GluR2 Ser880 phosphorylation significantly increased during reperfusion while the total level of GluR2 protein decreased (Fig. 16A and 16B). Collectively, these initial results indicated that OGD/R promotes the activation of PKCα, which associates with PICK1 to promote the Ser880 phosphorylation of the AMPAR GluR2 subunit.

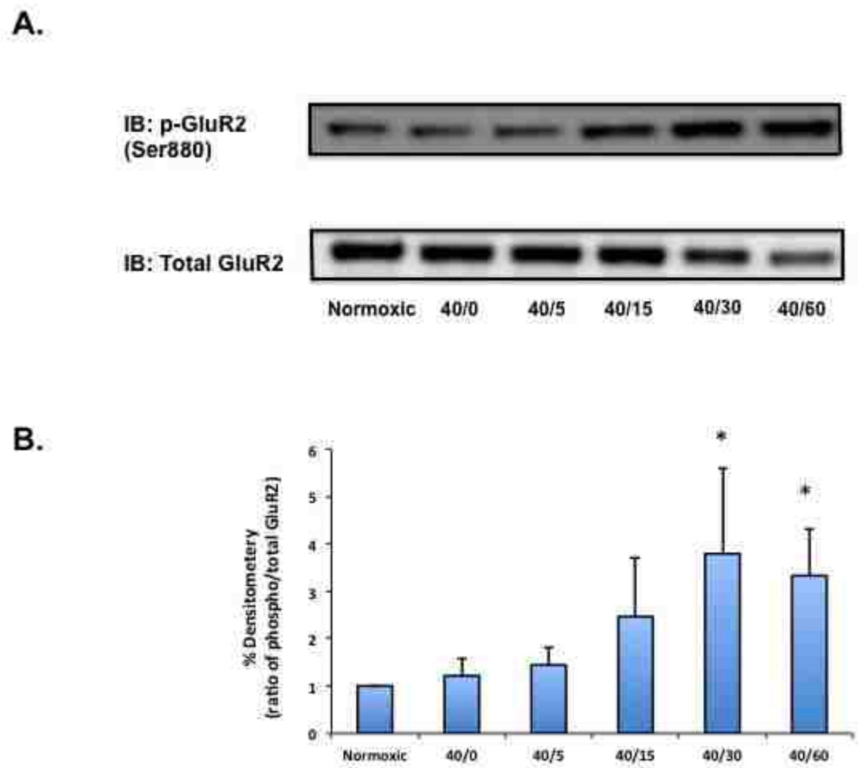

Figure 16. OGD/R exposure of adult rat hippocampal slices promotes the Ser880 phosphorylation of GluR2. Representative Western blot (A) from 3 independent experiments of hippocampal slices illustrates the time course of GluR2 Ser880 phosphorylation. Quantification (B) of GluR2 Ser880 phosphorylation levels expressed as a ratio of phospho-GluR2(Ser880) to total GluR2 protein levels. Data represent % densitometry mean (of normoxic control) ± S.D from three separate experiments. (askteriks * in (B) indicates a $p < 0.05$ from normoxic controls; ANOVA with post hoc Bonferroni test).

OGD/R promotes the association of GluR2 with PICK1 in acute adult rat hippocampal slices

The C-terminal Ser880 phosphorylation of GluR2 has been demonstrated to be involved in promoting the interaction of GluR2 with the PICK1, an event demonstrated to reduce surface expression of GluR2 (Terashima *et al.,* 2004, Terashima *et al.,* 2008). Ischemic-induced PICK1-GluR2 association has also been implicated in restricting GluR2 from recycling back to the plasma membrane (Dixon *et al.,* 2009), but has not been demonstrated in our model of stroke using acute adult rat hippocampal slices exposed to OGD/R. Therefore, experiments were performed to determine if the OGD/R-induced increase in Ser880 phosphorylation of GluR2 observed in rat hippocampal slices (Fig. 16A and 16B) functionally lead to an increase in GluR2-PICK1 association. Temporally consistent with the OGD/R-induced increase in activated PKCα-PICK1 and the increase in GluR2 Ser880 phosphorylation status, our results indicate a significant increase in GluR2-PICK1 association during reperfusion of OGD-treated slices (Fig. 17A and 17B). These results serve as a correlate with the increase in GluR2 Ser880 observed of GluR2 during the reperfusion of OGD-treated slices, and suggest a prevented recycling of GluR2 via PICK1-mediated membrane exclusion, data that is consistent with the findings of the previous study described in "CHAPTER 2" (see Fig. 9C and 9D).

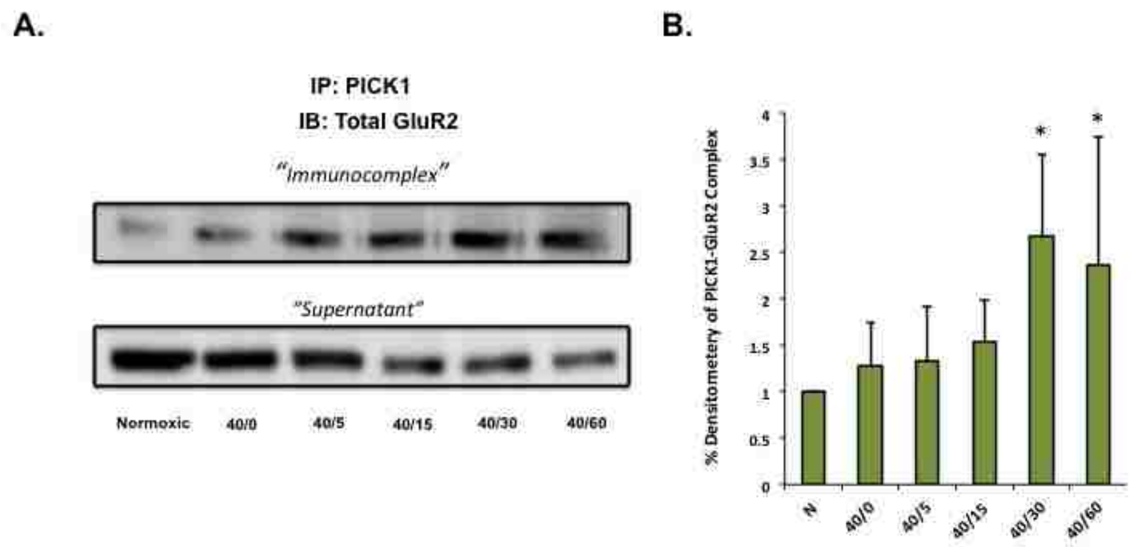

Figure 17. OGD/R promotes the association of PICK1 with GluR2. Lysates were prepared from hippocampal slices subjected to time matched normoxia, OGD alone, or OGD/R and immunoprecipitated with a PICK1 antibody (A). Also shown in (A) is the GluR2 immunoreactive band resulting from the supernatant following immunoprecipitation of PICK1, in addition to total levels of both PICK1 and GluR2. Quantification (B) of the density of the PICK1-GluR2 immunocomplex band are expressed as a % densitometry mean of normoxic controls ± S.D from three separate experiments. (askteriks * in (B) indicates a $p < 0.01$ from normoxic controls; ANOVA with post hoc Bonferroni test).

Inhibition of NADPH oxidase with apocynin decreases the OGD/R-induced increase in PKCα activation and subsequent Ser880 phosphorylation of GluR2

Apocynin, an inhibitor of NADPH oxidase activity, has been demonstrated by our lab and others to decrease ROS (Fig. 7; Genovese *et al.,* 2011), decrease damage to post-synaptic proteins (Murotomi *et al.,* 2011), and provide neuroprotection (Fig. 8; Wang *et al*., 2006) during ischemia/reperfusion. Oxidative stress has also been implicated in affecting ionic homeostasis during ischemia/reperfusion, through the enhancement of NMDAR currents (Hou *et al.,* 2007; Jian *et al.,* 2008), Phospholipase C mediated mobilization of intracellular calcium stores (Sato *et al*., 2009), mitochondrial calcium release (Clarke *et al*., 2008; Genovese *et al*., 2011) and the opening of cation channels (Hecquet and Malik, 2009) such as the transient receptor potential (melastatin) 2 (TRPM2). Therefore, we sought to determine if the reduction in oxidative stress observed with the inhibition of NADPH oxidase during OGD/R resulted in an attenuation of activated PKCα associated with PICK1. Our results illustrate that hippocampal slices pre-treated with apocynin (30 μM) prior to OGD/R showed a significant reduction in the activated form of PKCα associated with PICK1 (Fig. 18A and 18B), indicating that NADPH oxidase-mediated oxidative stress was involved in the OGD/R-induced increase in PKCα activity. Additionally, inhibition of NADPH oxidase activity also dampened the OGD/R-induced increase in GluR2 Ser880 phosphorylation (Fig. 18C and 18D). These experiments show that the increase in the oxidant environment following OGD/R resulting from NADPH oxidase activity contributes to the sustained activation of PKCα associated with PICK1 and the subsequent rise in GluR2 Ser880 phosphorylation.

A.

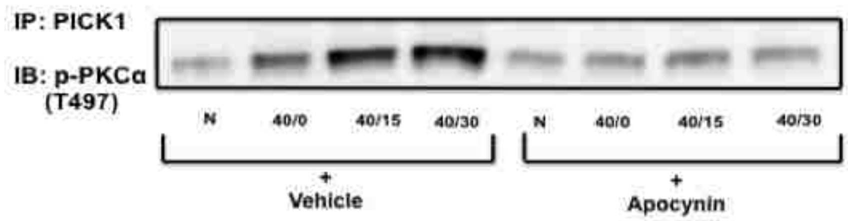
IP: PICK1
IB: p-PKCα
(T497)
N
40/0
40/15
40/30
N
40/0
40/15
40/30
+
Vehicle
+
Apocynin

B.

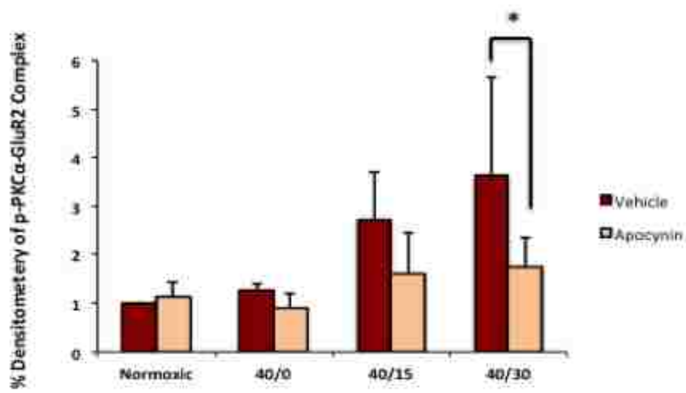
% Densitometery of p-PKCα-GluR2 Complex
Normoxic
40/0
40/15
40/30
Vehicle
Apocynin
*

C.

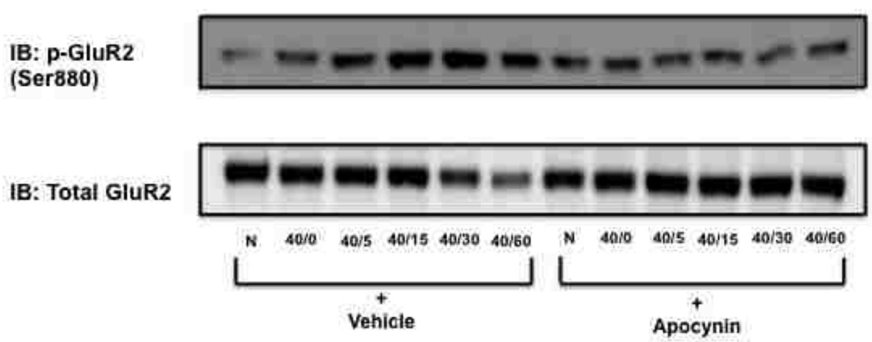
IB: p-GluR2
(Ser880)
IB: Total GluR2
N
40/0
40/5
40/15
40/30
40/60
N
40/0
40/5
40/15
40/30
40/60
+
Vehicle
+
Apocynin

D.

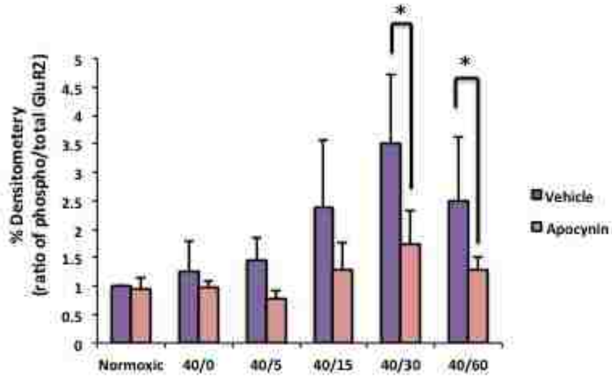
% Densitometery
(ratio of phospho/total GluR2)
Normoxic
40/0
40/5
40/15
40/30
40/60
Vehicle
Apocynin
*
*

Figure 18. The OGD/R-induced increase in activated PKCα associated with PICK1 and rise in Ser880 phosphorylation of Glur2 is blunted with inhibition of NADPH oxidase. Representative Western blot (A) from 3 independent experiments of hippocampal slices illustrates the pattern of PKCα (phospho-Thr497)-PICK1 association of slices exposed to OGD/R in the presence of vehicle (1:1000 DMSO) or apocynin (30 μM) pre-treatment. (C) Representative Western blot of the OGD/R-induced increase in GluR2 Ser880 phosphorylation. Quantification (B) of the density of the phospho-PKCα(Thr497)-PICK1 immunoreactive band expressed as the relative % mean densitometry of normoxic controls. Quantification (D) of GluR2 Ser880 phosphorylation levels expressed as a ratio of phospho-GluR2(Ser880) to total GluR2 protein levels. Data represent % densitometry mean (of normoxic control) ± S.D from three separate experiments. (askteriks * in (B) and (D) indicates a $p < 0.05$ from normoxic controls; ANOVA with post hoc Bonferroni test).

Inhibition of NADPH oxidase prevents the OGD/R-induced increase in GluR2-PICK1 association and OGD/R-induced loss of GluR2-GRIP1 association

On the C-terminal tail of GluR2, the sequence (IESVKI) serves as the PKCα mediated phosphorylation site at Ser880 and also as a PDZ binding domain. When GluR2 is in the dephospho-Ser880 state, it preferentially binds the PDZ binding scaffolding proteins GRIP1 and ABP, which have been demonstrated to be important in retaining GluR2 at the plasma membrane (Dong *et al,* 1997; Dong *et al.,* 1999). Upon Ser880 phosphorylation, the affinity for GRIP1 and ABP is reduced and the binding of another PDZ binding protein, PICK1 is promoted (Chung *et al.,* 2000), potentially facilitating the surface removal of GluR2. Therefore, experiments were performed to determine if the decrease in Ser880 GluR2 phosphorylation observed with NADPH oxidase inhibition during OGD/R resulted in maintenance of GluR2-GRIP1/ABP anchoring, as well as a decrease in GluR2-PICK1 association. Consistent with the findings from the previous figure (Fig. 18) of an OGD/R-induced increase in GluR2 Ser880 phosphorylation, inhibition of NADPH oxidase with apocynin prevented the disruption of GluR2-GRIP1/ABP anchoring (Fig. 19A-19D). Additionally, the interaction between GluR2-PICK1 was diminished (Fig. 19E and 19F), further confirming the role of NADPH oxidase in promoting the OGD/R-induced increase in GluR2 Ser880 phosphorylation and the interaction of GluR2 with its PDZ binding partners GRIP1, ABP, and PICK1.

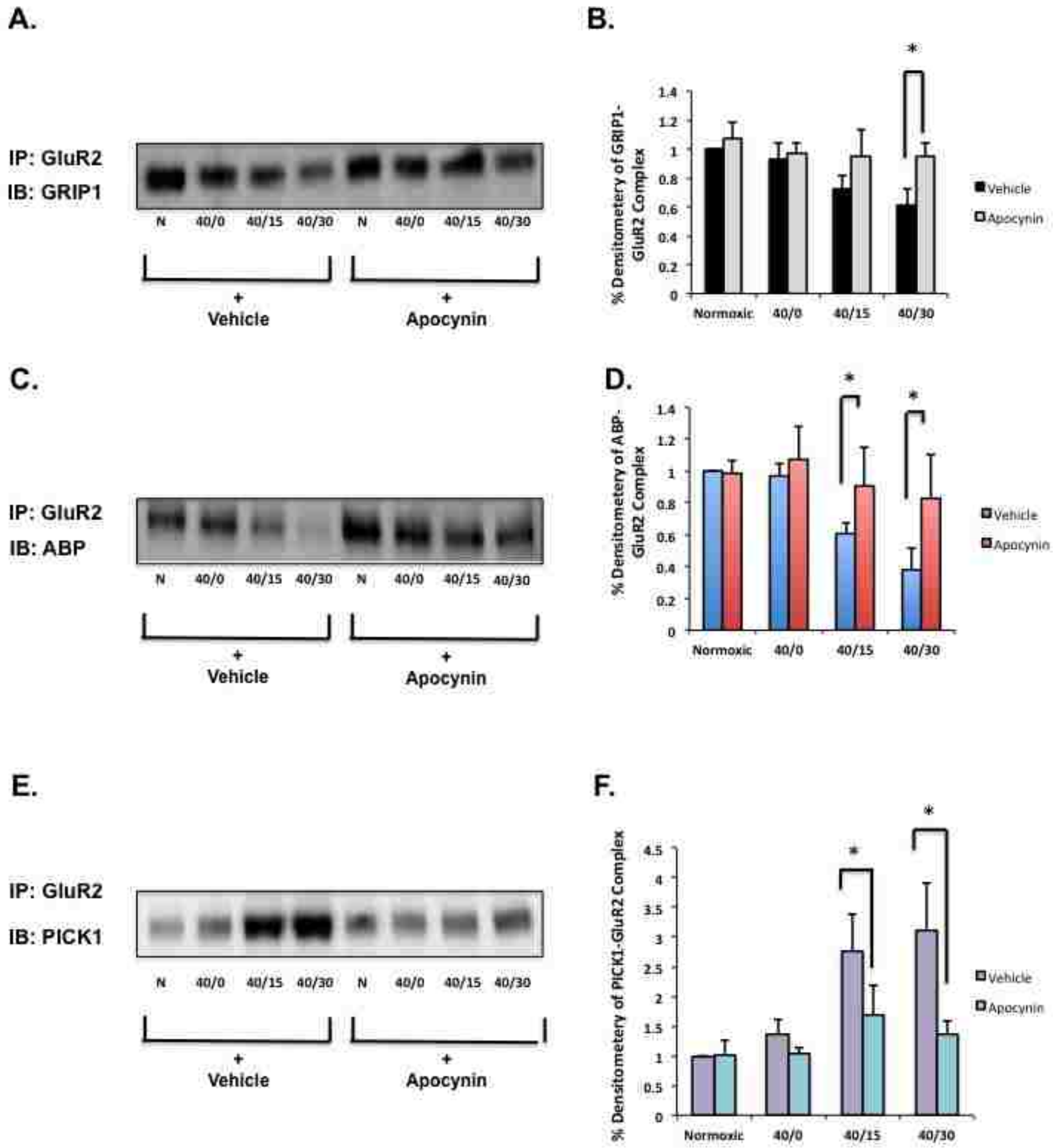
A.
IP: GluR2
IB: GRIP1
N
40/0
40/15
40/30
N
40/0
40/15
40/30
+
Vehicle
+
Apocynin
B.
% Densitometery of GRIP1-GluR2 Complex
Normoxic
40/0
40/15
40/30
Vehicle
Apocynin
C.
IP: GluR2
IB: ABP
+
Vehicle
+
Apocynin
D.
% Densitometery of ABP-GluR2 Complex
Normoxic
40/0
40/15
40/30
Vehicle
Apocynin
E.
IP: GluR2
IB: PICK1
+
Vehicle
+
Apocynin
F.
% Densitometery of PICK1-GluR2 Complex
Normoxic
40/0
40/15
40/30
Vehicle
Apocynin

Figure 19. Inhibition of NADPH oxidase restores the OGD/R-induced loss of GluR2-GRIP1/ABP anchoring and prevents the association of GluR2 with PICK1. Lysates were prepared from hippocampal slices subjected to time matched normoxia, OGD alone, or OGD/R in the presence of vehicle (1:1000) or apocynin (30 μM), followed by immunoprecipitation of GluR2 and subsequent immunoblotting for GRIP1 (A), ABP (C) and PICK1 (E) complex formation. Quantification (B, D, F) of the density of the GluR2-GRIP1, GluR2-ABP, and GluR2-PICK1 immunocomplex band are expressed as a % densitometry mean of normoxic controls ± S.D from three separate experiments. (askteriks * indicates a $p < 0.05$; ANOVA with post hoc Bonferroni test).

Disruption of the OGD/R-induced PICK1-GluR2 association does not effect Ser880 phosphorylation status of GluR2, but does rescue OGD/R-induced GluR2 degradation

PICK1 has been implicated to be involved in decreasing the surface expression of GluR2-containing AMPARs in both synaptic physiology (Xia *et al*., 2000; Lu and Ziff, 2005) and CNS pathology such as tramautic brain injury and ischemia (Bell *et al.,* 2009; Dennis *et al.,* 2011). To more precisely determine the importance of the GluR2-PICK1 interaction in GluR2 trafficking during OGD/R, a direct approach at disrupting the GluR2-PICK1 interaction was used with the compound FSC231, a small-molecule inhibitor of the PDZ domain on PICK1 (Thorsen *et al.,* 2010). Due to solubility issues in vehicle delivery, liposomal packaging was used for our drug delivery method. While slices treated to OGD/R alone or OGD/R with the empty liposomal vehicle resulted in an increase in PICK1-GluR2 association, the OGD/R-induced interaction of PICK1 with GluR2 was diminished when slices were treated with liposomes packaged with FSC231 (100 μM) (Fig. 20A and 20B). Interestingly, while FSC231 did not prevent the OGD/R-induced increase in Ser880 phosphorylation, it did significantly rescue total levels of GluR2 protein (Fig. 20C and 20D). These data suggest that the interaction of GluR2 with PICK1 serves as an important step in the OGD/R-induced selective degradation of GluR2 protein levels, either through an enhanced PICK1-mediated surface removal (Lu and Ziff, 2005; Bell *et al.* 2009) or a possible ubiquitin-PICK1 directed degradative trafficking mechanism (Joch *et al.,* 2007).

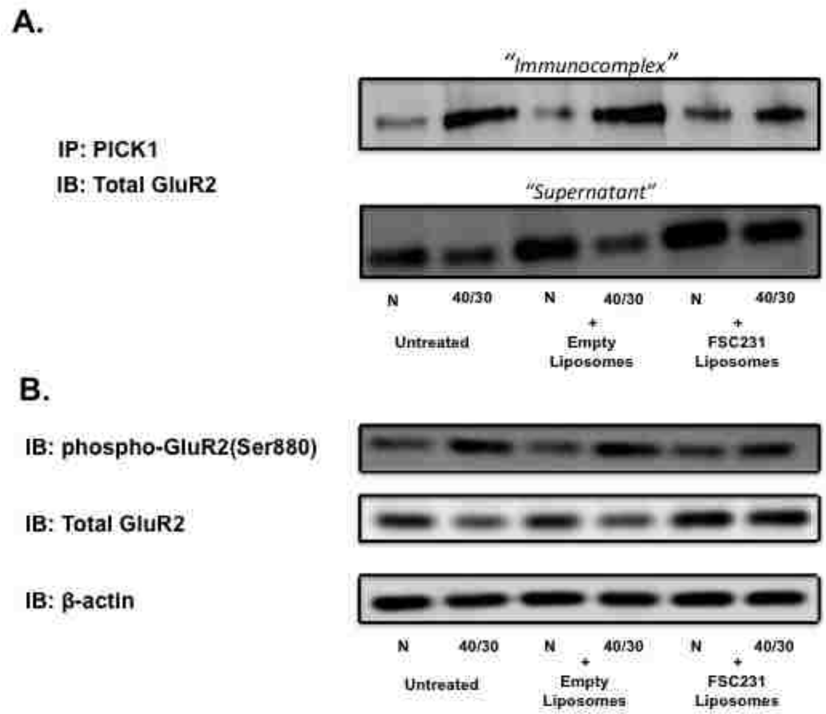

Figure 20. Direct inhibition of GluR2 association with PICK1 using the small-molecule inhibitor FSC231 rescues the OGD/R-induced loss of GluR2 protein levels. Lysates were prepared from hippocampal slices subjected to time matched normoxia or OGD/R in the presence of an empty liposomal vehicle or liposomes packaged with FSC231 (100 μM), followed by immunoprecipitation of PICK1 and subsequent immunoblotting for GluR2 (A). Also shown in (A) is the GluR2 immunoreactive band resulting from the supernatant following immunoprecipitation of PICK1. Lysates prepared from the same samples were also directly subjected to SDS-PAGE and immunoblotting (B) for determination of total protein levels of GluR2, phospho-GluR2(Ser880) and β-actin as a loading control.

Discussion

Multiple lines of evidence have shown that the activation of Ca^{2+}/Zn^{2+}-permeable AMPARs following ischemic injury significantly contributes to neuronal death (Yin *et al*., 2002; Anzai *et al.* 2003; Calderone *et al.,* 2004; Liu *et al.,* 2004; Noh *et al.* 2005; Liu *et al.* 2006). While it has been demonstrated that ischemia results in a decrease in GluR2 protein levels and an increase in AMPAR-mediated Ca^{2+} currents (Gorter *et al.,* 1997), the exact mechanistic signals resulting in GluR2-mediated surface removal have yet to be fully elucidated.

In this study, the data presented indicate that NADPH oxidase activity following OGD/R promotes the surface removal of GluR2 through increasing PKCα Ser880 phosphorylation of the GluR2 subunit. We found that inhibition of NADPH oxidase activity with apocynin during OGD/R not only dampened localized activation of PKCα with PICK1, but also attenuated the OGD/R-induced increase in Ser880 phosphorylation of GluR2. Furthermore, the decrease in Ser880 phosphorylation observed with NADPH oxidase inhibition during OGD/R also resulted in a decreased GluR2 interaction with PICK1, in addition to maintaining association of GluR2 with the membrane anchoring proteins GRIP1/ABP, ultimately rescuing the OGD/R-induced loss of GluR2 protein levels. Direct inhibition of the PICK1-GluR2 interaction with the small-molecule inhibitor FSC231 did not prevent the OGD/R-induced increase in GluR2 Ser880 phosphorylation, but did attenuate the interaction of PICK1 with GluR2 following exposure to OGD/R. Interestingly, FSC231 treatment during OGD/R also lead to a rescue of total GluR2 protein levels, suggesting the interaction of GluR2 with PICK1 serves as an important step in the ischemic-induced reduction in total GluR2 protein levels.

The PKCα-mediated Ser880 phosphorylation of GluR2 (Xia *et al*., 2000) has been shown to be important in the surface removal of GluR2 (Chung *et al*., 2000). While some studies have indirectly implicated that increased Ser880 phosphorylation of GluR2 occurs during ischemia/reperfusion (Liu *et al*., 2006), no studies to date have directly shown that an increase in Ser880 occurs with such treatment. We directly found that Ser880 phosphorylation of GluR2 increased significantly during reperfusion of OGD-exposed slices, but not during OGD without reperfusion. Our data also indicated that the association of activated PKCα with PICK1, a step necessary prior to Ser880 phosphorylation of GluR2 (Lu and Ziff, 2005), occurred maximally during reperfusion of OGD treated slices and not during OGD alone, data that is consistent with the time course established for the increase in Ser880 phosphorylaiton of GluR2.

Phosphorylation of GluR2 at Ser880 has been shown to disrupt the GluR2 association with GRIP1/ABP, proteins that are important in the anchoring of AMPARs to the cell surface (Matsuda *et al*., 2000). Dissociation from GRIP1/ABP exposes the PDZ binding domain on GluR2 where the Ser880 residue resides, and when phosphorylated, consequently has a high affinity for the PDZ binding domain of PICK1 (Dong *et al*., 1997), a protein important in restricting GluR2 from the cell surface (Terashima *et. al*. 2004; Terashima *et. al*. 2008). Ischemia has been shown previously to enhance the interaction of PICK1 with GluR2 and decrease the association of GRIP1/ABP with GluR2 (Liu *et al*., 2006). Consistent with these findings, the data presented in this study illustrates a significant increase in PICK1-GluR2 association as the GRIP1/ABP interaction with GluR2 decreases. Interestingly, inhibition of NADPH oxidase with apocynin maintains GluR2 anchoring to GRIP1/ABP and decreases PICK1-GluR2 association following OGD/R, findings in line with the decrease in GluR2 Ser880 phosphorylation observed with NADPH oxidase inhibition during OGD/R.

Additional studies need be performed to determine the precise manner in which NADPH oxidase contributes to the OGD/R-induced increase in PKCα activation and GluR2 Ser880 phosphorylation. The first possibility involves the direct redox-modulation of PKCα via NADPH oxidase derived ROS. Published reports have demonstrated that PKC activity is increased with oxidative stress (Ward *et al*. 1998), which can be attenuated with anti-oxidant treatment using α-tocopherol (de Diego-Ortero *et al*., 2009) or apocynin treatment (Tuttle *et al.,* 2009). However, studies have demonstrated that α-tocopherol reduces PKCα activity through non-antioxidant effects (Zingg and Azzi, 2004), potentially confounding the published results of redox-sensitive PKC activity. However, a reduction in glutathione levels has been reported to result in drastic increases in PKC activity (Ward *et al.,* 1998). Further research must be completed to fully understand the relationship between ROS and direct PKC activation.

A second possibility for OGD/R-induced NADPH oxidase-mediated increases in PKCα activity includes phosphatase inactivation. Protein phosphatase 1 (PP1) and protein phosphatase 2A (PP2A) have been demonstrated to be important in regulating PKC activity (Thiels *et al.,* 1996). Studies have shown that H_2O_2-induced oxidative stress inactivates both PP1 and PP2A, which is prevented with antioxidant treatment (O'Loghlen *et al*, 2003). Additionally, PP1 has been identified as the phosphatase responsible for the Ser880 dephosphorylation of GluR2 (Hu *et al.,* 2007). OGD/R-induced ROS-mediated inactivation of this phosphatase may therefore serve as an important mediator in not only regulating PKC activity, but also GluR2 Ser880 phosphorylation. Furthermore, studies have demonstrated that the filamentous actin binding protein neurabin is important in targeting PP1 to the post-synapse for GluR2 Ser880 dephosphorylation (Hu *et al*., 2007). Additionally, oxidative stress has been shown to result in the de-polymerization of actin (Tiago *et al.,* 2006), thereby potentially decreasing the synaptic localization of PP1 necessary for GluR2 Ser880 de-phosphorylation. Decreased synaptic localization in addition to increased phosphatase inactivation could be important steps involved in the sustained activation of PKCα and phosphorylation of GluR2, events that are attenuated with apocynin by decreasing NADPH oxidase-mediated oxidative stress during OGD/R.

A third possibility for the mechanism in which OGD/R-induced NADPH oxidase activity mediates PKCα activation involves enhancing intracellular Ca^{2+} concentrations. PKCα activity is positively regulated by increases in Ca^{2+} (Tiruppathi *et al*., 2006), therefore, any enhancement in Ca^{2+} concentrations will increase PKCα activity. Oxidative stress and NADPH oxidase activity has been linked to effecting Ca^{2+} levels through NMDARs (Hou *et al*., 2007; Murotomi *et al.,* 2008), phospholipase C-dependent release of intracellular Ca^{2+} stores (Sato *et al*., 2009), mitochondrial Ca^{2+} release (Clarke *et al.*, 2008; Genovese *et al.,* 2011) as well as the opening of cation channels (Hecquet and Malik, 2009). Therefore, inhibition of NADPH oxidase activity during OGD/R could potentially accomplish the dampening of PKCα activity not only through the maintenance of PP1 and PP2A phosphatase activity, but also through the attenuation of oxidative stress-enhanced rises in Ca^{2+} entry and intracellular Ca^{2+} release necessary for PKCα activation.

Taken together, this study, in combination with the data presented in “CHAPTER 2”, demonstrates the effect of OGD/R-induced NADPH oxidase-mediated oxidative stress on GluR2 membrane scaffolding as well as the effect on the endocytic machineries responsible for the surface removal of the AMPAR GluR2 subunit. Though these data provide a novel mechanism for the OGD/R-induced loss of GluR2 surface proteins, further studies will be necessary to fully characterize the upstream signaling pathways involved in mediating PKCα activation and the resultant increase in GluR2 Ser880 phosphorylation.

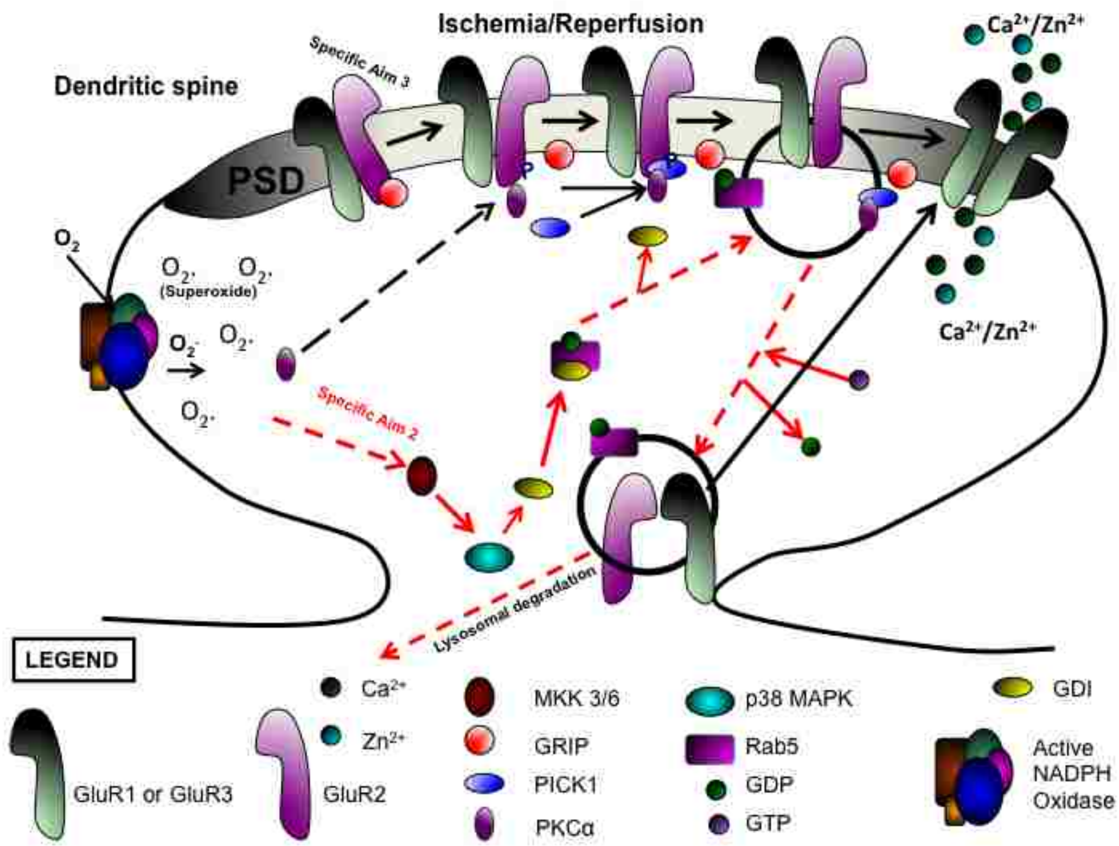

Diagram 9. Proposed Model for CHAPTER 2 and CHAPTER 3. Following Ischemia/Reperfusion, NADPH oxidase activity is responsible for the internalization of GluR1 and GluR2 AMPAR subunits via signaling for an increase in activity in the endocytic machinery (*red arrows*) and the Ser880 phosphorylation GluR2, leading to decreased GluR2 membrane scaffolding (*black arrows*).

OVERALL SUMMARY AND CONCLUSIONS

The focus of this research was to examine the role of the superoxide producing enzyme NADPH oxidase in signaling for altered receptor trafficking and function of post-synaptic ionotropic NMDA and AMPARs following ischemic/reperfusion-injury. Superoxide production arising from NADPH oxidase has been implicated in governing many processes of NMDA and AMPA receptor function (ex: LTP/LTD) under physiologic conditions, although the precise role of NADPH oxidase in contributing to these processes under pathologic insults such as ischemia/reperfusion has not been fully investigated.

The NADPH oxidase enzyme complex is responsible for superoxide production in wide variety of tissues and cells arising from the assembly of five NADPH oxidase subunits, two of which that are membrane bound ($gp91^{phox}$, $p22^{phox}$) and three of which are cytosolic activators ($p40^{phox}$, $p47^{phox}$, $p67^{phox}$) which translocate from the cytosol to the membrane in order to form the functional holoenzyme complex. Superoxide is produced via the one electron oxidation of NADPH to $NADP^+$ and the subsequent electron transfer along the NADPH oxidase enzyme subunits necessary for the single electron reduction of molecular oxygen (O_2) to superoxide ($O_2^{\bullet}$), a reactive free-radical due to its unpaired electron. The superoxide produced from NADPH oxidase activity has been demonstrated to be a critical step important in the processes learning and memory through a balanced and controlled redox environment. However, the overproduction of superoxide from NADPH oxidase has also been shown to be involved in contributing to neuronal death in a number of CNS pathologies, including stroke. Therefore, experiments were performed to investigate a potential link between the ischemia/reperfusion-induced over-activation of NADPH oxidase and possible downstream signaling events leading to the enhanced activity of NMDA and AMPA receptors known to contribute to excitotoxic cell death through enhanced calcium entry and resultant calcium cytotoxicity.

In the first study, we sought to determine the involvement of NADPH oxidase activity in mediating enhanced NMDAR function following oxygen-glucose deprivation/re-oxygenation (OGD/R). The influx of calcium ions through NMDAR channels has long been established as a critical mediator of synaptic plasticity. Additionally, calcium ion influx from NMDA receptors has also long been implicated in excitotoxic neuronal death following stroke. Studies have demonstrated that superoxide from NADPH oxidase is an important mediator of NMDA receptor function, specifically through potentiating NMDA receptor currents via redox signaling. Given the critical role of NADPH oxidase-dependent enhancement in synaptic plasticity, the role of NADPH oxidase activity in mediating NMDAR function following stroke is an important process to investigate.

Using cultured retinoic acid differentiated SH-SY5Y human neuroblastoma cells, we demonstrated that that OGD/R-treated cultures resulted in an increase in superoxide production, which was significantly diminished with pharmacologic inhibition of NADPH oxidase. Furthermore, following re-oxygenation of OGD-treated cultures, an increased tyrosine phosphorylation of the NR2A NMDA receptor subunit was observed, an event necessary for the potentiation of NMDAR currents. Additionally, the OGD/R-induced increase in NR2A tyrosine phosphorylation coincided with the time course of increased NADPH oxidase activity. In addition to diminishing superoxide production following oxygen-glucose deprivation/re-oxygenation, we found that pharmacologic inhibition of NADPH oxidase also attenuated the OGD/R-induced increase in NR2A tyrosine phosphorylation. We next examined the activation of Src family kinases (SKFs), a family of tyrosine kinases previously demonstrated to be important in mediating the tyrosine phosphorylation of NMDAR subunits and subsequent potentiation of NMDAR currents. We found that SFKs bound to the NMDA receptor scaffolding protein post-synaptic density protein 95 (PSD-95) increased in activity during re-oxygenation of OGD-treated cultures minutes prior to NR2A tyrosine phosphorylation. Furthermore, we found that direct inhibition of SFK activity diminished the OGD/R-induced increase in NR2A tyrosine phosphorylation, suggesting that SFKs are the tyrosine kinases involved in mediating NR2A tyrosine phosphorylation. SFKs have been shown to be redox sensitive in their activation patterns, so we next sought to determine if NADPH oxidase-dependent ROS was involved in mediating the activity of SFKs. Indeed, pharmacologic inhibition of NADPH oxidase during re-oxygenation of OGD-treated cultures diminished activated SFK scaffolding to PSD-95, implicating an involvement of NADPH oxidase derived ROS following OGD/R in the increase in tyrosine phosphorylation of the NMDA receptor NR2A subunit via increasing SFK activity. Lastly, to functionally examine that inhibition of NADPH oxidase decreased NMDAR signaling, we demonstrated that inhibition of NADPH oxidase attenuated the agonist-induced NMDAR mediated cellular death following OGD/R. Taken together, this study is the first to demonstrate a plausible downstream signaling event and cellular mechanism involved in the neuroprotection observed by various other labs with NADPH oxidase inhibition during ischemia/reperfusion.

In the second study, we examined whether the OGD/R-induced decrease total protein levels and surface expression of the AMPAR GluR2 subunit involved NADPH oxidase activity. AMPARs are another type of ionotropic glutamate receptors known to be critically important in synaptic plasticity. However, unlike NMDARs, most AMPARs in the CNS are impermeable to calcium influx upon glutamate stimulation and subsequent channel opening, especially in the hippocampus. The presence of the edited GluR2 (Q607R) subunit, one of four (GluR1-4) which combine in varying stoichiometeries to form a functional AMPA receptor tetramer, is responsible for governing this impermeability to divalent cations. However, following ischemic/reperfusion injury, AMPA receptors undergo an unusual subunit composition change from Ca^{2+}/Zn^{2+}-impermeable GluR2-containing AMPA receptors to Ca^{2+}/Zn^{2+}-permeable GluR2-lacking AMPA receptors, an event demonstrated to correlate with calcium cytotoxicity and subsequent delayed-neuronal death. Given that reactive oxygen species have been implicated in the endocytosis of numerous receptors, we sought to determine if NADPH oxidase mediated redox-signaling events were responsible for AMPAR sequestration and degradation following ischemia/reperfusion.

Using acute rat hippocampal slices prepared from adult (6-8 weeks old) males, we found that pharmacologic inhibition of NADPH oxidase diminished ROS generation in hippocampal slices during reperfusion of OGD-exposed slices. Through the use of surface labeling techniques, we found that OGD/R-treated hippocampal slices resulted in the internalization of the two most prominent AMPAR subunits, GluR1 and GluR2. However, when examining total protein levels of both receptor subunits, we found that only the GluR2 subunit was degraded, while GluR1 protein levels were mostly unaffected. Pharmacologic inhibition of NADPH oxidase activity following OGD/R not only rescued surface levels of both GluR1 and GluR2, but also prevented the selective decrease in GluR2 protein levels. Previously, the role of p38 mitogen-activated kinase (p38 MAPK) has been established as a key mediator in signaling for AMPAR surface removal by enhancing the activity of Rab5, a protein important in early endocytic trafficking. To investigate the possibility of p38 MAPK signaling, we found that the activity of p38 MAPK dramatically increased during reperfusion of OGD-treated hippocampal slices. Additionally, OGD/R resulted in Rab5 complex formation with guanosine nucleotide dissociation inhibitor (GDI) in a similar time-course as the increase in p38 MAPK activity. This event has been previously documented to be the mechanism through which p38 MAPK accomplishes increased surface removal of AMPA receptors. Given that p38 MAPK is in part regulated via cellular stress-signals such as oxidative stress, we sought to determine if NADPH oxidase served as an important signal for p38 MAPK activation following OGD/R. Indeed, inhibition of NADPH oxidase derived ROS during OGD/R not only decreased p38 MAPK activation, but also diminished Rab5-GDI complex formation, providing evidence that the rescue in surface AMPA receptor levels observed with NADPH oxidase inhibition during OGD/R is accomplished through attenuating p38 MAPK-dependent endocytic signals. Furthermore, direct pharmacologic inhibition of p38 MAPK activity also prevented Rab5-GDI complex formation, rescued AMPA receptor surface removal, and ultimately prevented the selective degradation of GluR2 subunit protein levels. Inhibition of clathrin-dependent endocytosis with hypertonic sucrose treatment also prevented the OGD/R-induced surface removal of

AMPA receptor subunits in addition to rescuing GluR2 protein loss, further illustrating the importance of early endocytic events in the OGD/R-induced degradation of GluR2.

In the third study, we sought to expand upon the OGD/R-induced NADPH oxidase-dependent GluR2 trafficking by examining phosphorylation and protein-protein interaction events known to be important in GluR2 surface removal. Using the same acute adult rat hippocampal slice model as previously discussed, we found that serine phosphorylation of the C-terminal tail of the GluR2 subunit at residue 880 increased following exposure to OGD/R. In its non-phosphorylated state, GluR2 is held at the plasma membrane via protein-protein interactions with the scaffolding proteins glutamate receptor interacting protein 1 (GRIP1) and AMPAR binding protein (ABP). When phosphorylated at serine residue 880 (Ser880), the affinity of GluR2 with GRIP1 and ABP is diminished, which enables the binding of GluR2 with protein interacting with C kinase (PICK1). PICK1 has been demonstrated to be important in decreasing the surface expression of GluR2. We found that in OGD/R-subjected rat hippocampal slices, GluR2-GRIP1 association is decreased, while GluR2-PICK1 association is increased. Additionally, the interaction of activated protein kinase C alpha (PKCα) with PICK1 has been shown to mediate delivery of PKCα to the plasma membrane, a step along with PICK1-ABP binding is necessary for the serine880 phosphorylation of GluR2. In OGD/R-treated rat hippocampal slices, we found that PKCα is activated and subsequently associates with PICK1 in a time course consistent with the OGD/R-induced increase in GluR2 Ser880 phosphorylation. Interestingly, we found that pharmacologic inhibition of NADPH oxidase during OGD/R attenuated GluR2 Ser880 phosphorylation, increased GluR2-GRIP1 association, decreased GluR2-PICK1 association, and dampened

PKCα activation and interaction with PICK1, ultimately preventing the selective degradation of the GluR2 subunit following OGD/R. Furthermore, we found that the interaction of GluR2 with PICK1 is a necessary step involved in the OGD/R-induced GluR2 degradation, as pharmacologic inhibition of the PICK1-GluR2 interaction failed to prevent GluR2 Ser880 phosphorylation, but succeeded in rescuing total GluR2 protein levels. This third study, in combination with the second, provides evidence for NADPH oxidase dependent pathways both at the level of the AMPAR as well as the level of the endocytic machinery responsible for internalization, with both signals ultimately contributing to the OGD/R-induced loss of GluR2 protein surface expression.

The research presented also opens up numerous avenues for future research direction. Other NMDAR subunits, such as the NR2B, also undergo tyrosine phosphorylation, an event that results in the extra-synaptic targeting of NMDARs. To date, the role of NADPH oxidase in mediating the OGD/R-induced increase in NR2B tyrosine phosphorylation has not been investigated. Additionally, other phosphorylation sites exist on NMDARs, and their role in effecting NMDAR function and synaptic targeting have not been fully studied, particularly in the context of OGD/R and NADPH oxidase-mediated signaling events.

Beyond internalization, the OGD/R-induced trafficking of AMPARs subunits has yet to be fully elucidated. While both GluR1 and GluR2 are internalized, differential sorting must occur to result in the drastic reduction of GluR2 protein following OGD/R. Investigation into the cellular signals, protein-protein interactions and endosomal trafficking patterns of all of the AMPAR subunits would be of great value to further understand the precise mechanisms involved in the OGD/R-induced degradation of

GluR2. Additionally, studies aimed at elucidating potential roles for NADPH oxidase-derived ROS in mediating AMPAR subunit recycling patterns would provide useful insight into the decreased surface expression of GluR2 following OGD/R. Experiments utilizing calcium imagining and/or electrophysiology technique in order to obtain functional confirmation of the biochemical changes following OGD/R presented in this dissertation would also be of interest. Lastly, characterization of these findings in an *in vivo* model of ischemia/reperfusion could also serve a potential future direction of study and provide useful knowledge on the role of NADPH oxidase following OGD/R in mediating cellular signaling events in a living animal model.

In summary, these studies have elucidated an ischemic-induced redox-sensitive signaling cascade for altered ionotropic glutamatergic receptor function that is dependent on NADPH oxidase activity. Through inhibition of NADPH oxidase ROS generation, we speculate that the OGD/R-induced enhancement of calcium entry from NMDAR potentiation and loss of calcium-impermeable AMPAR expression is prevented, ultimately increasing cellular viability in post-ischemic tissue. Further studies need be done to fully understand the intricacies of OGD/R-induced NADPH oxidase signaling, perhaps ultimately leading to possible NADPH oxidase targeted therapeutic intervention pharmaceuticals for stroke-patient care.

BIBLIOGRAPHY

Aarts MM and Tymianski M. Molecular Mechanisms Underlying Specificity of Excitotoxic Signaling in Neurons. (2011). *Current Molecular Medicine* **4**(2): 137-147.

Aarts M, Liu Y, Liu L, Besshoh S, Arundine M, Gurd JW, Want Y-T, Salter MW, Tymianski M. (2002). Treatment of Ischemic Brain Damage by Perturbing NMDA Receptor-PSD-95 Interactions. *Science* **298**(5594): 846-850.

Abramov AY, Scorziello A and Duchen MR. (2007) Three distinct mechanisms generate oxygen free radicals in neurons and contribute to cell death during anoxia and reoxygenation. *J. Neurosci.* **27**:1129-1138.

Adesnik H, Nicoll RA, England PM. (2005). Photoinactivation of native AMPA receptors reveals their real-time trafficking. *Neuron* **48**: 977-985.

Anzai T, Tsuzuki K, Yamada N, Hayashi T, Iwakuma M, Inada K, Kameyama K, Hoka S, Saji M. (2003). Overexpression of Ca^{2+}-permeable AMPA receptors promotes delayed cell death of hippocampal CA1 neurons following transient forebrain ischemia. *Neurosci. Res.* **46**: 41-51.

Atkins CM and Sweatt JD. (1999). Reactive oxygen species mediate activity-dependent neuron-glia signaling in output fibers of the hippocampus. *J. Neurosci.* **19**: 7241-7248.

Aukrust P, Muller F, Froland SS. (1994). Enhanced generation of reactive oxygen species in monocytes from patients with common variable immunodeficiency. *Clin. Exp. Immunol.* **97**: 232-238.

Arundine M, Tymianski M. (2003) Molecular mechanisms of calcium-dependent neurodegeneration in excitotoxicity. *Cell Calcium* **34:** 325-337.

Braithwaite SP, Xu J, Leung L, Urfer R, Nikolich K, Oksenberg D, Lombroso PJ, Shamloo M. (2008). Expression and function of striatal enriched protein tyrosine phosphatase is profoundly altered in cerebral ischemia. *Eur. J. Neurosci.* **27**: 2444-2452.

Banfi B, Molnar G, Maturana A, Steger K, Hegedus B, Demaurex N and Krause K.-H. (2001). A Ca(2+)-activated NADPH oxidase in testis, spleen, and lymph nodes. *J. Biol. Chem.* **276**: 37594-37601.

Banfi B, Malgrange B, Knisz J, Steger K, Dubois-Dauphin M and Krause K.-H. (2004). NOX3, a superoxide-generating NADPH oxidase of the inner ear. *J. Biol. Chem.* **279**: 46065-46072.

Barone FC, Irving EA, Ray AM, Lee JC, Kassis S, Kumar S, Badger AM, Legos JJ, Erhardt JA, Ohlstein EH, Hunter AJ, Harrison DC, Philpott K, Smith BR, Adams JL and Parsons AA. (2001) Inhibition of p38 mitogen-activated protein kinase provides neuroprotection in cerebral focal ischemia. *Med. Res. Rev.* **21**: 129-145.

Bass BL. (2002). RNA editing by adenosine deaminases that act on RNA. *Annu. Rev. Biochem.* **71**: 817-846.

Bedard K and Kruase KH. (2007). The NOX family of ROS-generating NADPH oxidases: physiology and pathophysiology. *Physiol. Rev*. **87**: 245-313.

Bell JD, Park E, Ai J, Baker AJ. (2009). PICK1-mediated GluR2 endocytosis contributes to cellular injury after neuronal trauma. *Cell Death and Differentiation* **16**: 1665-1680.

Bellone C, Luscher C, Mameli M. (2008). Mechanisms of synaptic depression triggered by metabotropic glutamate receptors. *Cell Mol. Life Sci.* **18**: 2913-2923.

Bennett JA and Dingledine R. (1995). Topology profile for a glutamate receptor: three transmembrane domains and a channel-lining reentrant membrane loop. *Neuron* **14**: 373-384.

Bianca VD, Dusi S, Bianchini E, Dal PI and Rossi F. (1999). Beta-amyloid activates the O-2 forming NADPH oxidase in microglia, monocytes, and neutrophils. A possible inflammatory mechanism of neuronal damage in Alzheimer's diseas. *J. Biol. Chem.* **274**: 15493-15499.

Blair AS, Hajduch E, Litherland GJ, and Hundal HS. (1999). Regulation of glucose transport and glycogen synthesis in L6 muscle cells during oxidative stress. Evidence for cross-talk between the insulin and SAPK2/p38 mitogen-activated protein kinases signaling pathways. *J. Biol. Chem* **274**: 36293-36299.

Borges K and Dingledine R. (1998). AMPA receptors: molecular and functional diversity. *Prog. Brain Res.* **116**: 153-170.

Brakeman PR, Lanahan AA, O'Brien R, Roche K, Barnes CA, Huganir RL, Worley PF. (1997). Homer: a protein that selectively binds metabotropic glutamate receptors. *Nature* **386(**6622): 284-288.

Bredt DS and Nicoll RA. (2003). AMPA Receptor Trafficking at Excitatory Synapses. *Neuron* **40**(2): 361-379.

Brennan AM, Suh SW, Won SJ, Narasimhan P, Kauppinen TM, Lee H, Edling Y, Chan PH, Swanson RA. (2009). NADPH oxidase is the primary source of superoxide induced by NMDA receptor activation. *Nature Neuro.* **12(**7): 857-863.

Broderick J, Connolly S, Feldmann E, et al. (2007). Guidelines for the management of spontaneous intracerbral hemorrhage in adults: 2007 update: a guideline from the American Heart Association/American Stroke Association Stroke Council, High Blood Pressure Research Council, and the Quality of Care and Outcomes in Research Interdisciplinary Working Group. *Circulation* **116**(16): 391-413.

Brown DI and Briendling KK. (2009). Nox proteins in signal transduction. *Free Radical Biology and Medicine* **47**(9):1239-1253.

Bucci C, Parton RG, Mather IH, Stunnesberg H, Simons K, Hoflack B, Zerial M. (1992). The small GTPase rab5 functions as a regulatory factor in the early endocytic pathways. *Cell* **70**: 715-728.

Calderone A, Jover T, Mashiko T, Noh KM, Tanaka H, Bennett MV, Zukin RS. (2004) Late calcium EDTA rescues hippocampal CA1 neurons from global ischemia-induced death. *J. Neurosci.* **24**: 9903-9913.

Calderone A, Jover T, Noh KM, Tanaka H, yokota H, Lin Y. (2003). Ischemic insults depress the gene silencer REST in neurons destined to die. *J. Neurosci.* **23**: 2112-2121.

Camacho A and Massieu L. (2005). Role of Glutamate Transporters in the Clearance and Release of Glutamate during Ischemia and its Relation to Neuronal Death. *Archives of Medical Research* **37**(1): 11-18.

Camps M, Nichols A, Arkinstall S. (2000). Dual specificity phosphatases: a gene family for control of MAP kinase function. *F.A.S.E.B. Journal* **14**: 6-16.

Carroll RC, Beattie EC, Xia H, Luscher C, Altschuler Y. (1999). Dynamin-dependent endocytosis of ionotropic glutamate receptors. *Proc. Natl. Acad. Sci. USA* **96**: 14112-14117.

Castillo J, Rama R, Devalos A. (2000). Nitric oxide-related brain damage in acute ischemic stroke. *Stroke* **31**: 779-786.

Cavalli V, Vilbois F, Corti M, Marcote MJ, Tamura K, Karin M, Srkinstall S, Gruenberg J. (2001). The stress-induced MAP kinase p38 regulates endocytic trafficking via the GDI:Rab5 complex. *Mol. Cell.* **7**: 421-432.

Chan PH. (1996). Role of oxidants in ischemic brain damage. *Stroke* **27**: 1124-1129.

Chen B-S and Roche KW. Regulation of NMDA receptors by phosphorylation. *Neuropharmacology* **53**(3): 362-368.

Chen C, Leonard JP. (1996) Protein tyrosine kinase-mediated potentiation of currents from cloned NMDA receptors. *J. Neurochem.* **67**: 194-200.

Chen K, Kirber MT, Xiao H, Yang Y and Keaney JF. (2008). Regulation of ROS signal transduction by NADPH oxidase 4 localization. *J. Cell Biol*. **181**: 1129-1139.

Chen M, Sun HY, Li SJ, Das M, Kong JM, Gao TM. (2009). Nitric oxide as an upstream signal of p38 mediates hypoxia/reoxygenation-induced neuronal death. *Neurosignals* **17**(2): 162-168.

Cheng G, Ritsick D, Lambeth JD. (2004). Nox3 regulation by NOXO1, p47phox, and p67phox. *J. Biol. Chem.* **279**: 34250-34255.

Christopherson KS, Sweeney NT, Craven SE, Kang R, El-Husseini Ael D. Bredt DS. (2003). Lipid-and protein-mediated multimerization of PSD-95: implications for receptor clustering and assembly of synaptic protein networks. *J. Cell Sci.* **116**: 3213-3219.

Chung HJ, Huang YH, Lau LF, Huganir RL. (2004). Regulation of the NMDA receptor complex and trafficking by activity-dependent phosphorylation of the NR2B subunit PDZ ligand. *J. Neurosci.* **24**: 10248-10259.

Chung HJ, Xia J, Scannevin RH, Zhang X, Huganir RL. (2000). Phosphorylation of the AMPA receptor subunit GluR2 differentially regulates its interaction with PDZ domain-containing proteins. *J. Neurosci.* **20**: 7258-7267.

Clarke SJ, Khaliulin I, Das M, Parker JE, Heesom KJ, Halestrap AP. (2008). Inhibition of mitochondrial permeability transition pore opening by ischemic preconditioning is probably mediated by reduction of oxidative stress rather than mitochondrial protein phosphorylation. *Circ. Res.* 102(9): 1082-1090.

Clem RL, Anggono V, Huganir RL. (2010). PICK1 regulates incorporation of calcium-permeable AMPA receptors during cortical synaptic strengthening. *J. Neurosci.* **30**(18): 6360-6366.

Conrad KL, Tseng KY, Uejima JL, Reimers JM, Heng LJ, Shaham Y. (2008). Formation of accumbens GluR2-lacking AMPA receptors mediates incubation of cocaine craving. *Nature* **454**: 118-121.

Corasanitl MT, Maiuolo J, Maida S, Fratto V, Navarra M, Russo R, Amantea D, Morrone LA, Bagetta G. (2007). Cell signaling pathways in the mechanisms of neuroprotection afforded by bergamot essential oil against NMDA-induced cell death in vitro. *Br. J. Pharmacol.* **151**(4): 518-529.

Cotton PC, Brugge JS. (1983) Neural tissues express high levels of cellular src gene product pp60c-src. *Mol. Cell Bio.* **3**(6): 1157-1162.

Crack PJ and Taylor JM. (2005). Reactive oxygen species and the modulation of stroke. *Free Rad. Biol. and Med.* **38**(11): 1433-1444.

Crump FT, Killman KS, Craig AM. (2001). cAMP-dependent protein kinase mediates activity-regulated synaptic targeting of NMDA receptors. *J. Neurosci.* **21**: 5079-5088.

Cuenda A and Rousseau S. (2007) p38 MAP-Kinase pathway regulation, function, and role in human diseases. *Biochimica et Biophysica Acta* **1173**: 1358-1375.

Culmsee C, Zhu C, Landshamer S, Becattini B, Wagner E, Pellecchia M, Blomgren K, and Plesnila N. (2005). Apoptosis-Inducing Factor Triggered by Poly(ADP-Ribose) Polymerase and Bid Mediates Neuronal Cell Death after Oxygen Glucose Deprivation and Focal Cerebral Ischemia. *Neurobiology of Disease* **25**(44): 10262-10272.

Cull-Candy S, Brickley S and Farrant M. (2001). NMDA receptor subunits: diversity, development and disease. *Curr, Opin, Neurobiol*. **11**: 327-335.

Cui XL, Brockman D, Campos B and Myatt L. (2006). Expression of NADPH oxidase isoform 1 (Nox1) in human placenta: involvement in preeclampsia. *Placenta* **27**: 422-431.

De Deken X, Wang D, Many MC, Costagliola S, Libert F, Vassart G, Dumont JE and Miot F. (2000). Cloning of two human thyroid cDNAs encoding new members of the NADPH oxidase family. *J. Biol. Chem.* **275**: 23227-23233.

Dejean LM, Martinez-Caballero S and Kinnally KW. (2006). Is MAC the knife that cuts cytochrome *c* from mitochondria during apoptosis? *Cell Death and Differentiation* **13**: 1387-1395.

Dennis SH, Jaafari N, Cimarosti H, Hanley JG, Henley JM, Mellor JR. (2011). Oxygen/glucose deprivation induces a reduction in synaptic AMPA receptors on hippocampal CA3 neurons mediated by mGluR1 and adenosine A3 receptors. *J. Neurosci.* **31**(33): 11941-11952.

Denu JM, Tanner KG. (1998). Specific and reversible inactivation of protein tyrosine phosphatases by hydgrogen peroxide: evidence for a sulfenic acid intermediate and implications for redox regulation. *Biochemistry* **37**: 5633-5642.

de Diego-Otero Y, Romero-Zerbo Y, el Bekay R, Decara J, Sanchez L, Rodriguez-de Fonseca R, del Arco-Herrera I. (2009). Alpha-Tocopherol Protects Against Oxidative Stress in Fragile X Knockout Mouse: an Experimental Therapeutic Approach for the Fmr1 Deficiency. *Neuropsychopharmacol*ogy **34**: 1011-1026.

Dixon RM, Mellor JR, Hanley JG. (2009). PICK1-mediated glutamate receptor subunit 2 (GluR2) trafficking contributes to cell death in oxygen/glucose-deprived hippocampal neurons. *J. Biol. Chem.* **284**(21): 14230-14235.

Dohi K, Ohtaki H, Nakamachi T, Yofu S, Satoh K, Miyamoto K, Song D, Tsunawaki S, Shioda S, Aruga T. Gp91phox (NOX2) in classically activated microglia exacerbates traumatic brain injury. *J. Neuroinflammation* **7**(41).

Dong H, Zhang P, Song I, Petrailia RS, Liao D, Huganir RL. (1999). Characterization of the glutamate receptor-interacting proteins GRIP1 and GRIP2. *J. Neurosci*. **19**: 6930-6941.

Dong H, O'Brien RJ, Fung ET, Lanahan AA, Worley PF, and Huganir RL. (1997). GRIP: a synaptic PDZ domain-containing protein that interacts with AMPA receptors. *Nature* **386**: 279-284.

Dunah AW, Wyszynski M, Martin DM, Sheng M, Standaert DG. (2000). Alpha-actinin-2 in rat striatum: localization and interaction NMDA glutamate receptor subunits. *Brain Res. Mol. Brain Res.* **79**: 77-87.

Dupuy C, Kaniewski J, Deme D, Pommier J, Virion A. (1989). NADPH-dependent H_2O_2 generation catalyzed by thyroid plasma membranes. Studies with electron scavengers. *Eur. J. Biochem* **185**: 597-603.

Ehlers MD. (2000). Reinsertion or degradation of AMPA receptors determined by activity-dependent endocytic sorting. *Neuron* **28**: 511-525.

El Benna J, Faust RP, Johnson JL and Babior BM. (1996). Phosphorylation of the respiratory burst oxidase subunit p47phox as determined by two-dimernsional phosphopeptide mapping. Phosphorylation by protein kinase C, protein kindase A, and mitogen-activated protein kindase. *J. Biol. Chem.* **271**: 6374-6378.

Endo H, Kamada H, Nito C, Nishi T, Chan PH. (2006). Mitochondrial translocation of p53 mediates release of cytochrome c and hippocampal CA1 neuronal death after transient global ischemia in rats. *J Neurosci* **26**: 7974-7983.

English JD and Sweatt JD. (1997). A Requirement for Mitogen-activated Protein Kinase Cascade in Hippocampal Long Term Potentiation. *J. Biol. Chem.* **272**: 19103-19106.

Falluji N, Abou-Chebl A, Rodriguez-Castro CE, Mukherjee D. (2011) Reperfusion Strategies for Acute Ischemic Stroke. *Angiology* **1**(8).

Farooq A, Zhou MM. (2004). Structure and regulation of MAPK phosphatases. *Cell Signal* **16**: 769-779.

Feigin VL. (2005). Stroke epidemiology in the developing world. *Lancet* **365**(9478): 2160-2161.

Ford LM, Sanberg PR, Norman AB, Fogelson MH. (1989). MK-801 prevents hippocampal neurodegeneration in neonatal hypoxic-ischemic rats. *Arch. Neurol.* **46**(10): 1090-1096.

Forder JP and Tymianski M. (2009) Postsynaptic mechanisms of excitotoxicity: Involvement of postsynaptic density proteins, radicals, and oxidant molecules. *Neuroscience* **158**(1): 293-300.

Furukawa H and Gouaux E. (2003). Mechanisms of activation, inhibition, and specificity: crystal structures of the NMDA receptor NR1 ligand-binding core. *EMBO J* **22**: 2873-2885.

Gardner SM, Takamiya K, Xia J, Suh JG, Johnson R. (2005). Calcium-permeable AMPA receptor plasticity is mediated by subunit-specific interactions with PICK1 and NSF. *Neuron* **45**: 903-15.

Gardoni F, Polli F, Cattabeni F, Di Luca M. (2006). Calcium-calmodulin-dependent protein kinase II phosphorylation modulcated PSD-95 binding to NMDA receptors. *Eur J Neurosci* **24**: 2694-2704.

Genovese T, Mazzon E, Paternitl I, Esposito E, Bramanit P, Cuzzocrea S. (2011). Modulation of NADPH oxidase activation in cerebral ischemia/reperfusion injury in rats. *Brain Res.* **1372**: 92-102.

Gerges NZ, Backos DS, Rupasinghe CN, Spaller MR, Esteban JA. (2006). Dual role of the exocyst in AMPA receptor targeting and insertion into the postsynaptic membrane. *EMBO J.* **25**: 1623-1634.

Goebel-Goody SM, Davies KD, Alvestad Linger RM, Freund RK, and Browing MD. (2009). Phospho-regulation of synaptic and extrasynaptic N-methyl-D-aspartate receptors in adult hippocampal slices. *Neuroscience* **158**: 1446-1459.

Glickman MH and Ciechanover A. (2002). The ubiquitin-proteasome proteolytic pathway: destruction for the sake of construction. *Physiol Rev* **82**: 373-428.

Gladding CM and Raymond LA. (2011) Mechanisms underlying NMDA receptor synaptic/extrasynaptic distribution and function. *Molec and Cell Neuro* [in press].

Gladstone DJ, Black SE, Hakim AM. (2002). Towards Wisdom From Failure: Lessons From Neuroprotective Stroke Trails and New Therapeutic Directions. *Stroke* **33**: 2323-2136.

Globus MY, Busto R, Martinez E. (1990). Ischemia induces release of glutamate in regions spared from histopathologic damage in the rat. *Stroke* **21**: 11143-11146.

Giannoni E, Letizia T, Chiarugi P. (2010) Src redox regulation: Again in the front line.

Free Rad Bio & Med **49**: 516-527.

Girouard H, Wang G, Gallo EF, Anrather J, Zhou P, Pickel VM, Iadecola C. (2009). NMDA Receptor Activation Increases Free Radical Production through Nitric Oxide and NOX2. *J Neurosci* **29**(8): 2545-2552.

Gorter JA, Petrozzino JJ, Aronica EM, Rosenbaum DM, Optiz T, Bennett MV. (1997). Global ischmia induces downregulation of GluR2 mRNA and increases AMPA receptor-mediated Ca2+ influx hippocampal CA1 neurons of gerbil. *J. Neurosci.* **17**: 6179-6188.

Gorvel JP, Chavrier P, Zerial M, Gruenberg J. (1991). Rab5 controls early endosome fusion in vitro. *Cell* **64**: 915-925.

Grant ER, Guttmann RP, Seifert KM, Lynch DR. (2001). A region of the rat N-methyl-D-aspartate receptor 2A subunit that is sufficient for potentiation by phorbol esters. *Neurosci Lett* **310**: 9-12.

Groce L, Bard L, Choquet D. (2009). Surface trafficking of N-methyl-D-aspartate receptors: physiological and pathological perspectives. *Neuroscience* **158**: 4-18.

Guttman RP, Baker DL, Seifert KM, Cohen AS, Coulter DA, Lynch DR. (2001). Specific proteolysis of the NR2 subunit at multiple sites by calpain. *J Neurochem* **78**: 1083-1093.

Hakim AM. (1998). Ischemic penumbra: the therapeutic window. *Neurology* **51**(3 Suppl 3): 44046.

Hanley JG, Khatri L, Hanson PI, Ziff EB. (2002). NSF ATPase and alpha-/beta-SNAPs disassemble the AMPA receptor-PICK1 complex. *Neuron* **34**:53-67.

Hardingham GE and Bading H. (2010). Synaptic versus extrasynaptic NMDA receptor signaling: implications for neurodegenerative disorders. *Nat Rev Neurosci* **11**: 682-696.

Hardingham GE, Fukunaga Y, Bading H. (2002). Extrasynaptic NMDARs oppose synaptic NMDARs by triggering CREB shut-off and cell death pathways. *Nat Neurosci* **5**: 405-414.

Hayashi T and Huganir R. (2004). Tyrosine phosphorylation and Regulation of the AMPA Receptor by Src Family Tyrosine Kinases. *J. Neurosci.* **24**(27): 6152-6160.

Hayashi Y, Shi SH, Esteban JA, Piccini A, Poncer JC, Malinow R. (2000). Driving AMPA receptors into synapses by LTP and CaMKII: requirement for GluR1 and PDZ domain interactions. *Science* **287**: 2262-2267.

Hecquet CM and Malik AB. (2009). Role of H(2)O(2)-activated TRPM2 calcium channel in oxidant-induced endothelial injury. *Thromb. Haemost.* **101**(4): 619-625.

Heuser JE and Anderson RG. (1989). Hypertonic media inhibit receptor-mediated endocytosis by blocking clathrin-coated pit formation. *J. Cell Biol.* **108**(2): 389-400.

Hou N, Torii S, Saito N, Hosaka M, Takeuchi T. (2008). Reactive oxygen species-mediated pancreatic beta-cell death is regulated by interactions between stress-activated protein kinases, p38 and c-Jun N-terminal kinase, and mitogen-activated protein kinase phosphatases. *Endocrinology* **149**: 1654-1665.

Hou XY, Zhang GY, Zong YY. (2003) Supression of postsynaptic density protein 95 expression attenuates increased tyrosine phosphorylation of NR2A subunits of N-methyl-D-aspartate receptors and interactions of Src and Fyn with NR2A after transient brain ischemia in rat hippocampus. *Neuro Lett* **343**: 125-128.

Hou XY, Liu Y and Zhang GY. (2007) PP2, a potent inhibitor of Src family kinases, protects against hippocampal CA1 pyramidal cell death after transient global brain ischemia. *Neurosci Lett* **420:** 235-239.

Hu X, Huang Q, Yang X, Xia H. (2007). Differential Regulation of AMPA Receptor Trafficking by Neurabin-Targeted Synaptic Protein Phosphatase-1 in Synaptic Transmission and Long-Term Depression in Hippocampus. *J. Neurosci.* **27**(11): 4674-4686.

Huang CC, You JL, Wu MY, Hsu KS. (2004). Rap1-induced p38 mitogen-activated protein kinase activation facilitates AMPA receptor trafficking via the GDI.Rab5 complex. Potential role in (S)-3,5-dihydroxyphenylglycene-induced long term depression. *J Biol Chem* **279**(13): 12286-12292.

Infanger DW, Sharma RV, Davisson RL. (2006). NADPH oxidases of the brain: distribution, regulation, and function. *Antioxid Redox Signal* **8**(9-10): 1583-1596.

Isaac JTR, Ashby MC, McBain CJ. (2007). The Role of the GluR2 Subunit in AMPA Receptor Function and Synaptic Plasticity. *Neuron* **54**(6): 859-871.

Jackson DA, Mou L, Gates A, Mosser VA, Tobin A. (2006). Transient hypoxia induces sequestration of M1 and M2 muscarinic acetylcholine receptors. *J Neurochem* **96**(2): 510-519.

Jagnandan D, Church JE, Banfi B, Stuehr DJ, Marrero MB and Fulton DJ. (2007). Novel mechanism of activation of NADPH oxidase 5: caclium sensitization via phosphorylation. *J. Biol. Chem.* **282**: 6494-6507.

Jane DE, Lodge D., Collingridge GL. (2009). Kainate receptors: pharmacology, function, and therapeutic potential. *Neuropharmacology* **56**(1): 90-113.

Jayakar SS and Dikshit M. (2004). AMPA receptor regulation mechanisms: future target for safer neuroportective drugs. *Int. J. Neurosci.* **114**(6): 695-734.

Jiang F, Zhang Y, Dusting GJ. (2011). NADPH oxidase-mediated redox signaling: roles in cellular stress response, stress tolerance, and tissue repair. *Pharmacol. Rev.* **63**(1): 218-242.

Jiang X, Mu D, Biran V, Faustino J, Chang S, Rincon C.M, Sheldon R.A. Ferriero DM. (2008) Activated Src kinases interact with the N-methyl-D-aspartate receptor after neonatal brain ischemia. *Ann Neurol* **65**(5): 632-641.

Joch M, Ase AR, Chen CX, MacDonald PA, Kontogiannea M, Corera AT, Brice A, Seguela P, Fon EA. (2007). Parkin-mediated monoubiquitination of the PDZ protein PICK1 regulates the activity of acid-sensing ion channels. *Mol. Biol. Cell* **18**(8): 3105-3118.

Kalia LV, Pitcher GM, Pelkey KS and Salter MW. (2006). PSD-95 is a negative regulator of the tyrosine kinase Src in the NMDA receptor complex. *EMBO J* **25**: 4971-4982.

Kalia LV, Gingrich JR, Salter MW. (2004) Src in synaptic transmission and plasticity. *Oncogene* **23**(48): 8007-8016.

Kamada H, Nito C, Endo H, Chan PH. (2007). Bad as a converging signaling molecular between survival PI3-K/Akt and death JNK in neurons after transient focal ischemia in rats. *J. Cereb. Blood Flow Metab.* **27**: 521-533.

Klann E, Roberson ED, Knapp LT and Sweatt JD. (1998) A role for superoxide in protein kinase C activation and induction of long-term potentiation. *J Biol Chem* **273**: 4516-4522.

Kim E and Sheng M. (2004). PDZ domain proteins of synapses. *Nat. Rev. Neurosci.* **5**: 771-781.

Kishida KT, Hoeffer CA, Hu D, Pao M, Holland SM, and Klann E. (2006) Synaptic plasticity deficits and mild memory impairments in mouse models of chronic granulomatous disease. *Mol Cell Biol* **26**: 5908-5920.

Kishida KT, Pao M, Holland SM, Klann E. (2005). NADPH oxidase is required for NMDA receptor-dependent activation of ERK in hippocampal area CA1. *J. Neurochem.* **94**(2): 299-306.

Koike M, Iino M, and Ozawa S. (1997). Blocking effect of 1-naphtyl acetyl spermine on Ca^{2+} - permable AMPA receptors in cultured rat hippocampal neurons. *Neurosci Res* **29**: 27-36.

Kwak S and Weiss JH. (2006). Calcium-permeable AMPA channels in neurodegenerative disease and ischemia. *Curr. Opin. Neurobiology* **16**: 281-287.

Lai TW, Shyu W-C, Wang YT. (2011). Stroke intervention pathways: NMDA receptors and byond. *Trends Mol Med* **17**(5): 266-275.

Lau A and Tymianski M. (2010). Glutamate receptors, neurotoxicity, and neurodegeneration. *Eur J Physiol* **460**(2): 525-542.

Lau LF, Huganir RL. (1995) Differential tyrosine phosphorylation of N-methyl-D-aspartate receptor subunits. *J Biol Chem* **270**(34): 20036-20041.

Lee BI, Lee DJ, Cho KJ, Kim GW. (2005). Early nuclear translocation of endonuclease G and subsequent DNA fragmentation after transient focal cerebral ischemia in mice. *Neuroscience Letters* **386**(1): 23-27.

Lee HK, Takamiya K, Han JS, Man H, Cim CH. (2003). Phosphorylation of the AMPA receptor GluR1 subunit is required for synaptic plasticity and retention of spatial memory. *Cell* **112**: 631-643.

Lee NK, Choi YG, Baik JY, Han SY, Jeong DW, Bae YS, Kim N and Lee SY. (2005). A crucial role for reactive oxygen species in FANKL-induced osteoclast differentiation. *Blood* **106**: 852-859.

Lefkowitz, RJ., Drake MT, Shenoy SK. (2006). Trafficking of G protein coupled receptors. *Circulation Research* **99**: 570-582.

Legos JJ, McLaughlin B, Skaper SD, Strijbos PJ, Parsons AA, Aizenman E, Herin GA, Barone FC, Erhardt JA. (2002). The selective p38 inhibitor SB-239063 protects primary neurons from mild to moderate excitotoxic injury. *Eur. J. Pharmacol.* **447**(1): 37-42.

Legos JJ, Erhardt JA, White RF, Lenhard SC, Chandra S, Parsons AA, Tuma RF, Barone FC. (2001). SB 239063, a novel p38 inhibitor, attenuates early neuronal injury following ischemia. *Brain Res.* **892**: 70-77.

Levey AI, Volpicelli LA, Lah, JJ. (2001). Rab5-dependent trafficking of the m4 muscarinic acetylcholine receptor to the plasma membrane, early endosomes, and multivesicular bodies. *Journal of Biological Chemistry* **276**: 47590-47598.

Li B-S, Sun M-K, Zhang L, Takahashi S, Ma W, Vinade L, kulkarni AB, Brady RO, Pant HC. (2001). Regulation of NMDA receptors by cyclin-dependent kinase-5. *PNAS USA* **98**(22): 12742-12747.

Li Q, Zhang Y, Marden JJ, Banfi B, Engelhardt JF. (2008). Endosomal NADPH Oxidase regulated c-Src activation following hypoxia/reoxygenation injury. *Biochem J.*

411(3): 531-541.

Lin D-T, Huganir RL. (2007). PICK1 and Phosphorylation of the Glutamate Receptor 2 (GluR2) AMPA Receptor Subunit Regulates GluR2 Recycling after NMDA Receptor-Induced Internalization. *J. Neurosci*. **27**(50): 13903-13908.

Lipton SA, Choi YB, Takahashi H, Zhang D, Li W, Godzik A, and Bankston LA. (2002) Cyesteine regulation of protein function: as exemplified by NMDA-receptor modulation. *Trends Neurosci* **25**: 474-480.

Liu AL, Wang XW, Liu AH, Su XW, Jian WJ, Qui PX, Yan GM. (2009). JNK and p38 were involved in hypoxia and reoxygenation-induced apoptosis of cultured rat cerebellar granule neurons. Exp. Toxicol. Pathol. 61(2): 127-143.

Liu B, Liao M, Mielke JG, Ning K, Chen Y, Li L, El-Hayek YH, Gomez E, Zukin RS, Fehlings MG, Wan Q. (2006). Ischemic Insults Direct Glutamate Receptor Subunit 2-Lacking AMPA Receptors to Synaptic Sites. *J. Neurosci.* **26**(20): 5309-5319.

Liu SJ, Gasperini R, Foa L, Small DH. (2010). Amyloid-beta decreases cell-surface AMPA receptors by increasing intracellular calcium and phosphorylation of GluR2. *J. Alzheimers Dis.* **21**(2): 655-666.

Liu S, Lau L, Wei J, Zhu D, Zou S, Sun HS, Fu Y, Liu F, Lu Y. (2004). Expression of Ca(2+)-permeable AMPA receptor channels primes cell death in transient forebrain ischemia. *Neuron* **43**: 43-55.

Liu Y, Wong TP, Aarts M, Rooyakkers A, Liu L, Lai TW, Wu DC, Lu J, Tymianski M, Craig AM, Wang YT. (2007). NMDA receptor subunits have differential roles in mediating excitotoxic neuronal death both in vitro and in vivo. *J Neurosci* **27**: 2846-2857.

Liu Y, Zhang G, Gao, C, Hou, X. (2001) NMDA receptor activation results in tyrosine phosphorylation of NMDA receptor subunit 2A(NR2A) and interaction of Pyk2 and Src with NR2A after transient cerebral ischemia and reperfusion. *Brain Res.* **909**(1-2): 51-58.

Lu Q, Rau TF, Hariss V, Johnson M, Poulsen DJ, Black SM. (2011). Increased p38 mitogen-activated protein kinase signaling is involved in the oxidative stress associated with oxygen and glucose deprivation in neonatal hippocampal slice cultures. *Eur. J. Neurosci.* **34**(7): 1093-1010.

Lu YM, Yin HZ, Chiang J, and Weiss JH. (1996). Ca(2+)-permeable AMPA/kainate and NMDA channels: high rate of Ca2+ influx underlies potent induction of injury. *J. Neurosci.* **16**: 5457-5465.

Lu W and Ziff EB. (2005). PICK1 interacts with ABP/GRIP to regulate AMPA receptor trafficking. *Neuron* **47**(3): 407-421.

Lu W, Man H, Ju W, Trimble WS, MacDonald JF, Wang YT. (2001). Activation of synaptic NMDA receptors induces membrane insertion of new AMPA receptors and LTP in cultured hippocampal neurons. *Neuron* **29**: 243-254.

Mackay K, Mochly-Rosen D. (1999). An inhibitor of p38 mitogen-activated protein kinase protects neonatal cardiac myocytes from ischemia. *J. Biol. Chem*. **274**: 6272-6279.

Man HY, Lin JW, Ju WH, Ahmadian G, Liu L. (2000). Regulation of AMPA receptor-mediated synaptic transmission by clathrin-dependent receptor internalization. *Neuron* **25**: 649-662.

Mansour M, Nagarajan N, Nehring RB, Clements JD, and Rosenmund C. (2011). Heteromeric AMPA receptors assemble with a preferred subunit stoichiometry and spatial arrangement. *Neuron* **32**: 841-853.

Martel MA, Wyllie DJA, Hardingham GE. (2009). In developing hippocampal neurons, NR2B-containing N-methyld-D-aspartate receptors (NMDARs) can mediate signaling to neuronal survival and synaptic potentiation, as well as neuronal death. *Neuroscience* **158**(1): 334-343.

Martin HG and Wang YT. (2010). Blocking the deadly effects of the NMDA receptor in stroke. *Cell* **140**: 174-176.

McCracken E, Valeriani V, SimpsonC, Jover T, McCulloch J, Dewar D. (2000). The lipid peroxidation by-product 4-hydroxynonenal is toxic to axons and oligodendrocytes. *J Cereb Blood Flow Metab* **20**: 1529-1536.

Mcintosh TK, VinkR, Soares H, Hayes R. Simon R. (1989). Effects of the N-methyl-D-aspartate receptor blocker MK-801 on neurologic function after experimental brain injury. *J. Neurotrauma* **6**(4): 247-259.

McLauchlan H, Newell J, Morrice N, Osborne A, West M, Smythe E. (1998). A novel role for Rab5-GDI in ligand sequestration into clathrin-coated pits. *Curr. Biol.* **8**: 34-45.

Miller AA, Dusting GJ, Roulston CL and Sobey CG. (2006). NADPH-oxidase activity is elevated in penumbral and non-ischemic cerebral arteries following stroke. *Brain Research* **111**: 111-116.

Mitani A, Namba S, ikemune K, Yanase H, Arai T, Kataoka K. (1998). Postischmic Enhancements of N-Methyl-D-Aspartic Acid (NMDA) and Non-NMDA Receptor-Mediated Responses in Hippocampal CA1 Pyramidal Neurons. *J Cereb Blood Flow and Metab* **18**: 1088-1098.

Murotomi K, Takagi N, Takeo S, Tanonaka K. (2011). NADPH oxidase-mediated oxidative damage to protein in the postsynaptic density after transient cerebral ischemia and reperfusion. *Mol. and Cell. Neuro.* **46**(3): 681-688.

Murotomi K, Takagi N, Mizutani R, Honda T, Ono M, Takeo S, Tanonaka K. (2010) mGluR1 antagonist decreased NADPH oxidase activity and superoxide production after transient focal cerebral ischemia. *J Neuro Chem* **114**: 1711-1719.

Murotomi K, Takagi N, Takayanagi G, Ono M, Takeo S, Tanonaka K. (2008). mGlur1 antagonist decreases tyrosine phosphorylation of NMDA receptor and attenuates infarct size after transient focal cerebral ischemia. *J Neuro Chem* **105**: 1625-1634.

Naisbitt S, Kim E, Tu JC, Xiao B, Sala C. (1999). Shank, a novel family of postsynaptic density proteins that bind to the NMDA receptor/PSD-95/GKAP complex and cortactin. *Neuron* **23**: 569-582.

Newpher TM and Ehlers MD. (2009). Spine microdomains for postsynaptic signaling and plasticity. *Trends Cell Biol* **19**: 218-227.

Niizuma K, Yoshioka H, Chen H, Kim GS, Jung JE, Katsu M, Okami N and Chan PH. (2010) Mitochondrial and apoptotic neuronal death signaling pathways in cerebral ischemia. *Biochimica et Biophysica Acta* **1802**(1): 92-99.

Nishimune A, Isaac JT, Molnar E, Noel J, Nash SR. (1998). NSF binding to GluR2 regulates synaptic transmission. *Neuron* **21**: 87-97.

Noh KM, Yokota H, Mashiko T, Castillo PE, Zukin RS, and Bennett MV. (2005). Blockade of calcium-permeable AMPA receptors protects hippocampal neurons against global ischemia-induced death. *PNAS USA* **102**: 12230-12235.

Norris EH and Giasson BI. (2005). Role of oxidative damage in protein aggregation associated with Parkinson's disease and related disorders. *Antioxid. Redox Signal* **7**: 672-684.

Novick P, Ortiz B, Grosshans L. (2006). Rabs and their effectors: Achieving specificity in membrane traffic. *Proc. Natl. Acad. Sci.* **8**: 11821-11827.

Novick P and Zerial M. (1997). The diversity of Rab proteins in vesicle transport. *Curr. Opin. Cell Biol*. **9**: 496-504.

Ogura M and Kitamura M. (1998). Oxidant stress incites spreading of macrophages via extracellular signal-regulated kinases and p38 mitogen-activated protein kinases. *J. Immunol.* **161**: 3569-3574.

O'Loghlen A, Perez-Morgado MI, Salinas M, Martin ME. (2003). Reversible inhibition of the protein phosphatase 1 by hydrogen peroxide. Potential regulation of elF2 alpha phosphorylation in differentiated PC12 cells. *Arch. Biochem. Biophys.* **417**(2):194-202.

Optiz T, Grooms SY, Bennet MV and Zukin RS. (2000). Remodeling of alpha-amino-3-hydroxy-5-methyl-4-isoxazole-propionic acid receptor subunit composition in hippocampal neurons after global ischemia. *Proc. Natl. Acad. Sci. USA* **97**: 13360-13365.

Ozawa H, Shioda S, Dohi K, Matsumoto H, Mizushima H, Zhou CJ, Funahashi H, Nakai Y, Nakajo S, Matsumoto K. (1999). Delayed neuronal cell death in the rat hippocampus is mediated by the mitogen-activated protein kinase signal transduction pathway. *Neurosci. Lett.* **262**: 57-60.

Passafaro M, Piech V, and Sheng M. (2001). Subunit-specific temporal and spatial patters of AMPA receptor exocytosis in hippocampal neurons. *Nat. Neurosci.* **4**: 917-926.

Patterson MA, Szatmari EM, Yasuda R. (2010). AMPA receptors are exocytosed in stimulated spines and adjacent dendrites in a Ras-ERK-dependent manner during long-term potentiation. *PNAS USA* **107**(36): 15951-15956.

Pellegrini-Giampietro DE, Gorter JA, Bennett MV, Zukin RS. (1997). The GluR2 (GluR-B) hypothesis: Ca^{2+}-permeable AMPA receptors in neurological disorders. *Trends Neurosci.* **20**: 464-470.

Pellegrini-Giampietro DE, Zukin RS, Bennett MV, Cho S and Pulsinelli WA. (1992). Switch in glutamate receptor subunit gene expression in CA1 subfield of hippocampus following global ischemia in rats. *Proc. Natl. Acad. Sci. USA* **89**: 10499-10503.

Pei L, Li Y, Zhang GY, Cui ZC, and Zhu ZM. (2000). Effects of two types of calcium channel antagonists on tyrosine phosphorylation of NMDA receptor subunit 2B in the hippocampus following transient cerebral ischemia. *Acta. Pharmacol. Sin*. **21**: 695-700.

Peng PJ, Zhong X, Tu W, Soundarapandian MM, Molner P, Zhu D, Lau L, Liu S, Liu F, Lu Y. (2006). ADAR2-dependent RNA editing of AMPA receptor subunit GluR2 determines vulnerability of neurons in forebrain ischemia. *Neuron* **49**(5): 719-733.

Perez JL, Khatri L, Chang C, Srivastava S, Osten P, and Ziff EB. (2001). PICK1 targets activated protein kinase C alpha to AMPA receptor clusters in spines of hippocampal neurons and reduces surface levels of the AMPA-type glutamate receptor subunit 2. *J. Neurosci.* **21**: 5417-5428.

Prybylowski K, Chang K, Sans N, Kan L, Vicini S, Wenthold RJ. (2005). The synaptic localization of NR2B-containing NMDA receptors is controlled by interactions with PDZ proteins and AP-2. *Neuron* **47**: 845-857.

Racz B, Blanpied TA, Ehlers MD, Weinberg RJ. (2004). Lateral organization of endocytic machinery in dendritic spines. *Nat. Neurosci.* **7**: 917-918.

Rakhade SN, Zhou C, Aujla PK, Fishman R, Sucher NJ, and Jensen FE. (2008). Early alterations of AMPA receptors mediate synaptic potentiation induced by neonatal seizures. *J. Neurosci*. **28**: 7979-7990.

Robinson MJ and Cobb MH. (1997). Mitogen-activated protein kinase pathways. *Curr. Opin. Cell Biol.* **9**: 180-186.

Rokutan K, Kawahara T, Kuwano Y, Tominage K, Nishida K and Teshima-Kondo S. (2008) Nox enzymes and oxidative stress in the immunopathology of the gastrointestinal tract. *Semin. Immunopathol.* **30**: 315-327.

Rosenbaum DM, Gupta G, D'Amore J, Singh M, Weidenheim K, Zhang H, Kessler JA. (2000). Fas(CD95/APO-1) plays a role in the pathophysiology of focal cerebral ischemia. *J Neurosci Res* **61**: 686-692.

Rumbaugh G, Adams JP, Kim JH., and Hungair RL. (2006). SynGAP regulates synaptic strength and mitogen-activated protein kinases in cultured neurons. *PNAS USA* **103**: 4344-4351.

Saeed SA, Shad KF, Saleem T, Javed F, Khan MU. (2007). Some new prospect in the understanding of the molecular basis of the pathogenesis of stroke. *Exp Brain Res* **182**: 1-10.

Salter MW and Kalia LV (2004). Src kinases: a hub for NMDA receptor regulation. *Nat. Rev. Neurosci.. Lett*. **416**: 317-328.

Sato H, takeo T, Liu Q, Nakano K, Osani T, Suga S, Wakui M, Wu J. (2009). Hydrogen peroxide mobilizes Ca2+ through two distinct mechanisms in rat hepatocytes. *Acta. Pharmacol. Sin.* **30**(1): 78-89.

Schaller B and Graf R. (2004). Cerebral ischemia and reperfusion: the pathophysiologic concept as a basis for clinical therapy. *J. Cereb. Blood Flow Metab* **27**(6): 351-371.

Seidenman KJ, Steinberg JP, Huganir R, Malinow R. (2003). Glutamate receptor subunit 2 Serine 880 phosphorylation modulates synaptic transmission and mediates plasticity in CA1 pyramidal cells. *J. Neurosci.* **23**: 9220-9228.

Serrander L, Cartier L, Bedard K, Banfi B, Lardy B, Plastre O, Sienkiewica A, Forro L, Schlegel W and Krause K.-H. (2007). NOX4 activity is determined by mRNA levels and reveals a unique patter of ROS generation. *Biolchem. J.* **406**: 105-114.

Serrano F, Kolluri NS, Wientjes FB, Card JP and Klann E. (2003) NADPH oxidase immunoreactivity in the mouse brain. *Brain Research* **988**: 193-198.

Seth D, Rudolph J. (2006). Redox regulation of MAP kinase phosphatase 3. *Biochemistry* **45**: 8476-8487.

Sheng M and Lee SH. (2000). Growth of the NMDA receptor industrial complex. *Nat. Neurosci*. **3**: 633-635.

Shepherd, JD. and Huganir RL. (2007). The Cell Biology of Synaptic Plasticity: AMPA Receptor Trafficking. *Annu. Rev. Cell Dev. Biol.* **23**: 613-643.

Shigemoto R, Kinoshia A, Wada E, Nomura S, Ohishi H, Takada M, Flor PJ, Neki A, Abe T, Nakanishi S, Mizuno N. (1997). Differential presynaptic localization of metabotropic glutamate receptor subtypes in the rat hippocampus. *J. Neurosci.* **17**(19): 7503-7522.

Shu SW, Shin BS, Ma H, Van Hoecke M, Brennan A.M, Yenair M.A, Swanson R.A. (2008). Glucose and NADPH Oxidase Drive Superoxide Production in Stroke. *Ann. Neurology* **64** (6): 654-653.

Smotrys JE and Linder ME. (2004). Palmitoylation of interacellular signaling proteins: regulation and function. *Annu. Rev. Biochem.* **73**: 559-587.

Spruston N, Jonas P and Sakmann B. (1995) Dendritic glutamate receptor channels in rat hippocampal CA3 and CA1 pyramidal neurons. *J. Physiol.* **482** (Pt 2): 325-352.

Soderling TR, Derkach VA. (2000). Postsynaptic protein phosphorylation and LTP. *Trends. Neurosci.* **23**: 75-80.

Sonnichsen B. De Renzis S, Nielsen E. Rietdorf J, Zerial M. (2000). *Journal of Cellular Biology* **149(**4): 901-914.

Sorce S and Krause K.-H. (2009). NOX Enzymes in the Central Nervous System: From Signaling to Disease. *Antioxid and Redox Signal* **11**(10): 2481-2504.

Soundarapandian MM, Tu WH, Peng PJ, Zervos AS, Lu YM. (2005). AMPA receptor subunit GluR2 gates injurious signals in ischemic stroke. *Mol. Neurobiol.* **32**(2): 145-155.

Srivastava S, Osten P, Vilim FS, Khatri L, Inman G, States B. (1998). Novel anchorage of GluR2/GluR3 to postsynaptic density by the AMPA receptor-binding protein ABP. *Neuron* **21**: 581-591.

Stavrovskaya IG and Kristal BS. (2005) The powerhouse takes control of the cell: is the mitochondrial permeability transition a viable therapeutic target against neuronal dysfunction and death? *Free Rad. Biol. and Med.* **38**(6): 687-697.

Steinacker P, Aitken A, Otto M. (2011). 14-3-3 proteins in neurodegeration. *Semi. Cell Dev. Biol.* [epub ahead of print].

Stenmark H, Olkkonen VM. (2001). The Rab GTPase family. *Genome Biology* **2**(5).

Stephenson FA, Cousisns SL, Kenny AV. (2008). Assembly and forward trafficking of NMDA receptors. *Mol. Membr. Biol.* **25**: 311-320.

Sugino T, Nozaki K, Takagi Y, Hattori I, Hashimoto N, Moriguchi T, Nishida E. (2000). Activation of mitogen-activated protein kinases after transient forebrain ischemia in gerbil hippocampus. *J. Neurosci.* **20**: 4506-4514.

Suppiramaniam V, Dhanasekaran M, Parameshwaran K. (2007) Amyloid beta peptides and glutamatergic synaptic dysregulation. *Experimental Neurology* **210**: 7-13.

Szydlowska K and Tymianski M. (2010). Calcium, ischemia and excitotoxicity. *Cell Calcium* **47**: 122-129.

Takagi N, Besshoh S, Morita H, Terao M, Takeo S, Tanonaka K. (2010). Metabotropic glutamate mGlu5 receptor-mediated serine phosphorylation of NMDA receptor subunit NR1 in hippocampal CA1 region after transient global ischemia in rats. *Eur. J. Pharmacol.* **644**(1-3): 96-100.

Takagi N, Shinno K, Teves L, Bissoon N, Wallace M.C, and Gurd J.W. (1997) Transient ischemia differentially increases tyrosine phosphorylation of NMDA receptor subunits 2A and 2B. *J Neurochem* **69**: 1060-1065.

Tafani M, Karpinich NO, Hurster KA, Pastorino JG, Schneider T, Russo MA and Farber JL. (2002) Cytochrome c Release upon Fas Receptor Activation Depends on Translocation of Full-length Bid and the Induction of the Mitochondrial Permeability Transition. *J. Biol. Chem.* **277**: 10073-10082.

Tanaka H, Grooms SY, Bennett MV, Zukin S. (2000). The AMPAR subunit GluR2: still front and center stage. *Brain Research* **886**: 190-207.

Tejada-Simon MV, Serrano F, Villasana LE., Kanterewicz BI, Wu GY, Quinn MT and Klann E. (2005) Synaptic localization of a functional NADPH oxidase in the mouse hippocampus. *Mol. Cell. Neurosci.* **29**: 97-106.

Terashima A, Pelkey KA, Rah JC, Such YH, Roche KW, Collingridge GL. (2008). An essential role for PICK1 in NMDA receptor-dependent bidirectional synaptic plasticity. *Neuron* **57**: 872-882.

Terashima A, Cotton L, Dev KK, Meyer G, Zaman S, Duprat F. (2004). Regulation of synaptic strength and AMPA receptor subunit composition by PICK1. *J. Neurosci.* **24**: 5381-5390.

Thiels E, Urban NN, Gonzalez-Burgos GR, Kanterewicz BI, Barrionuevo G, Chu CT, Oury TD, Klann E. (2000). Impairment of long-term potentiation and associative memory in mice that overexpress extracellular superoxide dismutase. *J Neurosci* **20**: 7631-7639.

Thiels E, Norman ED, Barrioneuvo G, Klann E (1998). Transient and persistent increase in protein phosphatase activity during long-term depression in the adult hippocampus in vivo. *Neuroscience* **86**: 1024-1029.

Thorsen TS, Madsen KL, Rebola N, Rathje M, Anggono V, Bach A, Moreira IS, Stuhr-Hansen N, Dyhring T, Peters D, Beuming T, Huganir R, Weinstein H, Mulle C, Stromgaard K, Ronn LC, Gether U. (2010). Identification of a small-molecule inhibitor of the PICK1 PDZ domain that inhibits hippocampal LTP and LTD. *Proc. Natl. Acad. Sci. U.S.A.* **107**(1): 413-418.

Tiago T, Ramos S, Aureliano M, Gutierrez-Merino C. (2006). Peroxynitrite induces F-actin depolymerization and blockade of myosin ATPase stimulation. *Biochem. Biophys. Res. Commun.* **342**(1): 44-49.

Tingley WG, Ehlers MD, Kameyama K, Doherty C, Ptak JB, Riley CT, Huganir RL. (1997). Characterization of protein kinase A and protein kinase C phosphorylation of the N-methyl-D-aspartate receptor NR1 subunit using phosphorylation site-specific antibodies. *J Biol Chem* **272**: 5157-5166.

Tiruppathi C, Ahmmed GU, Vogel SM, Malik AB. (2006). Ca2+ signaling, TRP channels, and endothelial permeability. *Microcirc.* **13**(8): 693-708.

Traynelis SF, Wollmuth LP, McBain CJ, Menniti FS, Vance KM, Ogden KK, Hansen KB, Yuan H, Myers SJ, and Dingledine R. (2010). Glutamate Receptor Ion Channels: Structure, Regulation, and Function. *Pharmacol Rev* **62**: 405-496.

Tu JC, Xiao B, Yuan JP, Lanahan AA, Leoffert K. (1998). Homer binds a novel proline-rich motif and links group 1 metabotropic glutamate receptors with IP3 receptors. *Neuron* **21**: 717-726.

Tuttle KR, Anderberg RJ, Cooney SK, Meek RL. (2009). Oxidative Stress Mediates Protein Kinase C Activation and Advanced Glycation End Product Formation in a Mesangial Cell Model of Diabetes and High Protein Diet. *Am. J. Nephrology* **29**: 171-180.

Uneo N, Takeya R, Miyano K, Kikuchi H, Sumioto H. (2005). The NADPH oxidase

Nox3 consitiutively produces superoxide in a p22phox-dependent manner: Its regulation by oxidases organizers and activators. *J. Biol. Chem.* **280**: 23328-23339.

Von Engelhardt J, Coserea I, Pawlak V, Fuchs EC, Kohr G, Seeburg PH, Monyer H. (2007). Excitotoxicity in vitro by NR2A- and NR2B-containing NMDA receptors. *Neuropharmacology* **53**(1): 10-17.

Wandinger-Ness A, Dong J, Stein MP. (2003) Rab proteins and endocytic trafficking: potential targets for therapeutic intervention. *Advanced Drug Delivery Reviews* **55**: 1421-1437.

Wang Q, Tompkins KD, Simonyl A, Korthuis RJ, Sun AY, Su GY. (2006) Apocynin protects against global cerebral ischemia-reperfusion-induced oxidative stress and injury in the gerbil hippocampus. *Brain Res.* **1090**(1):182-189.

Walder CE, Green SP, Darbonne WC, Mathias J, Rae J, Dinauer MC, Curnutte JT, Thomas GR. (1997). Ischemic stroke injury is reduced in mice lacking a functional NADPH oxidase. *Stroke* **28**: 2252-2258.

Ward NE, Pierce DS, Chung SE, Gravitt KR, O'Brian CA. (1998). Irreversible inactivation of protein kinase C by glutathione. *J. Biol. Chem.* **273**: 12558-12566.

Xi HJ, Zhang TH, Tao T, Song CY, Lu SJ, Cui XG, Yue ZY. (2011). Propofol improved neurobehavioral outcome of cerebral ischemia-reperfusion rats by regulating Bcl-2 and Bax expression. *Brain Research* **1410**: 24-32.

Xia J, Chung HJ, Wihler C, Huganir RL, Linden DJ. (2000). Cerebellar long-term depression requires PKC-regulated interactions between GluR2/3 and PDZ domain-containing proteins. *Neuron* **28**: 499-510.

Xu, W. (2011). PSD-95-like membrane associated guanylate kinases (PSD-MAGUKs) and synaptic plasticity. *Curr. Opin. Neurobiol*. **21**(2): 306-312.

Yashiro K and Philpot BD. (2008) Regulation of NMDA receptor subunit expression and its implications for LTP, LTD, and metaplasticity. *Neuropharmacology* **7**: 1081-1094.

Yi Z, Petralia RS, Fu Z, Swanwick CC, Wang YX, Prybylowski K, Sans N, Vicini S, and Wenthold RJ. (2007). The role of the PDZ protein GIPC in regulating NMDA receptor trafficking. *J. Neurosci.* **27**: 11663-11675.

Yin HZ, Sensi SL, Ogoshi F, Weiss JH. (2002). Blockade of Ca^{2+}-permeable AMPA/kainate channels decreases oxygen-glucose deprivation-induced Zn^{2+} accumulation and neuronal loss in hippocampal pyramidal neurons. *J. Neurosci.* **22**: 1273-1279.

Yu XM, Askalan R, Keil GJ 2nd, Salter MW. (1997). NMDA channel regulation by channel-associated protein tyrosine kinase Src. *Science* **275**(5300): 674-68.

Zhang X, Chen Y, Jenkins LW, Kochanek PM, Clark RSB. (2005). Bench-to-bedside review: Apoptosis/programmed cell death triggered by traumatic brain injury. *Crit. Care.* **9(**1): 66-75.

Zhong P, Liu W, Gu Z, Yan Z. (2008). Serotonin facilitates long-term depression induction in prefrontal cortex via p38 MAPK/Rab5-mediated enhancement of AMPA receptor internalization*. J. Physiol.* **586**(18): 4465-4479.

Zhu JJ, Qin Y, Zhao M, Van Aelst L, Manilow R. (2002). Ras and Rap control AMPA receptor trafficking during synaptic plasticity. *Cell* **110**: 443-455.

Zingg JM and Azzi A. (2004). Non-antioxidant activities of vitamin E. *Curr. Med. Chem.* **11**: 1113-1133.